

Copyright is owned by the Author of the thesis. Permission is given for a copy to be downloaded by an individual for the purpose of research and private study only. The thesis may not be reproduced elsewhere without the permission of the Author.

Testing the potential of mycobacteriophage endolysins fused to biodegradable nanobeads for controlling Mycobacteria

A thesis presented in partial fulfilment of the requirements for the degree of

Master of Natural Sciences

at Massey University, Albany,

New Zealand



MASSEY UNIVERSITY
TE KUNENGA KI PŪREHUROA
UNIVERSITY OF NEW ZEALAND

Courtney Grace Davies

2019

Abstract

10.4 million people are diagnosed with tuberculosis, worldwide, every year, according to the World Health Organisation. *Mycobacterium tuberculosis* is a Gram-positive bacterial pathogen that can easily be transmitted to health care professionals and people supplying aid in these nations. Fortunately, over the last 100 years, the bacteriophage has gained traction as a suitable therapeutic, antibiotic-alternative against bacterial pathogens, such as *M. tuberculosis*. Herein I describe my work utilising endolysins the lytic protein that bacteriophages usually employ to burst out of the cell, but instead using these proteins to lyse “from without”. In order to develop a proof-of-principle product, we used the expansive *M. smegmatis* bacteriophage collection and chose eight endolysin candidates for testing against *M. smegmatis*. These endolysins were bioinformatically analysed for active domains before being synthesised and inserted into an expression vector to produce fused biodegradable nanobeads made of polyhydroxyalkanoate. These nanobeads were tested for activity against *M. smegmatis*, a safe mycobacterium closely related to pathogenic tuberculosis. Four distinct tests were carried out to test the efficiency of these beads in causing cell death in different situations (45 minutes and 5 hours, across concentrations of 10mg/ml, 20mg/ml and 80mg/ml. Ultimately the nanobead fusions of endolysin Inca (lysin B) caused the most cell death at 80mg/ml after exposure to *M. smegmatis* for 5 hours in a standing culture, at 78.87% cell death \pm 5.21. When the nanobeads were applied to filter paper to mimic application to a hospital mask as a proof-of-concept approach before spraying with a bacterial aerosol, we saw that endolysin nanobead Jaws (lysin B) caused the most cell death with 75.54% \pm 3.15 at 80mg/ml. These results are promising and present a unique opportunity to take advantage of an existing natural mechanism to use as a prophylactic defense against pathogenic bacteria in hospital settings.

Acknowledgements

First and foremost, I wish to acknowledge the wisdom and support of my supervisor and Chief Phage Hunter, Dr. Heather Hendrickson, whom opened my eyes to the small and incredibly versatile world of the humble bacteriophage. Her intellectual challenges and ongoing support throughout this research have enabled me to grow and succeed in many ways.

Secondly, I would also like to acknowledge Dr. Eric Altermann, Kerri Reilly and the team at AgResearch, Palmerston North, for taking me under their wing and guiding me through the fascinating world of biodegradable nanobeads and their potential to save the world.

I would also like to acknowledge my parents, Johanne and James, for the hours of devotion listening to my trials and tribulations, encouraging me to keep going and accompanying me to the laboratory in the evenings when a zombie movie has made me second guess my research path.

Additionally, to my friends and colleagues who have been there through each practice talk, phage pun, mid-thesis crisis and procrastination lunch, I extend my sincere gratitude to you.

My amazing friend Piper was my inspiration for beginning this field of research to find an antibiotic alternative to support her as she dealt with her unfair share of life-threatening bacterial infections. I dedicate this thesis to her and my best friend Chiff, who was and will always be, my shining light, who started this journey by my side and ended it in my heart. Last but not least my late family members Aunty Trish and Taid who would always encourage me to succeed and whose memories I cherish as I go forward into the future.



Contents

List of figures	v
List of tables	vi
List of abbreviations	vii
1 Introduction	1
1.1 Bacterial infection of <i>Mycobacterium</i> species	1
1.1.1 Implications of untreated <i>Mycobacterium</i> in New Zealand	2
1.1.2 Diagnosis and treatment of tuberculosis	3
1.2 Antibiotic resistant tuberculosis	4
1.3 Transmission of tuberculosis	4
1.3.1 Infection of health-care workers	5
1.4 Bacteriophages	7
1.4.1 Bacteriophage life cycle	7
1.4.2 Bacterial resistance to bacteriophages	8
1.5 Gram-positive cell walls	13
1.6 Endolysins	14
1.6.1 D29 mycobacteriophage lysin B demonstrates cell lysis from without	16
1.6.2 Endolysin diversity	18
1.6.3 Advantages of endolysins	18
1.6.4 Complications associated with endolysins	19
1.7 <i>Mycobacterium smegmatis</i> mc ² 155 as a model organism	20
1.8 PhagesDB.org	21
1.9 Mycobacteriophage clusters	24
1.10 Biodegradable nanobeads	24
1.10.1 PHA biodegradability	25
1.10.2 PHA synthase	26
1.11 Aims	27
1.12 Summary for remainder of the thesis	29
2 Materials and Methods	30
2.1 Bacteriophage endolysin selection through bioinformatics	30
2.1.1 Online databases and tools; PhagesDB and NCBI BLASTp annotations	30
2.1.2 Clustal Omega	30
2.1.3 HHpred	31
2.1.4 Plasmid constructs	32
2.2 Media	33
2.2.1 Antibiotics, supplements, media,	33
2.2.2 Bacterial strains	33
2.2.3 <i>M. smegmatis</i> growth	33
2.2.4 Growing and maintaining bacteriophage	34

2.2.5	Transforming chemically-competent <i>E. coli</i> BL21	34
2.3	Nanobead production	34
2.3.1	Nile Red stain.....	36
2.3.2	Bead extraction	36
2.3.3	Ultrasonic Processor	36
2.3.4	Bead purification and storage	37
2.4	Testing cell death of <i>M. smegmatis</i>	37
2.4.1	Test one: detecting cell death through fluorescent microscopy	38
2.4.2	Test two: detecting cell death through a plate-reader assay	39
2.4.3	Test three: detecting difference in colony counts.....	40
2.4.4	Test four: detecting cell death using filter paper for a proof-of-concept applied approach 41	
2.4.5	Statistical analysis.....	42
3	Results and Discussion	43
3.1	PART ONE: Gene selection process and domain confirmation	43
3.1.1	Rationale behind choosing the final mycobacteriophage endolysin candidates	43
3.1.2	Checking for evidence of lysin function using NCBI BLASTp.....	48
	Bacteriophage selection candidates	48
3.1.3	48
3.1.4	Verifying lysin-like domains are present using HHpred	51
3.1.5	PhaC pET-14b plasmid construct.....	55
3.2	PART TWO: Expression and production of biodegradable lysin nanobeads	57
3.2.1	Establishing expression of PhaC in <i>E. coli</i> with a Nile Red stain	57
3.2.2	Purifying nanobeads.....	58
3.2.3	Dealing with contamination	59
3.2.4	Endolysin nanobead size differences	61
3.3	PART THREE: Testing antimicrobial activity against <i>M. smegmatis</i>	67
3.3.1	Test one: detecting cell death through fluorescent microscopy	67
3.3.2	Test two: detecting cell death through a plate-reader assay	73
3.3.3	Test three: detecting difference in colony counts.....	78
3.3.4	Test four: detecting cell death using hospital masks as a proof of concept applied approach 96	
3.4	Summary.....	103
3.5	Future directions	104
4	Conclusion.....	105
5	References	106

List of figures

Figure 1: Bacteriophage lytic cycle	8
Figure 2: Different types of cell wall structure	14
Figure 3: Crystalline structure of D29 lysin B	17
Figure 4: Phylogenetic tree of mycobacterium species	21
Figure 5: Mycobacteriophage diversity	23
Figure 6: Polyhydroxyalkanoate nanobead with endolysin proteins fused to surface	25
Figure 7: Production of PHA nanobeads with fused endolysins	35
Figure 8: Testing cell death induced by bead exposure by colony count	40
Figure 9: Lab-made spray system	42
Figure 10: Cladogram of a selection of lysin A mycobacteriophages (clusters labelled)	44
Figure 11: Cladogram of a selection of lysin B mycobacteriophages from each cluster (clusters labelled)	45
Figure 12: Bacteriophage endolysin geographic location	50
Figure 13: pET-14b endolysin fusion plasmid constructs	55
Figure 14: Nile Red stain to detect presence of lipid nanobeads	58
Figure 15: Purified nanobeads indicated by the white band in the glycerol gradient	58
Figure 16: Contamination across increasing dilutions	60
Figure 17: Gram stained contamination indicated Gram-negative bacterium present	60
Figure 18: Endolysin nanobead size differences	62
Figure 19: Scanning Electron Microscopy of three lysin nanobeads	63
Figure 20: Phase contrast 100X microscopy of unstained lysin nanobeads	64
Figure 21: Fluorescent microscopy of <i>M. smegmatis</i> exposed to nanobeads (1)	69
Figure 22: Fluorescent microscopy of <i>M. smegmatis</i> exposed to nanobeads (2)	70
Figure 23: Fluorescent microscopy of <i>M. smegmatis</i> exposed to nanobeads (3)	71
Figure 24: Plate reader graphs of <i>M. smegmatis</i> cell states	73
Figure 25: Endolysin nanobead controls in 96-well plate, no bacteria	74
Figure 26: <i>M. smegmatis</i> after exposure to 10mg/ml endolysin nanobeads in the 96-well plate reader, shaking	75
Figure 27: <i>M. smegmatis</i> cell death after 45 minutes exposure to 10mg/ml, 20mg/ml and 80mg/ml nanobead concentrations in a standing culture of at room temperature	80
Figure 28: Giles is the most effective endolysin nanobead at 45 minutes	82
Figure 29: <i>M. smegmatis</i> cell death after 5 hours exposure to 10mg/ml, 20mg/ml and 80mg/ml nanobead concentrations in standing culture at room temperature	84
Figure 30: Inca is the most effective endolysin nanobead at 5 hours	86
Figure 31: All endolysin combinations at each trial point	88
Figure 32: Comparison of cell death with <i>M. smegmatis</i> WT and <i>M. smegmatis</i> colonies cultured from surviving colonies	91
Figure 33: Surviving <i>M. smegmatis</i> colonies cultured and infected by Inca bacteriophage serial dilution 3µl spot test	94
Figure 34: 10µl of nanobeads on filter paper compared to a hospital mask	96
Figure 35: <i>M. smegmatis</i> colonies stamped after exposure to nanobeads on filter paper	97
Figure 36: Distribution of colony counts	100

List of tables

Table 1: The lysin A and lysin B genes chosen for this project	32
Table 2: Antibiotic concentrations	33
Table 3: Bacterial strains used in this work.....	33
Table 4: NCBI BLASTp output	47
Table 5: Domain analysis of Lysin-like proteins by HHpred.....	52
Table 6: Amount of nanobeads harvested	58
Table 7: Endolysin nanobead mean bead sizes	61
Table 8: Live/dead stain of <i>M. smegmatis</i> after exposure to nanobeads	68
Table 9: <i>M. smegmatis</i> average cell death and significance after 45 minutes of exposure to 10mg/ml, 20mg/ml and 80mg/ml nanobead concentrations	81
Table 10: <i>M. smegmatis</i> average cell death and significance after 5 hours of exposure to 10mg/ml, 20mg/ml and 80mg/ml nanobead concentrations	85
Table 11: Comparison of <i>M. smegmatis</i> colony morphologies between WT and endolysin nanobead-surviving colonies.....	90
Table 12: Raw colony counts of nanobead stamping experiment	98
Table 13: Average cell death of <i>M. smegmatis</i> after being sprayed on nanobead-coated filter paper “masks”	99

List of abbreviations

AMP	Ampicillin
AMR	antimicrobial resistant
ATCC	American Type Culture Collection
BLAST	Basic Local Alignment Search Tool
BLASTn	Basic Local Alignment Search Tool (nucleotides)
BLASTp	Basic Local Alignment Search Tool (proteins)
CB	Carbenicillin disodium salt
CHX	Cycloheximide
CM	Chloramphenicol
CRISPR	Clustered Regularly Interspaced Palindromic Repeats
<i>E. coli</i>	<i>Escherichia coli</i>
FASTA	Fast Alignment Search Tool A
IPTG	isopropyl β -D-1-thiogalactopyranoside
HGT	horizontal gene transfer
lysA	Lysin A
lysB	Lysin B
<i>M. smegmatis</i>	<i>Mycobacterium smegmatis</i>

<i>M. tuberculosis</i>	<i>Mycobacterium tuberculosis</i>
MAC	maximum accuracy algorithm
MDR	multidrug-resistant
MPI	Max Planck Institute
MSA	multiple sequence alignment
OD	optical density
P011	passage 0 from frozen stock
P1FF	passage 1 from frozen stock
P2FF	passage 2 from frozen
PBS	phosphate buffer solution
PHA	polyhydroxyalkanoate
PhagesDB	www.phagesdb.org
SIE	superinfection exclusion systems
WT	wild type

1 Introduction

For centuries bacterial pathogens have been an issue for human health by compromising physical health, economic stability and environmental prosperity. We are entering a new era of antibiotic consciousness, so it is important to be more aware of the current treatments to these pathogens and the sustainability of their effectiveness. The following introduction will establish the basis of mycobacterial impact as well as introducing the bacteriophage as a therapeutic alternative to antibiotics. We will then introduce this project in more depth, focussing on attaching mycobacteriophage endolysins to biodegradable nanobeads to test against *Mycobacterium smegmatis*.

1.1 Bacterial infection of *Mycobacterium* species

As at 2017, the *Mycobacterium* genus comprises of over 150 recognised species, with many environmental and pathogenic to humans and animals alike (King et al., 2017). This genus includes some well-known pathogens such as *Mycobacterium tuberculosis*, the causative bacterial pathogen responsible for infecting one third of the human population with tuberculosis (Sreevatsan et al., 1997). The World Health Organisation 2018 Global Tuberculosis report states that *M. tuberculosis* currently infects 1.7 billion people, causing 1.3 million deaths in 2017 and further predicts that by 2050 there will be 10,000,000 tuberculosis deaths in comparison to 8,200,000 deaths from cancer (WHO, 2018). When *M. tuberculosis* bacteria become active in the bloodstream, the human immune system cannot stop the bacteria from multiplying and this is what causes the disease (CDC, 2018). Lillebaek and colleagues state that out of the infected patients, only 10% of infected individuals appear to develop active disease which they have shown to activate 33 years past the first infection with the remaining 90% of cases remaining latent (*M. tuberculosis* bacteria is dormant and inactive with the possibility to be reactivated) (Lillebaek et al.,

2002; Zumla, Raviglione, Hafner, & Fordham von Reyn, 2013). Latently infected individuals can still develop the disease, but it cannot be spread in latent form.

A 2016 report published by O'Neill estimates that by 2050, 10 million lives per year and a cumulative 100 trillion USD of economic output are at risk from the rise of drug resistant infections if solutions are not found now (O'Neill, 2016).

1.1.1 Implications of untreated *Mycobacterium* in New Zealand

The 2010 Ministry of Health report states that tuberculosis notification rates in New Zealand have been around 10 per 100,000 (0.01%) , decreasing to 0.007% in recent years (MoH, 2010). New Zealand has higher rates of *M. tuberculosis* than other developed countries (including 0.004% in the United States, 0.005% in Canada and 0.006% in Australia) and this may be attributed to immigration from countries with high incidence of *M. tuberculosis* and socioeconomic deprivation, with over two thirds of all cases in New Zealand from individuals born in a foreign country (MoH, 2010). More specifically, the highest rates of tuberculosis are seen in individuals occupying urban areas such as Auckland and South Auckland, along with individuals who are not of “European” descent (most notably Pacifica people and those who identify as “Other”) (MoH, 2010). However, from these reports of tuberculosis infection, New Zealand has comparatively low rates of resistance to antimicrobials used for treatment of tuberculosis (MoH, 2017).

Other prominent members of the *Mycobacterium* genus include *Mycobacterium smegmatis* (the model organism for this research) and *Mycobacterium bovis*, the causative agent for zoonotic tuberculosis (Cosivi et al., 1998). The dairy industry is New Zealand’s largest export market worth in excess of \$13.7 billion NZD and uncontrolled mycobacterial outbreaks have the potential to wreak havoc economically (Warren & Allen, 2017). Past studies have identified *M. bovis* present in swine and cattle populations

with the effect emphasised by the boom in possum population, however the strict regulations imposed by the New Zealand bovine tuberculosis control programme have reduced tuberculosis rates from 11% in mature cattle in 1905 to less than 0.003% in cattle in 2012/2013 (Livingstone, Hancox, Nugent, & de Lisle, 2015).

1.1.2 Diagnosis and treatment of tuberculosis

Tuberculosis is one of the most ancient diseases currently known to researchers, dating back 17,000 years (Sandhu, 2011). The unique intracellular location of the pathogen shields it from antibodies and airborne nature of *M. tuberculosis* can easily be spread from one infected host to the next (Kaufmann, 2001). The ease of spread and difficulty of diagnosis and treatment correlates with statistics suggesting 95% of developing nations are currently infected with tuberculosis, contributing to one third of the world's current population latently infected (Oren, Bell, Garcia, Perez-Velez, & Gerald, 2017).

Screening methods for the detection of tuberculosis include a field chest x-ray and culture along with the tuberculin skin test (TST) and the interferon- γ release assays (IGRA) which involve a blood test although it cannot determine the difference between latent and disease cases of tuberculosis (Linaz, Wong, Freedberg, & Horsburgh, 2011; WHO, 2018).

Some of the major difficulties in managing tuberculosis include the rigorous treatment, some toxicity in drugs used as well as the non-compliance of some patients, leading to complications in treatment success. First-line anti-tuberculosis drugs include isoniazid, rifampicin, pyrazinamide, ethambutol and streptomycin and fixed-dose combinations of these drugs are used to prevent drug resistance that could occur with separate drug treatments (WHO, 2010). Treatment of multi-drug resistant tuberculosis is more intensive with over 20 months of treatment resulting in a cost of \$134,000 USD per case of MDR-TB and \$430,000 per XDR-TB (Suzanne et al., 2014).

1.2 Antibiotic resistant tuberculosis

Not only do the effects of tuberculosis in the present-day concern human health, agricultural development and economic prosperity, they are also shaping the future of the world. In 2017, the World Health Organisation estimated that 558,000 people developed tuberculosis that was resistant to the most effective frontline drug rifampicin, a further 82% of these reported cases were multi-drug resistant indicating they do not respond to at least rifampicin and isoniazid which are the two most powerful anti-tuberculosis drugs (WHO, 2018). Communities with those infected with HIV/AIDS are at further risk with the 2018 WHO report stating 464,633 tuberculosis cases among HIV-positive people were reported. It is therefore important for future treatments to take into consideration the current increasing rates of MDR tuberculosis, as well as the relationship to other diseases such as HIV.

1.3 Transmission of tuberculosis

Tuberculosis is an airborne pathogen, spread from person to person through the air through infected individuals coughing, sneezing or spitting (CDC, 2018; WHO, 2018). Living in a slum increases the risk of tuberculosis transmission due to over-crowding, air-pollution and under-nutrition (WHO, 2018). Despite increasing access to treatment, WHO has estimated that over 3 million incidents of tuberculosis cases go undiagnosed and untreated every year, which perpetrates the continuous transmission (von Delft et al., 2015). Even with a diagnosis, access to medication and treatment is often delayed, sometimes with a 2-month interval between symptom onset and the start of effective treatment (Salaniponi et al., 2000; von Delft et al., 2015).

1.3.1 Infection of health-care workers

In 2017, 9,299 health-care workers from 65 countries were reported with tuberculosis, with the highest rate in Mozambique (WHO, 2018). The idea of increasing treatment coverage of tuberculosis to over 90% is one of the top 10 indicators for monitoring implementation of the *End TB Strategy* by WHO. The rationale for this is that high-quality tuberculosis care is essential to prevent suffering and death from the disease (WHO, 2018). This report also states that current health interventions for TB prevention are the mitigation of tuberculosis transmission opportunities through prevention and control of infection. The most recent report addressing the risk for health care associated transmission of tuberculosis is the 2005 CDC report, stating that the transmission of tuberculosis to health care workers has been linked to close contact with tuberculosis-infected patients during aerosol-generating or aerosol-producing procedures (CDC, 2005). An updated administrative refocus on “Finding (patient) cases Actively, Separate temporarily and Treat effectively (FAST)” has been advocated despite the difficulty of applying all of these measures in low resource, high tuberculosis settings where most occupational (health-care workers are effected) tuberculosis cases occur (Ehrlich, 2018). This has resulted in health care workers calling for advocacy and pressure from the government to take the need for preventative transmission seriously (Ehrlich, 2018). Because these health care workers are not always adequately protected, we want to take advantage of the antimicrobial lysis properties of bacteriophage and use these as a prophylactic prevention method as a barrier aid to minimise the risk of aerosol-generated tuberculosis pathogens on objects where the bacteria can interact with the lytic mechanism, including hospital masks and bench surfaces. This research focusses on the use of lytic enzymes from bacteriophages fused to polyhydroxyalkanoate nanobeads as a

proposed prophylactic treatment to individuals at risk of infection including health care workers in the field, discussed further at the end of this section.

The infection does not end with the health-care worker alone. Those infected can further transmit tuberculosis to their families and those around them, which is why it is important to protect and target this mycobacterial pathogen at the front line. An example from a study by Sterling and colleagues, reported the first documented tuberculosis transmission from a cadaver with partially treated tuberculosis to an embalmer who had previously been tested to not have tuberculosis. The study concluded that aerolisation from the airway from the airway of the cadaver to the embalmer was the mode of tuberculosis transmission and this aerolisation remains a risk to our health care workers today (Daniel, 2001; Sterling et al., 2000).

It is important to realise that the effects of tuberculosis infections of healthcare workers extend to their family beyond physical implications, including risk of transmission to loved ones, financial hardship, community stigma and career limitations, with von Delft and colleagues stating one physician called her husband weeping “I could die”, as she threw up blood in her basin sink a few weeks before being diagnosed with extreme drug-resistant tuberculosis (von Delft et al., 2015). Daniel and colleagues state that it is difficult to generalise the magnitude of occupational tuberculosis risk for non-hospital workers, however they acknowledge the idea that ventilation, recognition of tuberculosis cases and isolation procedures may be less than ideal in non-hospital settings (Daniel, 2001). This correlates with the statistics that state 95% of tuberculosis cases occur in developing nations where one third of the world’s population is latently infected (Daniel, 2001; Oren et al., 2017). It is therefore crucial to have correct protection measures and alternatives to antibiotic treatment in place in order to prevent the unnecessary spread of tuberculosis through the people trying to stop it on the frontline.

1.4 Bacteriophages

Bacteriophages were first noticed through “glassy and transparent” zones of dead bacteria by English physician, Frederick Twort, in 1915 (Keen, 2015). They are viruses that only infect bacteria and occupy a profound role in environmental and biological processes with over 10^{31} phage particles – the most abundant living entity on Earth (Comeau et al., 2008; Keen, 2015). Bacteriophages have a large environmental impact and can infect between 15% - 40% of the ocean’s bacterial population each day which can thereby influence dissolved carbon ratios through to phytoplankton productivity (Danovaro et al., 2011). However, it is their unique host specificity which gives them an advantage over more broad range antibiotics in healthcare, with lytic bacteriophages (that kill bacteria as opposed to lysogenic bacteriophage that integrate into the host bacterium’s DNA) having considerable therapeutic potential (d’Herelle, 1931; Keen, 2015). There have been numerous studies that use bacteriophage as antimicrobials in health care, agriculture and food production that will be discussed in more depth throughout this section.

1.4.1 Bacteriophage life cycle

Bacteriophages are viral parasites that bind to the cell surface of a specific bacteria, inject in their genetic material and take advantage of the hosts cellular machinery needed to replicate, prior to bursting out of the cell through a lysis event, causing bacterial death shown in Fig. 1 (Kingwell, 2015). Some bacteriophage carry out a lysogenic life cycle, wherein they inject their DNA into the bacterial chromosome, however these types of bacteriophage are less desirable from an antimicrobial phage therapy option, as they can spread virulence factors or antimicrobial resistance throughout the bacterial host (Higgins et al., 2005; Kingwell, 2015).

Figure 1: Bacteriophage lytic cycle.

Bacteriophage bind to specific receptors on the bacterial cell wall and inject their DNA. The lytic cycle demonstrates how bacteriophage replicate within the cell before bursting through the cell wall, rupturing the bacteria and releasing new viruses. Adapted from (Kingwell, 2015).

1.4.1.1 Lysis from without

“Lysis from without” or exogenous lysis refers to the lysis event as a result of extracellularly applied lysis agents (such as endolysins) (Abedon, 2011). An earlier definition defines the external lysis phenomenon as “abortive infection accompanied by prompt lysis of a cell, typically following excessive multiple infection” (Schuster, 1962). Nevertheless, throughout this thesis the simplified idea of lysis from without will refer to the exposure of bacterial cells to endolysins fused to biodegradable nanobeads and the subsequent effect these will have.

1.4.2 Bacterial resistance to bacteriophages

Bacteriophages are strong drivers of bacterial evolution as bacteria are constantly evolving to evade their viral predators (Chibani-Chennoufi, Bruttin, Dillmann, & Brüssow, 2004). Because we are interested in developing methods of infecting and killing the bacteria that do not have a large suite of resistance mechanisms to counteract the lytic

process, it is useful to understand the processes behind bacterial lysis and the resistance mechanisms at each existing step.

Work by Hofnung and colleagues suggest bacterial resistance can involve mutations that result in a change in structure, or even the entire loss, of the bacteriophage binding site through deletion mutations (Hofnung, Jezierska, & Braun-Breton, 1976). Although the Hofnung study focussed on *E. coli* K12 λ bacteriophage, we will explore these mechanisms in relation to mycobacteria. Because of these conclusions, we are looking into a way of avoiding these resistance strategies highlighted below, using the framework of the lytic infection cycle (Fig. 1) in order to lyse the bacterial cell prior to resistance.

Throughout evolution, bacteria have evolved resistance methods to counteract the impact of the bacteriophages that target various steps within the bacteriophage life cycle, specifically blocking adsorption, preventing DNA injection, rejecting the incoming DNA and abortive infection systems (Chibani-Chennoufi et al., 2004; Sturino & Klaenhammer, 2006). Because this work focusses on the possibility of using mycobacteriophage-derived proteins for mycobacterium cell lysis, we will also describe what is known of mycobacteriophage-specific resistance in each instance, although often their contributions to mycobacteriophage host preferences are poorly understood (Jacobs-Sera et al., 2012).

1.4.2.1 Bacteriophage attachment prevention

Bacterial strains have evolved to prevent bacteriophage adsorption to cell receptors through three key strategies; receptor blocking (using bacteria-specific proteins), extracellular matrix production and competitive inhibitor production (Labrie, Samson, & Moineau, 2010). Bacteriophages initiate infection by attaching and binding to specific receptors upon the surface of their host bacteria, before inserting their DNA (J. Chen et

al., 2009). Bacteria can also produce extracellular polymers (hydrolases and lyases) that can protect the bacteria from its environment as well as providing a physical barrier between the bacteriophage and their receptors (Labrie et al., 2010). Although some bacteriophage are able to recognise these polymers with the potential to even degrade them, the means of bacteriophage attachment to the cell wall are limited, especially in regards to mycobacterial infections (McNerney & Traoré, 2005; Stummeyer et al., 2006). However, there have been multiple studies looking into the relationship between specific mycobacteriophage D29 and cell wall receptors. Hatfull suggests that the loss of cell wall receptor in mycobacteria does not prevent D29 from attaching, thereby not conferring resistance, however an earlier study with colleague Barsom showed that an *M. smegmatis* mutation with an insertion upstream of the *mpr* gene, when the *mpr* gene was overexpressed, resistance to D29 occurred (Barsom & Hatfull, 1996; Hatfull, 2014; McNerney & Traoré, 2005). The resistance occurs by inhibiting the transport of bacteriophage DNA across the cell wall (McNerney & Traoré, 2005).

1.4.2.2 Bacteriophage entry prohibition

Superinfection exclusion systems (SIE) are proteins that block bacteriophage entry into potential bacterial host cells and are predicted to be anchored or strongly associated with membrane components (Labrie et al., 2010). In other words, SIE occurs when infection by an existing bacteriophage prevents and secondary infection by that bacteriophage or another closely related virus. Hopkins and Ptashne describe a potential mechanism to superinfection exclusion through a prophage, where bacterial “escape” is infrequent (Hopkins & Ptashne, 1971). The 1971 study further explains that at least three mutations would be required in order to confer the virulent phenotype (Hopkins & Ptashne, 1971; Jacobs-Sera et al., 2012). Jacobs-Sera and colleagues state that SIE in mycobacteria are still poorly understood.

1.4.2.3 Bacteriophage nucleic acid modifications

Bacteria have modification systems that cleave bacteriophage genomic DNA (site specific sequences if they do not carry methylation marks specific to the system) and these systems can be classified into at least four groups, type I – IV (Labrie et al., 2010). When unmethylated bacteriophage DNA enters into a bacterial cell which carries out one of these nucleic acid modification systems, it is immediately recognised and cleaved by a specific restriction enzyme to be degraded or at the least methylated to ensure the bacteriophage lytic cycle is not initiated (Kruger & Bickle, 1983). Bacteriophage have developed defense to this system by modifying their genomes to avoid DNA cleavage, by incorporating unusual bases in their systems, such as *Bacillus subtilis* bacteriophages that replaces thymine with 5-hydroxymethyluracil (Hopkins & Ptashne, 1971; Jacobs-Sera et al., 2012). Bacteriophage can also defend themselves by employing “palindromic avoidance” through avoiding palindromic repeats in their genetic sequences, as type II bacterial restriction endonucleases can often recognise these palindromic repeats (Rocha, Danchin, & Viari, 2001; Stern & Sorek, 2011). In the case of mycobacterium, there have been five restriction modification systems identified in five closely related mycobacterium (Roberts & Macelis, 2001; Rocha et al., 2001). Although there are few examples of mycobacterium employing these systems to evade bacteriophage infection nevertheless this is a prime example of the ongoing coevolution between bacteria and bacteriophages.

1.4.2.4 CRISPR Cas systems

Clustered regularly interspaced palindromic repeats (CRISPR) and the associated Cas genes are another effective mechanism becoming more prominent in evolution throughout the bacterial kingdom for reducing the infection by bacteriophages (Godde & Bickerton, 2006). CRISPR is an immunity system that targets foreign nucleic acids

including those of bacteriophage genomes and plasmids by taking up genetic material from invasive elements such as bacteriophage and building up an inheritable DNA-encoded immunity over time (Marraffini & Sontheimer, 2008). The CRISPR systems work by having loci which typically consist of several non-contiguous direct repeats separated by stretches of variable sequences called spacers that correspond to segments of captured bacteriophage sequences, often adjacent to associated Cas genes (Horvath & Barrangou, 2010). In turn, these Cas genes encode a large and heterogeneous family of proteins carrying the functional domains that are typical of nucleases, helicases, polymerases and polynucleotide-binding proteins which allow the bacterial cell to cleave the recognised bacteriophage DNA upon initial entry into the bacterial cell (Haft, Selengut, Mongodin, & Nelson, 2005; Horvath & Barrangou, 2010).

The constant exposure to exogenous DNA as a result of transduction, conjugation, and transformation have forced over 90% of bacterial species to establish an array of defense mechanisms (Horvath & Barrangou, 2010). Although there is limited knowledge around *M. smegmatis* mc²155, He and colleagues state that there CRISPR Cas systems active against mycobacteriophages can be found throughout 14 mycobacteria (He, Fan, & Xie, 2012; Jacobs-Sera et al., 2012; Liu et al., 2014; Samaddar et al., 2015). Choudhary and colleagues also note that specifically there are no type II CRISPR Cas systems in mycobacterium, not ruling out the presence of other CRISPR type systems (Choudhary, Thakur, Pareek, & Agarwal, 2015).

Some bacteriophages can defend against CRISPR Cas systems by employing anti-CRISPR proteins, however this does not always provide immunity against the CRISPR Cas system and the success depends on how many bacteriophages are present for infection. In bacteriophages that do have this defense mechanism, the first bacteriophage to infect a CRISPR-encoded bacterium will most likely be destroyed by the CRISPR Cas

system before it is able to make enough anti-CRISPR proteins, nevertheless the anti-CRISPR proteins that it does make will still persist in the bacterial cell that will help to suppress its defense systems. Therefore, the next bacteriophages that come along will help to contribute to the eventual overturn of CRISPR with an influx of anti-CRISPR proteins that will take down the immune system and render the bacterial cell viable for infection. It can be thought of as a sacrificial cooperative effect, with the bacteriophage that are the slowest to infect having the greatest chance of a full lytic cycle.

We are interested in developing methods to infect bacteria where they do not have resistance mechanisms to counteract the bacteriophage. In the last step of the lytic cycle shown in Fig. 1, bacteriophage use a programmed timed response from the holin protein enabling the access of endolytic enzymes to make contact and cleave the peptidoglycan cell wall. By taking advantage of the endolysin proteins that operate in the final stage of the lytic cycle whereby bacteria can no longer establish resistance mechanisms, we can initiate lysis “from without” at the very beginning enabling us to overcome the resistance mechanisms aforementioned.

1.5 Gram-positive cell walls

Gram-positive bacterial species differentiate from their Gram-negative counterparts in that they lack an outer membrane yet compensate with a thicker cell wall, in comparison to Gram-negative bacteria which have an outer membrane present as shown in Fig. 2 below. The cell walls of mycobacteria (a Gram-positive organism) are composed of thin layers of peptidoglycan and arabinogalactan with a thick wall of mycolic acids which is unique to mycobacteria compared to other Gram-positive bacteria (Fig. 2) (Brennan; Lisa Brown, Julie M. Wolf, Rafael Prados-Rosales, & Arturo Casadevall, 2015). Therefore, it is important when identifying protein candidates, to select candidates that are capable of

cleaving through both the peptidoglycan component of the cell wall, in addition to the thick wall of mycolic acids present.

Figure 2: Different types of cell wall structure

A) Gram-negative cell wall with distinctive outer membrane, B) Gram-positive cell wall with lack of outer membrane and no mycolic acid layer, C) Mycobacterial cell wall displaying thick mycolic acid layer in addition to the peptidoglycan cell wall. The most significant difference between the Gram-negative and Gram-positive cell walls is that the Gram-negative cell wall has an outer membrane meaning bacteriophage attachment differs from Gram-positive bacteriophages. Adapted from (L. Brown, J. M. Wolf, R. Prados-Rosales, & A. Casadevall, 2015).

While mycobacterium species are Gram-positive bacteria that lack a traditional outer membrane and contain a relatively thick layer of PG, they also have a unique outer membrane structure that is analogous to the outer membrane of Gram-negative species (K. M. Payne, 2006). The cross-linked design of the bacterial cell wall is responsible for keeping the cell at a high internal pressure of between 15-25 atmospheres and therefore any damage or disruption to this cell wall can result in extrusion of the cell membrane to the outer environment and hypotonic lysis (Fischetti, 2010a). In natural systems, bacteriophage lyse from within to release bacteriophage progeny and as a result require a long tail protein to allow access to the cell membrane and consequently the cytoplasm.

1.6 Endolysins

Endolysins are enzymes produced by bacteriophage with the purpose of attacking one of the four major bonds in the peptidoglycan component, digesting the bacterial cell wall to

initiate bacteriophage progeny release (Fischetti, 2010a). In natural systems, bacteriophages do not have signal sequences (so they are not translocated through the cytoplasmic membrane), instead this function is controlled by another protein called holin (I. N. Wang, Smith, & Young, 2000). The endolysin accumulates into a fully-folded, active state in the cytoplasm, waiting for the small membrane holin protein to allow the endolysin access through the membrane due to a timing process “programmed” in to the holin itself (I. N. Wang et al., 2000). Once the endolysin makes contact with the cell wall, this lysis results in destruction of the cell and the bacterium’s ability to survive. In the past, studies have focussed on using the whole bacteriophage to exploit the bacterial cell, however only recent endeavours have focussed primarily on lytic enzymes in isolation of the whole virus (Fischetti, 2010a; Loeffler, Djurkovic, & Fischetti, 2003; Nelson, Loomis, & Fischetti, 2001; Schuch, Nelson, & Fischetti, 2002). These studies, specifically using mycobacteriophage D29, will be discussed further throughout this thesis.

Because bacteria have evolved resistance over time to bacteriophages, in the forms of attachment prevention, entry prohibition, nucleic acid modifications and CRISPR Cas, it is important to identify methods of cell lysis to lyse the cell before these mechanisms can initiate. Phage endolysins are both enzymatically and architecturally diverse with a large variation in both length and size. There are 24 enzymatic catalytic domains and 13 cell binding domains in bacteriophage endolysins (Oliveira et al., 2013). Lytic enzymes such as endolysins are suitable lysing agents as they are able to make direct contact with the cell wall carbohydrates and peptidoglycan when they are applied externally “from without”, without requiring the programmed response of the holin protein (Fischetti, 2010a).

In the case of Gram-positive *Streptococcus pneumoniae* bacteria, 2,000µg of the Cpl-1 pneumococcal bacteriophage lysin was able to kill *S. pneumoniae* within 15 minutes, reducing it from a median of log₁₀ 4.70cfu/ml to undetectable levels (Loeffler et al., 2003). In natural systems, once the holin protein has made the hole in the cell membrane, it takes only seconds for the endolysin to lyse through, releasing the bacteriophage particles into the environment (Gründling, Manson, & Young, 2001; I.-N. Wang, 2006).

Gram-positive cell endolysins exhibit a two domain structure with the N-terminal domain retaining peptidoglycan-hydrolysing activity to cleave one of the four major bonds in the peptidoglycan (highly conserved domain) whilst the C-terminal cell binding domain (connected via a short linker) binds to a substrate in the host cell wall (which is usually a carbohydrate but can vary) (Fischetti, 2008; Schmelcher, Donovan, & Loessner, 2012). Although the lytic domain of the endolysin that allows it to cleave through the peptidoglycan cell wall can be active on a variety of different bacteria, endolysins can still be extremely specific, often down to a specific serovar of host species through the specificity of the cell wall binding domain components.

1.6.1 D29 mycobacteriophage lysin B demonstrates cell lysis from without

Previous studies have shown that mycobacteriophage D29, crystalline structure shown in Fig. 3 below, has the capability to lyse *M. smegmatis* exogenously through an interaction between catalytic and cell wall binding domains (Pohane, Patidar, & Jain, 2015). Work by Payne in 2006, shows a decrease in cell accumulation by adding D29 lysin to a fresh culture of *Mycobacterium smegmatis* which resulted in some growth inhibition through biofilm degradation (K. M. Payne, 2006). The external lipid-rich cell wall structure of *M. smegmatis* is more likely to contain substrates for lysis through the lysin B protein, which is why there is more evidence supporting lysin B over lysin A (Ojha, Trivelli, Guerardel,

Kremer, & Hatfull, 2010). Through extensive research into D29 lysin B, the crystalline structure has suggested close similarity to other α/β hydrolase cutinases including esterases and lipases.

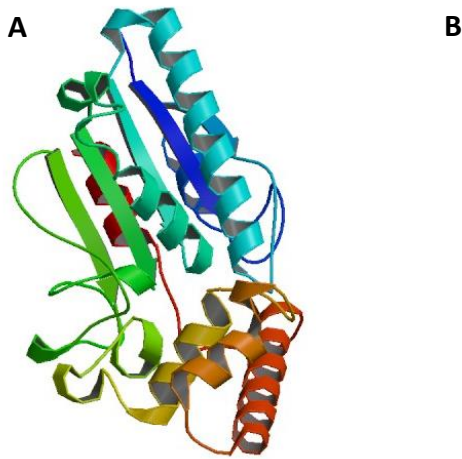


Figure 3: Crystalline structure of D29 lysin B

A) The biological assembly of the secondary structure of the D29 lysin protein. B) A magnified view at the catalytic triad of Ser82, His240 and Asp166 that occupy a similar position to other members of the α/β hydrolase family (K. Payne, Sun, Sacchettini, & Hatfull, 2009).

For bacterial cells to evade exogenous lysis “from without”, there would need to be a series of mutations in the mycolic acids and peptidoglycan components of the cell wall to prevent the lytic cleavage of these cell wall domains by the endolysins. This would require a significant genetic re-structuring of the cell wall, potentially compromising other important bacterial mechanisms, making this resistance opportunity extremely unlikely. This is one of the advantages for utilising an external lytic antimicrobial. The current differences in cell wall composition between Gram-negative and Gram-positive species already presents a boundary for increased host-range for bacteriophage, with most bacteriophage only being able to infect a narrow host range.

This D29 lysin B protein sequence is available on the publicly accessible PhagesDB.org and will be used as the positive control throughout this research.

1.6.2 Endolysin diversity

There is incredible diversity within mycobacteriophage endolysins, with enormous variation and up to a two-fold difference in size. More specifically, around 90% of endolysins have three conserved domains unlike other bacteriophage endolysins that only have two domains (K. M. Payne & Hatfull, 2012). These domains include; C-terminal domain which functionally corresponds to the C-terminal cell wall binding domain, allowing the endolysin to carry out peptidoglycan hydrolase (cleaving the peptidoglycan bonds in the cell wall), a centrally located amidase, muramidase or transglycosylase, and the N-terminal whose function is not as well understood but appears to encode a series of peptidases (K. M. Payne & Hatfull, 2012). Payne and Hatfull also explain that there are over 120 possible combinations of endolysins with six possible types of N-terminal domains, five types of amidase/glycosidase domains and a further four putative C-terminal cell wall binding motifs. This extraordinary diversity results in cell wall specificity when binding (K. M. Payne & Hatfull, 2012).

1.6.3 Advantages of endolysins

Using endolysins to lyse exogenously bypasses the possibility of initiating resistance mechanisms from the bacterial cell. As aforementioned, the bacterial host cell has a number of ways to defend itself against the infection of foreign matter. By using an exogenous application of endolysins independent of the bacteriophage lytic cycle, we are able to bypass this system and attack the peptidoglycan cell wall on the bacterial cell in order to signal lysis. In natural systems endolysins interact with the smaller holin molecule, however the endolysins themselves are the molecules that are the direct cause of lysis which requires fewer programmed pathways when using endolysins exogenously. Another advantage of Gram-positive-specific endolysins is that the exogenous nature of the cell wall enables the endolysins to be able to make direct contact with the

carbohydrates and peptidoglycan components as a potential proof-of-concept antimicrobial against pathogenic mycobacteria (Fischetti, 2010b). Because of the specificity required to lyse the cell wall components, endolysins provide no threat to internal microflora nor eukaryote cells if applied *in vivo*. Endolysins are fast acting, with studies suggesting they can infect and kill Gram-positive bacteria after seconds of contact which is further evidence towards the applied practicality of this research project (Loeffler, Nelson, & Fischetti, 2001; Nelson et al., 2001).

Lysins have also been demonstrated to be safe to use for humans and other eukaryotes as the murein hydrolases that are active domains of lysins, target the peptidoglycan cell wall that is only present in bacteria (Sharma, Vipra, & Channabasappa, 2018). A 2012 study from George and colleagues demonstrated that lysin P128 was completely inactive on eukaryotic cells, with no toxicity reported on cell lines Vero and HEp2 at the highest concentrations of 2.5mg/ml (George et al., 2012). Another Phase I clinical trial from Jun and colleagues in 2017 using lysin Sal-200 did not show any serious adverse effects on eukaryotic cells when tested using concentrations of 10mg/kg on healthy human male volunteers (Jun et al., 2017). Because the ultimate goal for this project is to develop a prophylactic tool to prevent mycobacteriophage infection, it is important to know the effects of lysins on human health.

1.6.4 Complications associated with endolysins

As previously mentioned, the endolysin requires the pre-programmed timing of the holin in order to initiate cell lysis through creating a hole in the cell membrane in natural systems. This can be a challenge when the endolysin is required to act as the sole lysing agent without the holin present as the lack of signal sequences prohibit the endolysin from its lysis ability. However, this can work as an advantage when applied externally, relying on environmental pressure to permeate the cell membrane after cell wall damage. A major

disadvantage compared to whole bacteriophage therapy, is the absence of self-replication by the endolysin proteins, unlike bacteriophage that self-replicate within the host cell (O'Flaherty, Ross, & Coffey, 2009). Another complication is the resistance mechanisms that the bacterial cell has evolved to counteract the bacteriophages lytic infections. There is an opportunity for bacteria to develop resistance to this exogenous lysis agent; however, this would require an almost complete reformation of the peptidoglycan and mycolic acid components of the cell wall which is improbable at this stage.

1.7 *Mycobacterium smegmatis* mc²155 as a model organism

Unlike most pathogenic bacteria that are slow-growing and harmful, *M. smegmatis* is fast-growing and non-pathogenic as well as being closely related to pathogenic bacteria *M. tuberculosis* and *M. bovis* as illustrated below in Fig. 4 (Snapper, Melton, Mustafa, Kieser, & Jr, 1990; Vishnoi et al., 2010).

Contrary to the cell wall structure of most Gram-positive bacteria, *M. smegmatis* has an additional lipid layer, similar to *M. tuberculosis*, observed in Fig. 2 (Jayawardana et al., 2015). In addition, there is a large, publicly accessible database where over 1,600 *M. smegmatis* bacteriophage genome sequences are stored, detailed below (Russell & Hatfull, 2017). This database enables the access of lysin candidates from bacteriophage discovered throughout the world.

M. smegmatis also has evidence of mycobacteriophage D29 having lysed the cell exogenously resulting in observable cell death. Because of these qualities, *M. smegmatis* was selected as the model organism for this project.

Figure 4: Phylogenetic tree of mycobacterium species

Based on 16S rRNA, this phylogenetic tree indicates that *M. smegmatis* is the most closely-related yet non-pathogenic bacterial species to *M. tuberculosis* which makes it a suitable bacterium to use for this project (Vishnoi, Roy, Prasad, & Bhattacharya, 2010).

1.8 PhagesDB.org

Phagesdb.org (PhagesDB) is a comprehensive and interactive Actinobacteriophage website that provides open-access information related to the discovery, characterisation, and genomics of bacteriophage that infect Actinobacterial hosts, including both *M. smegmatis* and *M. tuberculosis* (Russell & Hatfull, 2017). As at February 2019, PhagesDB contained 15,059 bacteriophages uploaded, 10,416 of which infect *Mycobacterium* species and 1,729 of which are sequenced. PhagesDB accepts bacteriophage isolations from different countries throughout the world, encompassing both hemispheres and a range of environments resulting in a diverse array of bacteriophage genomes and characterisation present. When bacteriophages are genome-sequenced and annotated, the information becomes available down to the annotation of

each specific gene, resulting in a detailed resource available. Because of this layout, PhagesDB is a significant preliminary measure to identify the location of endolysins within mycobacteriophage. To date, there has been one published article discussing a mycobacteriophage isolated from New Zealand, StepMih (Butela et al., 2017).

Bacteriophages are added to the database through high school, college and undergraduate “phage hunting” programmes which means an extra series of bioinformatic tests will be carried out in this research to provide further evidence that the lytic enzymes selected are in fact the same as the annotation call (Russell & Hatfull, 2017).

A

B



Figure 5: Mycobacteriophage diversity

A) 2015 literature illustrates the diversity of gene content relationships through 627 sequenced mycobacteriophages displayed as a network phylogeny. The multiple branches reflect the phylogenetic complexities as a result of the mosaic bacteriophage genomes where many genes within the genome have a distinct evolutionary history (Pope et al., 2015). B) Mycobacteriophage also have diverse isolation locations throughout the world (PhagesDB, 2019).

1.9 Mycobacteriophage clusters

One of the useful features of PhagesDB is the display of bacteriophage clusters. It has been proposed that two mycobacteriophage genomes that display over 50% nucleotide sequence similarity should be grouped into the same cluster, with some clusters containing bacteriophage with over 90% nucleotide sequence similarity such as mycobacteriophage Bxz1 and Catera (Fig. 5) (Hatfull, Cresawn, & Hendrix, 2008; Sassi, Bebeacua, Drancourt, & Cambillau, 2013). Currently on PhagesDB there are 29 known mycobacteriophage clusters (including a Singleton cluster for bacteriophage that do not fit into any existing cluster), with 56 sub clusters. Although the research from Hatfull and colleagues suggests inclusion of mycobacteriophage genomes within clusters is largely on an “ad hoc” basis, rather than with strict criteria, this research aimed to identify endolysin candidates capable of exogenous mycobacterium lysis from a range of bacteriophages therefore this initial cluster identification and assortment is a tool to begin exploration with.

1.10 Biodegradable nanobeads

Polyhydroxyalkanoates (PHA) are the largest group of natural biopolymers, produced in various microorganisms as carbon and energy reserves when the main growth nutrient is limited (Kamravamanesh, Lackner, & Herwig, 2018; Li, Yang, & Loh, 2016). These PHAs consist of hydroxyalkanoic acids linked by oxoester bonds with an amorphous polyester core surrounded by a boundary layer of embedded or attached proteins (Fig. 6), including PHA synthase (PhaC) which can be N-terminally fused to a protein of interest, and can range in size from 100nm – 500nm (K. Grage et al., 2009; Rehm, 2003). PHAs have been developed for use in biomedical and industrial applications and have been shown to be well tolerated by mammalian systems (Katrin Grage et al., 2009) . There has

also been research in to using *E. coli* strains, including BL21, to produce PHA nanobeads with the overexpression of the corresponding plasmids which is the basis of this study (Blatchford, Scott, French, & Rehm, 2012).

These PHA nanobeads are water insoluble (although still biodegradable). Because PHA nanobeads are carbon reserves, they are naturally degraded by PHA depolymerase (PhaZ) during times of carbon starvation (Chek et al., 2017). PHA nanobeads offer two distinct advantages as proteins of interest are covalently bound in a uniform direction to the surface and these can be expressed through a one-step process (Lee, Parlane, Rehm, Buddle, & Heiser, 2017).

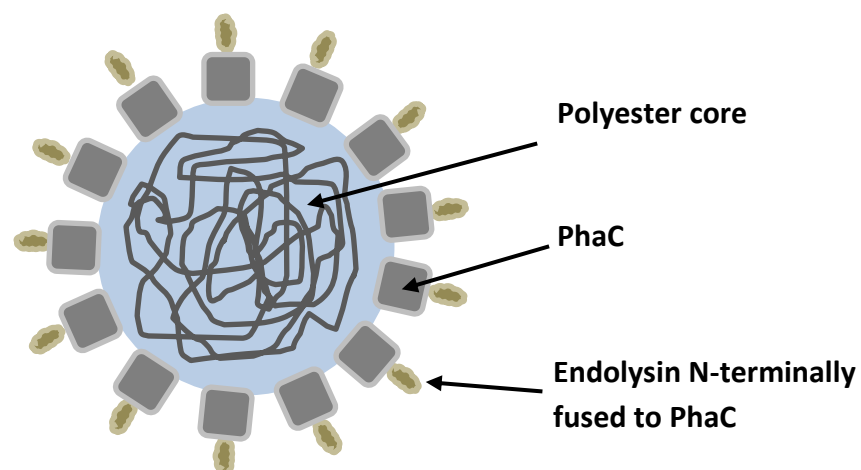


Figure 6: Polyhydroxyalkanoate nanobead with endolysin proteins fused to surface

Each PHA nanobead has only one type of lysin fused to the surface (either lysin A or lysin B). This is a “first generation” bead.

1.10.1 PHA biodegradability

A unique aspect of PHA nanobeads is their complete biodegradability. In various environmental conditions (including soil, sea water, lake water and anaerobic sludge), bacteria including *Acidovorax facilis*, *Aspergillus fumigatus*, *Comamonas* sp., *Pseudomonas lemoignei*, *Pseudomonas fluorescens*, *Comamonas testosterone* and

Ilyobacter delafieldii excrete extracellular PHA depolymerases which degrade the PHA molecules into water soluble monomers and oligomers to be reused as a carbon source (Anderson & Dawes, 1990). However, the rate of biodegradation is dependent on several factors including the microbial population present, pH and the temperature (Mergaert, Anderson, Wouters, Swings, & Kersters, 1992). Due to the changing landscape, studies surrounding the commercial viability of PHA are underway, exploring these biodegradable nanobeads as an antimicrobial drug delivery alternative in the biomedical field. Anticipation for commercial PHA use include high-end products with distinct properties and a definite purpose of utilisation where the PHA biocomplexity and biodegradability would aid as an advantage, such as drug delivery materials, tissue engineering and nanobiotechnology yet PHA's can also be utilised for low-end products where the biodegradability is an advantage but the main benefit would be the economic efficiency, such as organic waste bags, single use packaging and toys (Kovalcik, Obruca, Fritz, & Marova, 2019).

1.10.2 PHA synthase

PHA synthases catalyse the polymerisation of PHA polymers as the key enzyme in PHA synthesis. PhaC is the key enzyme involved in the biosynthesis of PHA and polymerises monomeric hydroxyalkanoate substrates (Chek et al., 2017). There are currently four reported classes of PHA synthase, including; Class I which forms a homodimer, Class II which contains synthases PhaCI and PhaCII, and Class III and IV synthases that form heterodimers and favour short chain length monomers (Chek et al., 2017). The subunit size of Class I and II have a subunit size of approximately 60 to 70kDa whereas the subunit size of Class III and IV are larger having two subunits (Jendrossek, 2009; Rehm, 2007). All PHA synthases share a conserved cysteine as a catalytic site and this is where the PHA chain is covalently attached (Jendrossek, 2009). Early evidence suggests that

activity from PHA synthase is directly associated with isolated PHA granules (Griebel & Merrick, 1971).

Phasins are PHA granule-associated proteins that promote bacterial growth and can influence the size, number and distribution of these granules (Mezzina & Pettinari, 2016). Phasins also amphiphilic proteins which shield the inner hydrophobic polymer from the cytoplasm of the cell (Maestro & Sanz, 2017). Pötter and colleagues suggest phasin homologue PhaP1 constitutes the major component of the layer at the surface of poly(3-hydroxybutyrate) granules (Pötter et al., 2004).

1.11 Aims

The aims of this thesis can be separated into three parts: (1) the bioinformatic identification of candidate mycobacteriophage endolysins capable of lysing exogenously, (2) the design and development of unique biodegradable nanobeads equipped with endolysins fused on the surface and (3) to test the capacity of these endolysin proteins delivered on biodegradable nanobeads to kill *M. smegmatis* cells through a series of quantifiable tests.

Aim 1: Choose endolysins to lyse exogenously

The objectives related to this aim revolve around using bioinformatics tools to identify appropriate endolysins using the PhagesDB database. Though D29 is a mycobacterial endolysin that is known to function in this way, this does not give us a screening method, other than to focus our attentions on lysin B homologues. I will use software-based approaches to ensure that the genes chosen for cloning have domains associated with lysis. I set out to choose two lysin A proteins and six lysin B proteins. I will then use the

available genome data from over 1,600 sequenced mycobacteriophage accessed from PhagesDB to, select candidates across a range of clusters. The first aim will be wrapped up with the comparisons of the selected candidates to increase accuracy of lysis candidate selection using NCBI BLAST, Clustal Omega and HHpred.

Aim 2: Design and develop unique biodegradable nanobeads

The objectives required to support this aim are based on using the selected candidates to go through a series of *in vitro* processes to produce a functioning and applicable biodegradable nanobead in order to transport these lysis candidates to infect the bacterial cell through surface fusion. This specific objectives for this aim were to work in conjunction with GeneArt and AgResearch to design and synthesize N-terminal fusion construct plasmids. Collaborate with the AgResearch Grasslands team to electroporate the synthesized plasmids into *E. coli*, express the PHA nanobeads in *E. coli* and harvest and purify the nanobeads to be used in *in vitro* experiments whilst also being able to construct these nanobeads at Massey University too.

Aim 3: Test endolysin nanobeads on *M. smegmatis* to see cell death

The objectives for this aim are to design and implement methods for testing the antimicrobial lytic activity of the endolysin nanobeads against *M. smegmatis*. A series of quantitative and statistically sound tests were devised to test the effectiveness of the beads produced, including live/dead microscopy to observe the degree to which whole cells appeared damaged but not completely lysed, a plate reader experiment to understand how the nanobeads lyse in shaking conditions, testing the nanobeads using colony forming unit assays to observe *M. smegmatis* cell death through a colony decrease after exposure in a standing culture and finally a nanobead test on filters or hospital masks to demonstrate

the degree to which they could serve as a prophylactic barrier against infection of *M. tuberculosis* in practical medical settings as a proof-of-concept.

1.12 Summary for remainder of the thesis

The remainder of this thesis will describe the materials and methods used to carry out the aims, including the software, strains and laboratory conditions used. Then I will discuss the results and discussion concurrently to describe the rationale behind the experiments and scientific thought. The thesis will then conclude with an overall summary and reference list.

2 Materials and Methods

2.1 Bacteriophage endolysin selection through bioinformatics

This section will introduce the bioinformatic software that assisted on endolysin confirmation through detailed output.

2.1.1 Online databases and tools; PhagesDB and NCBI BLASTp annotations

Two sequenced mycobacteriophages from each cluster (including sub clusters where appropriate) were selected from PhagesDB with the position of each lysin A, lysin B, holin (if present) and the amino acid sequences of these proteins recorded (PhagesDB, 2017). Each endolysin amino acid sequence was run through NCBI Standard Protein BLASTp to see if the annotated function is correct compared to other bacteriophage functions by e-value comparison. The database selected was Non-redundant protein sequences (nr) using the programme search algorithm blastp (protein-protein BLAST). The default parameters under the blastp algorithm included maximum of 100 target sequences, automatically adjusting parameters for short input sequences, expected threshold of 10, word size of six and zero maximum matches in query range. The scoring parameters included the default BLOSUM62 matrix, gap costs were 11 existence, extension 1 with conditional compositional score matrix adjustment.

2.1.2 Clustal Omega

All amino acid sequences from the selected mycobacteriophages were separated into “Lysin A” and “Lysin B” categories. It was decided at this stage to disregard the holin protein as this protein has a specific purpose within inter-cell bacteriophage lysis with no significant effect proposed for exogenous lysis. The Clustal programme was clustalo, version 1.2.4 (Goujon et al., 2010; McWilliam et al., 2013; Sievers et al., 2011). A set of proteins were selected for sequence analysis and the remaining default input parameters

were selected. The output format was ClustalW with character counts and input sequences not dealigned. The mBed-like clustering guide tree and clustering iterations were both true, with a default number of combined iterations (0), maximum guide tree iterations and HMM iterations. The output order was aligned.

2.1.2.1 FigTree

Using the amino acid sequence from each bacteriophage lysin A or lysin B gene identified from DNAMaster, FigTree v1.4.3 was used to make a phylogenetic tree of the output to gauge a visual understanding of genetic relationships.

2.1.3 HHpred

For further domain confirmation, Fast Alignment Search Tool A (FASTA) files were submitted to the Max Planck Institute (MPI) Bioinformatics Toolbox HHpred (Zimmermann et al., 2018). The NCBI_Conserved_Domain(CD)_v3.16 was selected and the default settings for the programme were used. Briefly, the multiple sequence alignment (MSA) generation method was (HHblits=>uniclust30_2018_08) with three MSA generation steps with an e-value minimum threshold of $1e-3$. The minimum sequence identity of MSA hits with query (%) was 0 and minimum coverage of MSA hits (%) was 20. The local alignment mode was used, the maximum accuracy (MAC) had no realignment and the secondary structure scoring was set during alignment. A total of 250 target sequences were selected with a minimum probability in the hit list ($>10\%$) of 20.

Table 1: The lysin A and lysin B genes chosen for this project

Phage name	Cluster	Gene position	Lysin type	Start site	Stop site	GenBank accession number
StarStuff (lysA)	A2	12	lysin A	4697	6178	KX89781
Pipsqueaks (lysA)	N	28	lysin A	22834	24342	KU935730
D29 (lysB)	A2	12	lysin B	6606	7370	AF022214
Jaws (lysB)	K1	31	lysin B	26448	27320	JN185608
Inca (lysB)	E	34	lysin B	30537	31394	MH576956
Giles (lysB)	Q	32	lysin B	28339	29574	EU203571
Dylan (lysB)	O	67	lysin B	43515	44555	KF024730
Bongo (lysB)	M1	38	lysin B	31794	32765	JN699628

The lysin proteins occur in different regions of each mycobacteriophage genome. The gene numbers in each genome are listed along with the start and stop of the ORF and the genome accession numbers. Both lysin A's come from different clusters and all lysin B's come from different clusters.

2.1.4 Plasmid constructs

This section of the research was carried out in conjunction with the support and assistance of Dr. Eric Altermann in AgResearch, Palmerston North. The N-terminal fusion sequences were mRNA stabilised and codon optimised by GeneArt, along with the gene synthesis and cloning into the vector.

2.2 Media

2.2.1 Antibiotics, supplements, media,

Table 2: Antibiotic concentrations

Antibiotic	Final concentration
Ampicillin (AMP)	10mg/ml
Chloramphenicol (CM)	34mg/ml
Carbenicillin disodium salt (CB)	50mg/ml
Cycloheximide (CHX)	10mg/ml

The antibiotic concentrations were made as above. Throughout the thesis I will refer to them through the abbreviated name and the concentration will be known as the final concentration above, unless stated otherwise.

2.2.2 Bacterial strains

Table 3: Bacterial strains used in this work

Bacterial strain	Supplied from	Reference
<i>E. coli</i> BL21	AgResearch	(Jeong, Kim, & Lee, 2015)
<i>M. smegmatis</i> mc ² 155	American Type Culture Collection (ATCC)	(Mohan, Padiadpu, Baloni, & Chandra, 2015)

We used *E. coli* BL21 as the host for the PHA expression using the strain to transform the pET-14b plasmid. *M. smegmatis* mc²155 was used as the bacterium specie to test cell death.

2.2.3 *M. smegmatis* growth

M. smegmatis was grown in Complete 7H9 media from a frozen glycerol stock of WT *Mycobacterium smegmatis* mc²155. *M. smegmatis* was streaked out from frozen stocks (onto 1.5% LB + CB + CHX plates) and incubated at 37°C for 72 hours. One colony was then picked and added to 50ml of Complete 7H9 and 250µl 20% Tween80 for a further incubation period at 37°C, shaking at 250rpm for 72 hours. For experiments using a bacteriophage, Tween80 was not used as it has been shown to inhibit adsorption of mycobacteriophages on the bacteria (White & Knight, 1958). This working stock was kept at 4°C for 5 weeks. Working stocks of *M. smegmatis* culture were used to make

actively growing cultures by taking 50µl of the stock added to the 7H9 Complete media and incubated at 37°C for 72 hours. Cultures were refreshed monthly for backup stocks, although *M. smegmatis* can still be usable for up to six months refrigerated at 4°C.

2.2.4 Growing and maintaining bacteriophage

Bacteriophage Inca (NCBI:txid2283256) was isolated on *M. smegmatis* mc²155 from soil in New Zealand and purified using the SEA-PHAGES guide (PhagesDB, 2015; SEA-PHAGES). Inca was frozen in glycerol and kept in the -80°C freezer until required.

2.2.5 Transforming chemically-competent *E. coli* BL21

2µl of lyophilised plasmids was added to 60µl already-chemically competent *E. coli* BL21 cells thawed on ice and heat shocked for 45 seconds on a 42°C heat block. These cells were put back on ice with 250µl of SOC broth, mixed gently and shaken at 200rpm at 37°C for 45 minutes. To observe colonies, 10µl of cells was spread onto 1.5% LB + AMP plates and incubated at 37°C overnight.

2.3 Nanobead production

For each successfully transformed plasmid, a single ampicillin resistant *E. coli* colony was picked and added to 5ml LB + AMP and incubated at 37°C shaking at 160rpm, allowing cells to grow in excess overnight. The following day, flasks of 100ml LB + AMP + CM and 20% glucose were added along with 2ml of the overnight *E. coli* culture. These flasks were then incubated at 37°C, shaking at 200rpm for two hours. 1.5 hours into the procedure, 1ml from a flask was extracted and tested at OD₆₀₀ – all flasks remained incubating until the two hours was complete, to reach an OD₆₀₀ of close to 0.5. When OD₆₀₀ ~0.5 was reached, 1ml of IPTG was added to each flask to induce expression the pET-14b plasmid which initiated the production of the PHA beads from the *E. coli*

(Abedi, Beheshti, Najafabadi, Sadeghi, & Akbari, 2012). They were then incubated at 20°C shaking at 160rpm for 48 hours. 24 hours through this procedure, a Nile red stain was carried out (described below) on a sample to visualise the nanobead expression within the *E. coli* under microscopy. After 48 hours of expression, the cells were separated into two balanced 50mL Falcon Tubes before centrifuging at 5,000g for 10 minutes. The supernatant was then discarded and the pellet frozen until the bacterial lysis commenced, as illustrated in Fig. 7.

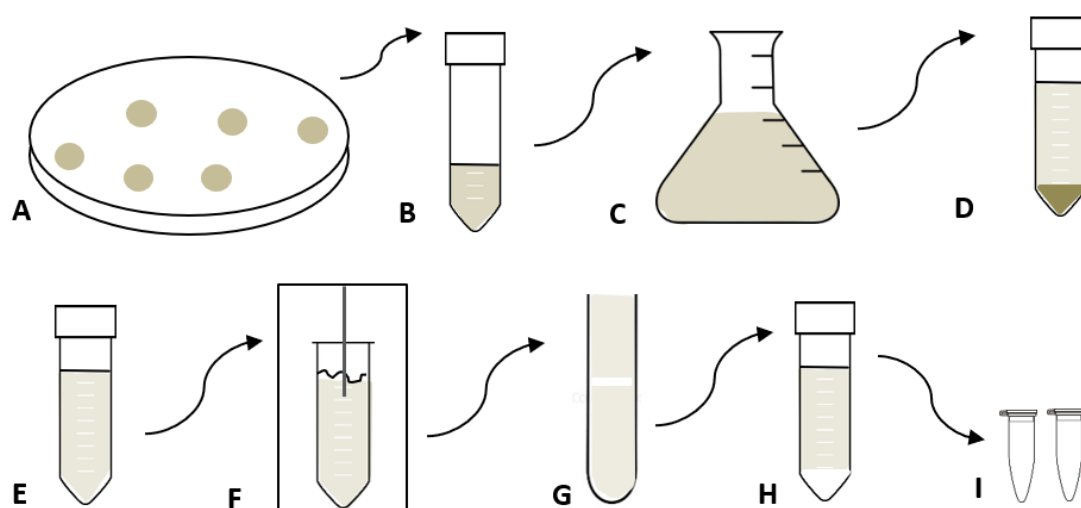


Figure 7: Production of PHA nanobeads with fused endolysins

A) the chemically competent *E. coli* BL21 containing pET-14b and PhaC plasmids are streaked out and one colony is picked into B) fresh media to incubate overnight. C) a sub-culture of 2ml overnight culture was transferred into fresh media and incubated until OD reached ~0.5 before inducing with IPTG and incubating for a further 48 hours. D) the *E. coli* is spun down, pelleted (discarding supernatant) and frozen until further use or lysed overnight. E) the pellet is resuspended in lysis buffer, lysozyme and DNase, standing at 4°C overnight. F) solution is sonicated and G) placed in glycerol gradient for ultra-centrifugation to isolate a white band of pure beads before H) spinning to pellet and remove excess glycerol then I) storing at -80°C at a concentration of 200 mg/ml until use.

2.3.1 Nile Red stain

In order to visualise bead production, 1ml of sample was resuspended in 1ml PB (Phosphate Buffer) and 10 μ l of Nile red stain (0.05 μ g/ml) before pelleting. This was repeated twice before finishing off with a final resuspension. 10 μ l of sample was examined under 100X microscopy using an Olympus BX-61 microscope and Nile Red stain to identify what cells had produced PHA nanobeads. This step was used to visualise the expression of the nanobead and if no nanobeads were visible, the culture would be remade.

2.3.2 Bead extraction

In order to extract the beads from the cells the bacterial pellet was lysed by resuspension in 10mL lysis buffer and 1mL lysozyme. This was left agitating in an icebox at 100rpm for 2-3 hours or until the solution became a mucus-like consistency. 150 μ L of 1000U DNaseI was then added to the mucus-like lysed resuspension and this solution was gently inverted to mix and then stored in the 4°C fridge overnight. The following day the sample was put through the sonicator as a physical lysis measure alongside the chemical lysis.

2.3.3 Ultrasonic Processor

Sonication at Massey University, Albany, was carried out using the Misonix Sonicator Ultrasonic Processor S-4000 for additional physical cell lysis. The microtip was cleaned with ethanol wipes before use and the solution of chemically lysed *E. coli* cells were taken up to 40ml with the addition of PBS and vortexed before being placed on ice for sonication. Programme settings were programmed as follows; Amplitude: 60, Process Time; 10 minutes, Pulse-ON Time; 30 seconds, Pulse-OFF Time; 30 seconds. Halfway through the elapsed time (at 5 minutes), the sonication process would be paused, and the

sample taken out and shaken to resuspend *E. coli* cells for maximum sonication opportunity.

2.3.4 Bead purification and storage

The collected solution was topped up with phosphate buffer (to a total volume of 40ml) and centrifuged at 8,000g for 20 minutes at 4°C. The supernatant was discarded before the pellet was resuspended with 4mL of 50mM phosphate buffer ensuring that it did not become too foam-like to distort the gradient. A glycerol gradient with 4mL of 88% glycerol on the base, 4mL of 44% glycerol in the middle and 2mL of resuspended pellets was made up in polypropylene tubes. The remaining bead solution was split across the tubes and balanced within 0.01g. The beads and glycerol gradients were centrifuged using an ultracentrifuge TW-641 rotor for 1 hour 45 minutes at 35,000g. At the conclusion of the centrifugation, the white band at the glycerol gradient interface was removed with the upper layer of glycerol discarded and the intermediate white band poured into a Falcon tube topped up to 45mL with PB, gently shaken and centrifuged at 8,000g for 20 minutes at 4°C to separate the purified nanobeads from the glycerol that may have become mixed in during the ultra-centrifugation process. The supernatant was then discarded, and the bead pellet was resuspended in phage buffer to a concentration of 20mg/ml with the addition of 20µl/ml Tween80 to prevent clumping. These were stored indefinitely at -80°C or until required for further experiments. Once in use, the tube of nanobeads was kept in the fridge at 4°C and not continuously frozen/refrozen.

2.4 Testing cell death of *M. smegmatis*

In order to determine the degree of cell death in populations of *M. smegmatis* that the nanobead exposure could induce in liquid, a series of exposure times and concentrations were tested as follows; 45 minutes and 5 hours and concentrations of 10mg/ml, 20mg/ml

and 80mg/ml per time allocation. There were these six experimental controls in this research, each with three replicates of *M. smegmatis* culture. For example, 10mg/ml nanobead exposure: 50µl of nanobeads were added to 1ml *M. smegmatis* culture (as stocks were stored at 200mg nanobeads, per ml of PBS, 20mg/ml for either 45 minutes or 5 hours. The control *M. smegmatis* culture had 5µl PBS added as this is what the nanobeads were stored in. Controls with similar volumes of PBS were used for each concentration.

Unless otherwise specified, these infections would be carried out at room temperature (21°C) using a standing culture of *M. smegmatis* stored at 4°C. Each time point and concentration of nanobeads would have a corresponding *M. smegmatis* control that remained at room temperature for the duration of the exposure experiment.

2.4.1 Test one: detecting cell death through fluorescent microscopy

The above infections were carried out and 4µl/ml of 1.67mM SYTO 9 nucleic acid stain, 18.3mM propidium iodide fluorescent stain solution in DMSO was added, mixed in and 2µl was placed onto an M9 + glucose 1% agarose pad. Once the 2µl bead solution had set, a coverslip was placed on the pad and examined under the Olympus BX-61 microscope using an Olympus U-RFL-T fluorescent lamp and microscope settings of 50ms GFP and 30ms RED. Images were captured using the cellSens Dimension software.

To calculate cell death, images were merged in Fiji Image J software. Green cells were recorded as “alive” and red cells were recorded as “dead”. Unstained beads were also photographed under the microscope, measuring 100 unstained beads at a 10^{-1} dilution on Fiji Image J software.

2.4.2 Test two: detecting cell death through a plate-reader assay

For this experiment, the concentration of nanobead exposure to *M. smegmatis* were set up as aforementioned in section 2.4 with three replicates as well as untreated *M. smegmatis*, water, empty wells and wells with an autoclaved glass bead in them, in a Greiner 96 well flat bottom plate.

Each well of the 96-well plate contained a particular concentration of nanobead (discussed above) exposed to a series of *M. smegmatis* dilutions from $10^0 - 10^{-11}$. 100µl of each sample was placed into a well as there would be fast shaking and 100µl would minimise the risk of contamination from overflow. A second set of trials involved the same set up but with an autoclaved glass bead to stimulate aerobic growth of *M. smegmatis*. This experiment was not set into the 45 minute and 5 hour time allocations for nanobead exposure as the experiment was run over a 24 hour timeframe.

The plate reader software was Gen5 2.06 and each experiment was run for 24 hours continuously shaking fast, the temperature set at 37°C, kinetic run, three replicates read at OD600 and with a lid.

2.4.3 Test three: detecting difference in colony counts

The first part of this experiment looked at the difference in colonies due to cell death caused by the nanobeads upon exposure. The bead exposures were set up as below in Fig. 8. After the two time points of 45 minutes and 5 hours, the exposure tests were serially diluted in 7H9 Complete media, 100µl of 10^{-6} dilution was added to a 1.5% LB + CB + CHX plate and spread using autoclaved glass beads. These plates were then inverted and incubated at 37°C for 72 hours. After 72 hours, colonies were counted across each of the plates, Fig 8.

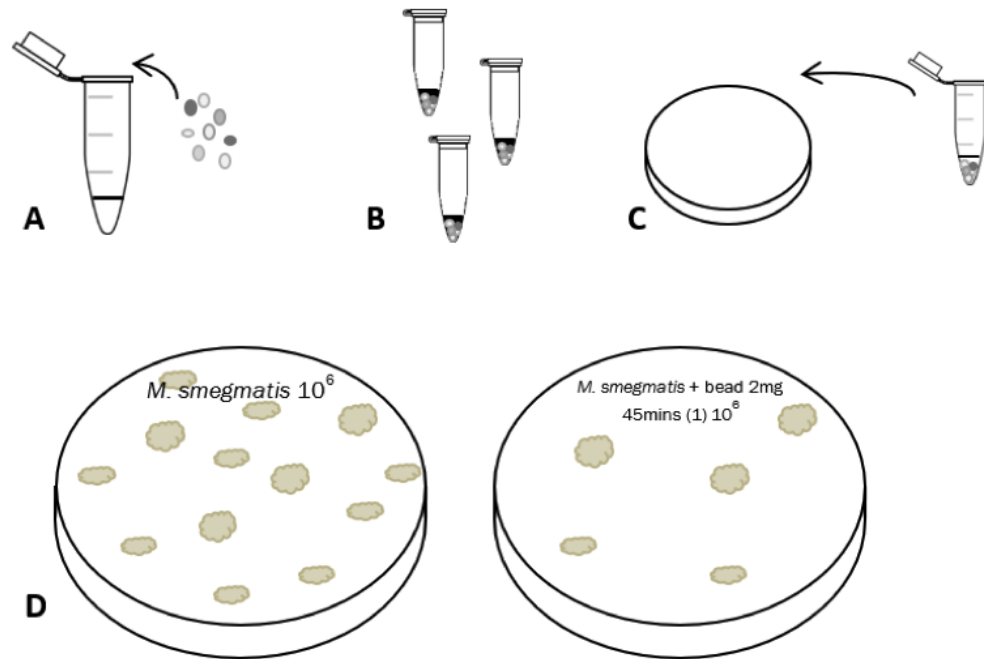


Figure 8: Testing cell death induced by bead exposure by colony count

A) a specified concentration of nanobeads are added to a standing culture of *M. smegmatis* at room temperature and B) left standing for a specified period of time. The nanobeads are then C) serially diluted and spread across an agar plate and incubated before D) counting the difference in colonies between the treated and untreated plates.

2.4.3.1 Testing for resistant colonies

The second part of this experiment aimed to understand if the remaining colonies were resistant to endolysins or if there had not been enough endolysin nanobeads to achieve a higher percentage of cell death. This was done by picking a colony from each plate with the highest cell death, growing it with the same preparation as above, and repeating the 80mg/ml 5 hour experiment to compare the cell death between the different cultures.

2.4.4 Test four: detecting cell death using filter paper for a proof-of-concept applied approach

Because hospital masks are hydrophobic and require commercial spray coaters, Grade 1 filter paper was used as a hydrophilic alternative. 1cm diameter filter paper pieces were autoclaved before use. Each concentration of nanobead solution was spread across the filter paper, let dry for ~5 minutes before spraying one spray of 10^{-5} *M. smegmatis* using a cosmetic atomiser which dispenses 100µl bacteria per spray using the contraption in Fig. 9. Each piece of filter paper was then left for 15 minutes before stamping onto a 1.5% LB + CB + CHX plate, inverted and incubated at 37°C for 72 hours. This crafty solution was created using a Harris Uni-Core-2.00 borer to make a small hole in an Eppendorf tube to put the tube of the spray nozzle into. This way, we were able to see exactly how much spray was used at a given time was able to be more reliably observed.



Figure 9: Lab-made spray system

Using the Harris Uni-Core-2.00 to make a hole in the Eppendorf tube, the experiment can use smaller volumes than the bottle that a traditional cosmetic atomiser bottle would hold (~30mls) and also to control how much spray is used.

2.4.5 Statistical analysis

Additional data analysis of results was carried out using Microsoft Excel 16 and RStudio version 1.1.46.

3 Results and Discussion

This section will include the motivation and results of each experiment alongside a critical analysis of results and a discussion of the interpretation. Both positive and negative results are included as they both had an impact on future directions. The results come in three parts; the selection of the endolysins for this work, expressing the endolysins on the nanobeads and testing the endolysin-nanobead fusions for their effect on cell viability.

3.1 PART ONE: Gene selection process and domain confirmation

The purpose of this project was to identify lysin proteins that would be capable of lysing *M. smegmatis* “from without” using the vast resource of completely sequenced mycobacteriophages available from PhagesDB. Ultimately, the aim was to attach these proteins to biodegradable nanobeads. Herein, I will describe the process that was undertaken in order to choose the type of proteins, the specific genes and how the identity of the proteins expressed from those genes was verified bioinformatically.

3.1.1 Rationale behind choosing the final mycobacteriophage endolysin candidates

Mycobacteriophage endolysins were selected for this project. In order to make the best use of these experiments we wanted to choose Lysin A and Lysin B genes for synthesis and expression in a nanobead expression vector, however we wanted the endolysins to be different from one another. Our strategy for choosing different genes is discussed below through four bioinformatic steps. This project required simple and practical lytic enzymes with the structural and biochemical simplicity to allow them to act as lytic agents when applied to *M. smegmatis* exogenously, fused to biodegradable nanobeads. (K. Payne et al., 2009; Pohane et al., 2015; Young, 2013).

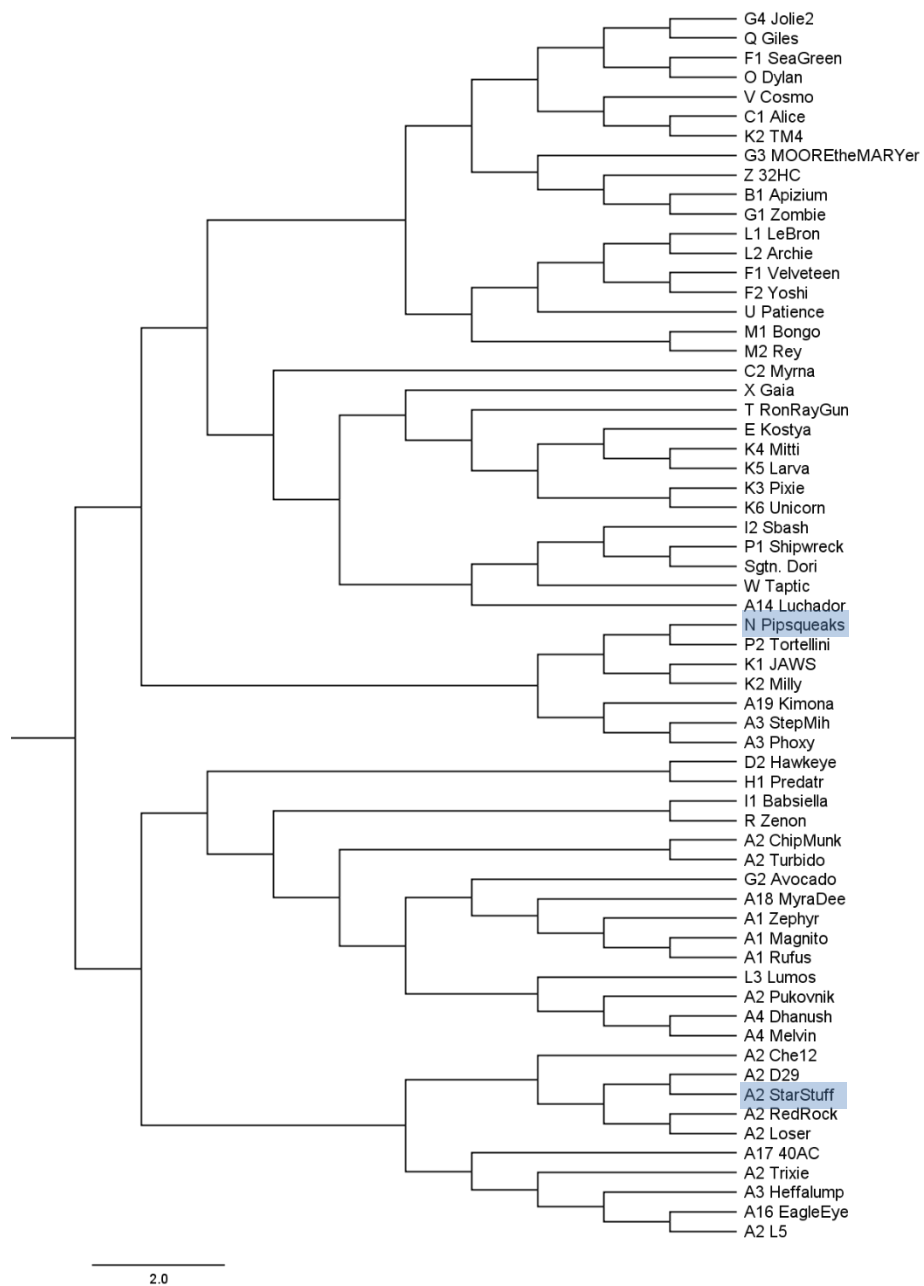


Figure 10: Cladogram of a selection of lysin A mycobacteriophages (clusters labelled)

The two mycobacteriophages highlighted in blue illustrate the two final candidates selected for the project; StarStuff and Pipsqueaks. We can see from this tree that the cluster A mycobacteriophages are close together, indicating similarity in lysin A amino acid sequence. StarStuff was chosen as it is one of the cluster A mycobacteriophages and it is closely related to other lysin A's that have shown "lysis from without" in other studies. Pipsqueaks was chosen as it is further away in the phylogenetic tree, amongst a group of mosaic-clustered mycobacteriophages.

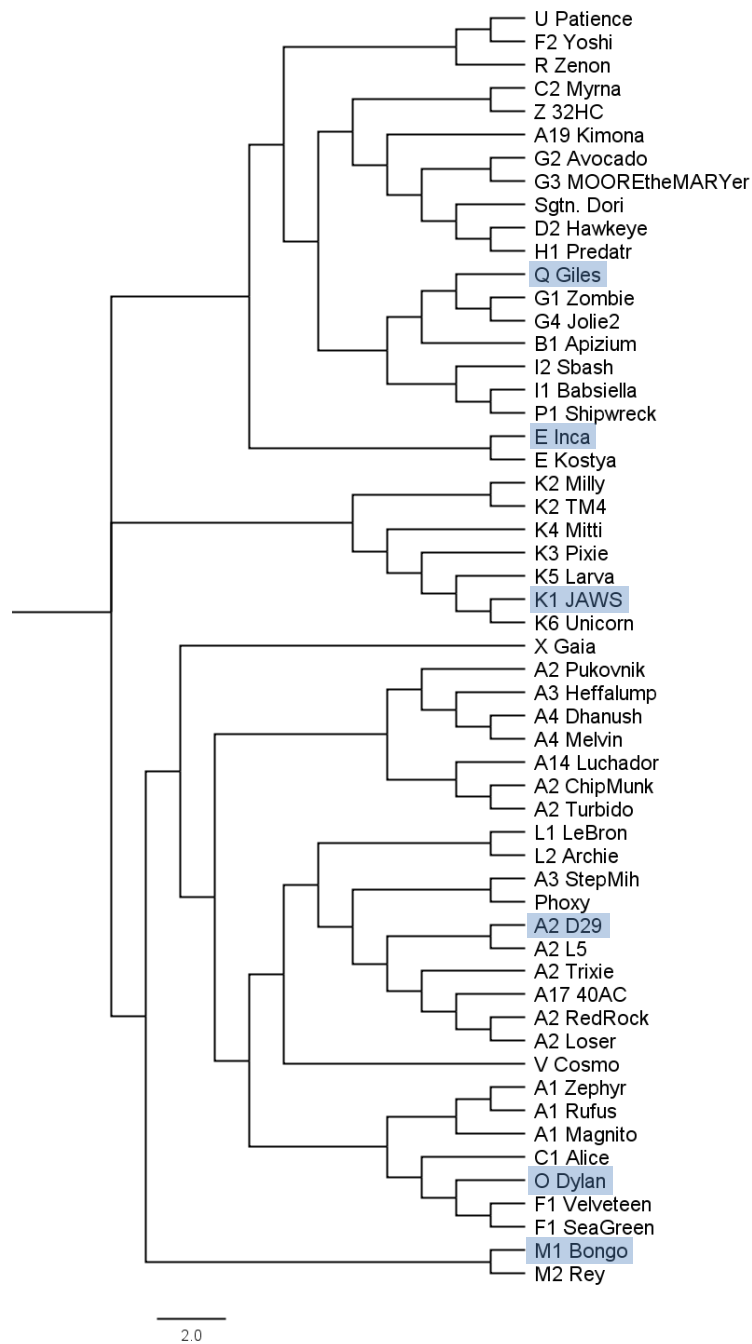


Figure 11: Cladogram of a selection of lysin B mycobacteriophages from each cluster (clusters labelled)

The six mycobacteriophages highlighted illustrate the six final candidates selected for the project; Giles (Q), Inca (E), Jaws (K1), D29 (A2), Dylan (O) and Bongo (M1). Not only are these six lysin B's from different clusters, they are also distinct on the phylogenetic tree. They are each from a monophyletic clade and this diversity was the reason they were selected for this project.

Ultimately, lysin B's were the focus due to their capacity to "lyse from without". Lysin B of mycobacteriophage D29 was shown to be active against a 5-day standing culture *M. smegmatis* biofilm as an applied protein in concentrations from 1µg/ml to 100µg/ml to (K. M. Payne, 2006). A few lysin A's were chosen as they lyse the peptidoglycan whereas lysin B's lyse at the junction between the mycolic acids and peptidoglycan component of the cell wall (Ford, Sarkis, Belanger, Hendrix, & Hatfull, 1998; K. Payne et al., 2009; Pohane et al., 2015). The set of Lysin A and Lysin B genes chosen are represented as a cladogram of amino acid similarity in Fig. 10 and Fig. 11. The six mycobacteriophages highlighted illustrate the six final candidates selected for the project; Giles (Q), Inca (E), Jaws (K1), D29 (A2), Dylan (O) and Bongo (M1). Not only are these six lysin B's from different clusters, they are also distinct on the phylogenetic tree. They are each from a monophyletic clade and this diversity was the reason they were selected for this project.

In order to choose bacteriophage genes that were more likely I chose mycobacteriophages from different "clusters". Clusters are way of grouping similar bacteriophages, in an ad hoc fashion that accounts for chimerism that was developed by Graham Hatfull and colleagues and applied to the bacteriophages in PhagesDB. Briefly, bacteriophages that display over 50% nucleotide sequence similarity are grouped into the same cluster (Hatfull et al., 2008; Sassi et al., 2013). Two bacteriophages were selected from each of 85 clusters for this project and these bacteriophages represented a geographical spread across the world (Fig. 12). I eventually chose a set of two lysin A and six lysin B spanning across a total of seven clusters (Table 4, Fig. 10 and Fig. 11).

Table 4: NCBI BLASTp output

Bacteriophage endolysin	Top hit description	Alignment score	Query cover (%)	E-value	Identity (%)	Accession number
StarStuff (lysA)	lysine A Mycobacterium phage Kerberos	1007	100	0.0	99	APC43063.1
Pipsqueaks (lysA)	lysine A Mycobacterium phage Carcharodon	1026	1001	0.0	100	YP_009197153.1
D29 (lysB)	lysine B Mycobacterium phage Pomar16	516	100	0.0	99	AOQ27846.1
Jaws (lysB)	lysine B Mycobacterium phage Crew	580	100	0.0	99	APU93135.1
Inca (lysB)	gp35 Mycobacterium phage CJW1*	582	100	0.0	99	NP_817485.1
Giles (lysB)	lysine B Mycobacterium phage Gancho	820	100	0.0	99	AYB69374.1
Dylan (lysB)	gp70 Mycobacterium virus Corndog**	715	100	0.0	100	NP_817921.1
Bongo (lysB)	lysine B Mycobacterium phage PegLeg	662	100	0.0	100	YP_008050970.1

Listing the bacteriophage's closest BLASTp "hit" and the corresponding e-value. * the second best hit was described as a "lysine B" with the same scores as CJW1 (except the identity which was 99%) and there was significant evidence to show that CJW1 was also a lysine B, unannotated. ** the second best hit was also described as a "lysine B" with the same scores as Corndog (except the alignment score which was 713 and the identity which was 99%) and there was significant evidence to show that Corndog was also a lysine B, unannotated.

I used bioinformatic tools BLAST and Clustal to analyse the active domains of my lysins following on the model of Payne and Hatfull (K. M. Payne & Hatfull, 2012). All eight of the endolysins chosen (Table 4) were confirmed to be endolysins in BLAST by having e-values of at least 10^{-5} or similarity scores of at least 20%. This rough bioinformatic analysis enabled the positive identification of hydrolase family domains that were also found in this project, discussed in more depth below.

3.1.2 Checking for evidence of lysin function using NCBI BLASTp

The bacteriophages in the PhagesDB database have been discovered, sequenced and annotated by undergraduates in the SEA-PHAGES programme (Jordan et al., 2014). As such, the annotations have been quality controlled within the program and are most likely accurate, nevertheless it is wise to double check that there is evidence for functional assignment of an annotation. Each of the lysin A and lysin B genes that we chose were individually submitted to the NCBI BLASTp database in order to verify that there is strong evidence for the annotation call (Fassler & Cooper, 2011).

Each of the lysin candidates had over 99% identity to an identical lysin protein in at least three other matches with e-values of 0.0 indicating strong evidence that the annotations were correct and each of the candidates is either a lysin A or a lysin B (Table 4). Although the information illustrated in Table 4 shows only the top hit, for every bacteriophage lysin output, there were at least three hits with similar statistics providing further evidence towards the accuracy of these annotations and less chance of two false-annotations occurring to match.

3.1.3 Bacteriophage selection candidates

The eight endolysin candidates comprised of six lysin B's and two lysin A's are located across the North and South hemisphere, throughout three countries encompassing island nations and landlocked countries. There were lysins from three different continents, spanning three countries across two hemispheres. For example, both a lysin A (StarStuff) and lysin B (Dylan) came from South Africa. Although to date we do not know of any studies demonstrating an effect of geography on lysin ability or bacteriophage characteristics, nevertheless it was interesting to select a group of bacteriophages from around the world to include in this project.

As aforementioned, D29 was included as a positive control in this experiment with previous research from Payne and colleagues demonstrated the lytic effects of D29 when it was applied to *M. smegmatis* biofilms “from without” resulting in a significant decrease in biofilm maturation (K. M. Payne, 2006).

The lysin B from bacteriophage Inca was also included in this project not only as a New Zealand bacteriophage representative but also as our laboratory has a frozen stock of Inca after my discovery of this bacteriophage in 2015. We can therefore use this bacteriophage to compare the lytic ability of lysin proteins to the bacteriophage. This may be important since the mechanisms that mycobacteria use to evade infection from mycobacteriophages, including SIE, nucleic acid modifications and CRISPR Cas, are expected to be in effect when a bacteriophage infects but should not interfere with “lysis from without” by endolysins.

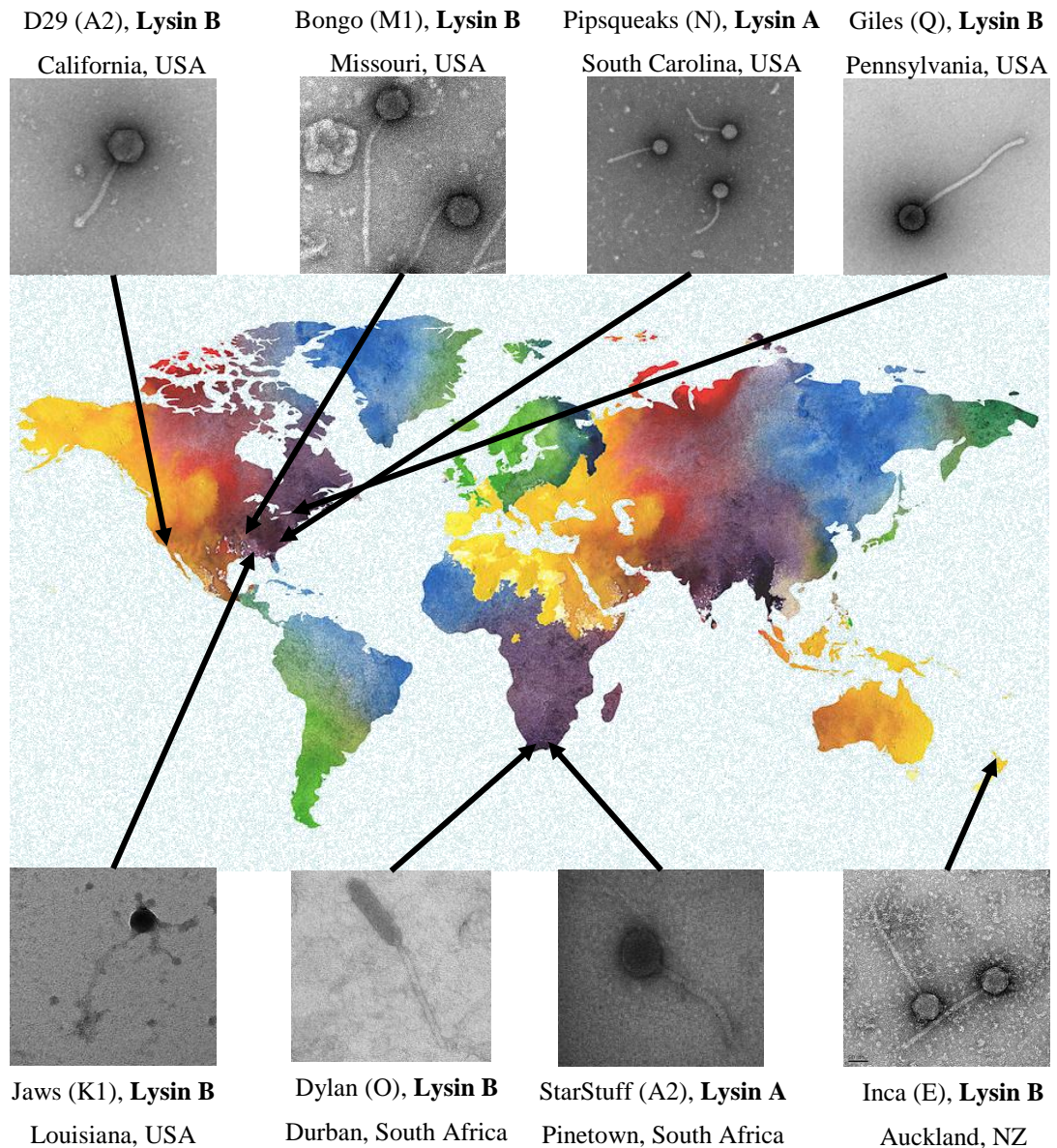


Figure 12: Bacteriophage endolysin geographic location

The eight endolysin candidates comprised of six lysin B's and two lysin A's are located across the North and South hemisphere, throughout three countries encompassing island nations and landlocked countries. Clusters are labelled in brackets. These bacteriophages are all siphoviridae (tailed bacteriophages), however Dylan is distinctly different displaying a longer capsid head approximately one third the size of the whole bacteriophage. The other bacteriophages vary in tail length but remain true to the siphoviridae morphotype. We can see that there is no correlation between phenotypic characteristics of these bacteriophage morphotypes based on geographic location.

3.1.4 Verifying lysin-like domains are present using HHpred

The last check we wanted to perform in order to confirm that the eight genes that we had selected for this project were true lysins, was to evaluate the domains in each gene using HHpred. HHpred used a multiple sequence alignment to detect protein homology and conserved domains.

D29 Lysin B, the positive control in this work causes “lysis from without” through the presence of the α/β hydrolase, with a catalytic triad common to cutinases, containing an additional four-helix domain involved in the binding of lipid substrates. (K. Payne et al., 2009). D29 is a mycolylarabinogalactan esterase that functions by cleaving the specific ester linking the mycolic acid-rich outer membrane to the arabinogalactan releasing free mycolic acids during lysis, is it therefore a crucial component for lysis (K. Payne et al., 2009). The presence of the α/β hydrolase domain will be a further indication that the genes we have selected will act as a lysin in this trial. We used the lysin B amino acid sequence from bacteriophage D29 as a primary reference to explore the presence or absence of domains that have similar lysin-like activities. Further comparing to the endolysin candidates selected from bacteriophage D29 lysin B, this protein was used as a reference to explore the presence of lysin-like domains. HHpred outputs give the name of the conserved domains that are part of the protein structure found four different conserved domains across all of the eight endolysins (Table 5).

Table 5: Domain analysis of Lysin-like proteins by HHpred

Lysin	Conserved domain ID	Name	Probability	E-value
StarStuff (lys A)	00325	chitinase_glyco_hydro_19	99.70	7.1e-20
Pipsqueaks (lys A)	00325	chitinase_glyco_hydro_19	99.75	2.8e-21
D29 (lys B)	00707	Pancreat_lipase_like	96.76	2.2e-4
Jaws (lys B)	00707	Pancreat_lipase_like	95.72	6.1e-3
Inca (lys B)	00741	Lipase	94.74	1.5e-2
Giles (lys B)	00741	Lipase	95.87	2.5e-3
Dylan (lys B)	00707	Pancreat_lipase_like	94.17	8.6e-2
Bongo (lys B)	00519	Lipase_3	97.14	2.6e-5

There are four different conserved domains listed as the top match (highest probability score and lowest e-value) for each of the lysins. Conserved domains chitinase_glyco_hydro_19 (a chitinase) was observed for both lysin A's, whereas a variation of lipase domains including Pancreat_lipase_like, Lipase and Lipase_3 were identified for each of the lysin B's. Upon further investigation, each of these slightly different conserved domains have the same function as a lipase.

One conserved domain chitinase_glyco_hydro19 was identified as the top hit for both lysin A proteins and although there were three conserved domains for the lysin B proteins, they were all associated with lipase activity. The interpretation of the lysin A and lysin B analyses are discussed further below.

3.1.4.1 Lysin A domain analysis

HHpred suggested strong evidence of lytic activity for StarStuff and Pipsqueaks with the chitainse_glyco_hydro_19 hit observed with over 99.7% probability for both lysin A's. HHpred lists this class of chitinase as “Glycoside hydrolase family 19 chitinase domain. Chitinases are enzymes that catalyse the hydrolysis of the beta-1,4-N-acetyl-D-glucosamine linkages in chitin polymers” (Zimmermann et al., 2018). Payne and colleagues identified lysin A candidates that also contain the 00325 chitinase domain and Catalão and colleagues noted that this domain has previously been identified mainly in cluster A mycobacteriophage (StarStuff is cluster A2), however there is little information

listed about chitinase presence in cluster N mycobacteriophages, which is the cluster of Pipsqueaks, although there is no evidence to suspect the contrary (Catalão & Pimentel, 2018; K. M. Payne & Hatfull, 2012). Based on the earlier definition of clusters from Hatfull and colleagues, the assignment of mycobacteriophage to clusters does not appear to correlate to any significant difference in lysin domain characterisation at this stage due to the highly mosaic nature of bacteriophage evolution and both inter-cluster and intra-cluster relatedness reveals a continuum of genetic diversity (Pope et al., 2015). We hypothesise that a reason for clusters to not be informative is the highly mosaic nature of bacteriophage evolution which means that each bacteriophage genome can be considered as a unique combination of modules that are exchangeable throughout the population (Hatfull, 2008). Once again, the inclusion of clusters in the early stages of this research was just to help group bacteriophage so we had a pool of largely differing bacteriophages. Proteins that encompass chitin-like domains generally act on the β -glycosidic linkages that are present in chitin and the peptidoglycan cell wall components (Catalão & Pimentel, 2018). These data therefore further support the assignment of lysin A properties to the two selected lysin A genes that are annotated in StarStuff and Pipsqueaks, both of which we will use for nanobead expression.

3.1.4.2 Lysin B domain analysis

In comparison, the conserved domains for the lysin B candidates suggest they are part of the lipase domain class. Basing the previous extensive research around lysin B lytic activity of D29, the D29 domains will form the basis of this analysis. It can be seen in Table 5, that D29, Jaws and Dylan share an identical match as the top hit; Pancreat_lipase_like, which HHpred describes as “Pancreatic lipase-like enzymes. Lipases are esterases that can hydrolyse long-chain acyl-triglycerides into di- and monoglycerides, glycerol, and free fatty acids at a water/lipid interface” (Zimmermann et

al., 2018). Similarly, to the lysin A cutinases, lysin B lipases, cutinases and esterases are all lipolytic enzymes, members of the serine hydrolase family that all fall into the large α/β hydrolase superfamily (Arpigny & Jaeger, 1999; Catalão & Pimentel, 2018; Z. Chen et al., 2007; Gupta, Gupta, & Rathi, 2004). The activity of these lipases is centred around the catalytic triad of specifically ordered Ser, Asp (or Glu) and His amino acid sequences, identified through the crystalline 3D structure of D29, Fig. 3, the Ser amino acid is highly conserved (Catalão & Pimentel, 2018). The primary lipase domain demonstrates the underlying lytic ability under the α/β hydrolase family, and the subsequent hits still fall into the hydrolytic enzyme classes.

Conserved domain 00741; Lipase, was the top hit for Inca and Giles. HHpred describes the lipase domain as “Lipases are esterases that can hydrolyse long-chain acyl-triglycerides into di- and monoglycerides, glycerol, and free fatty acids at a water/lipid interface” (Zimmermann et al., 2018). This definition is only slightly modified from that of conserved domain 00707 with the basic lipase function described. Therefore, we can be confident that these domains are very similar in function, suggesting further evidence towards correct annotation and proposed lytic ability for Inca and Giles too.

Bongo was the only lysin B with a top hit independent of the other five lysin B's; lipase_3. Nevertheless, the HHpred definition of lipase_3 is identical to domain 00741 “Lipase” suggesting the overarching function is based on the same lytic principles.

We can be confident progressing further into the pET-14b plasmid fusion and biodegradable nanobead construction and testing, with the bioinformatic evidence analysed.

3.1.5 PhaC pET-14b plasmid construct

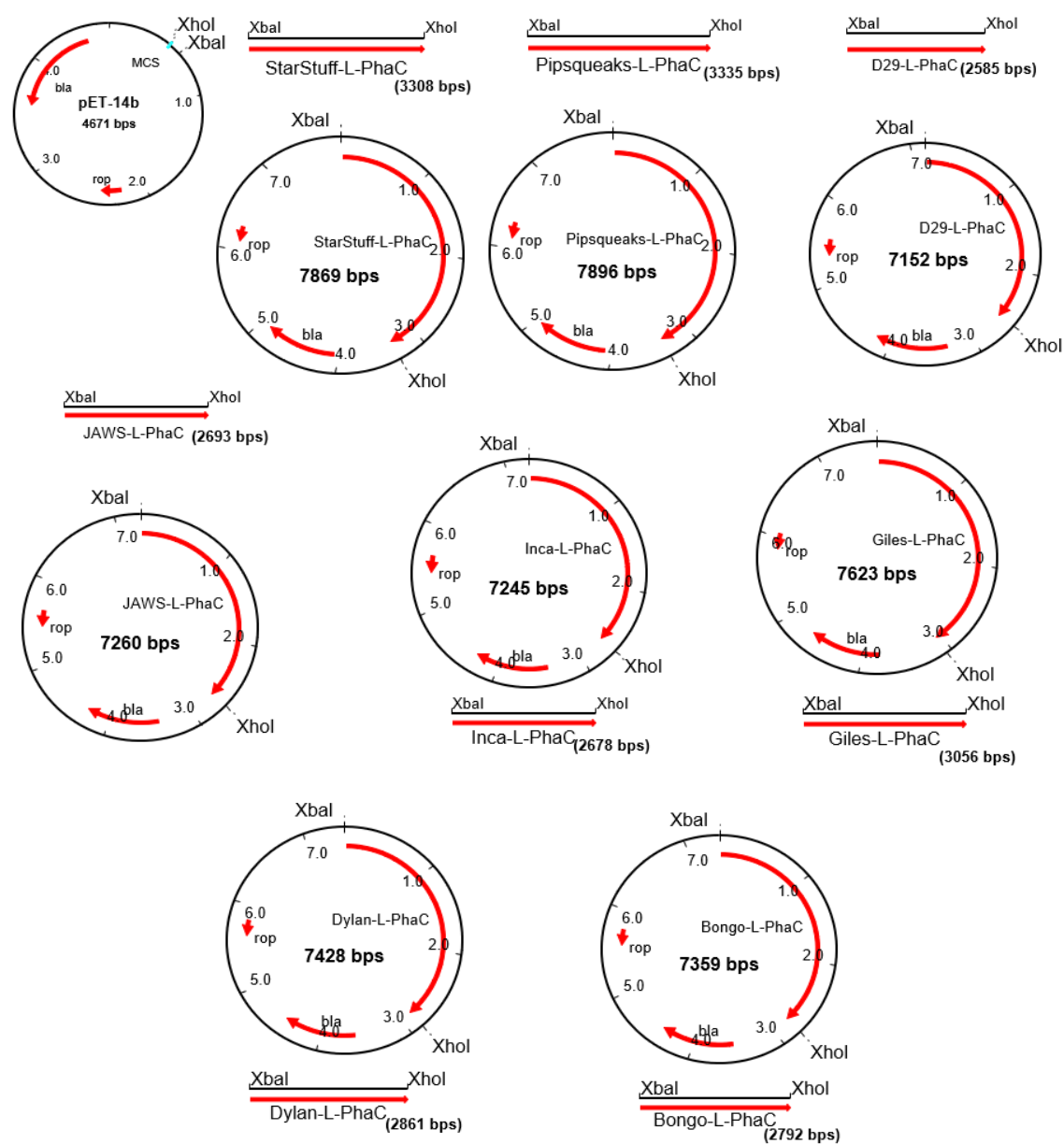


Figure 13: pET-14b endolysin fusion plasmid constructs

Designed by Eric Altermann (AgResearch) using Plasmid Map Enhancer for Windows 95. All molecules are drawn to scale with pET-14b as a reference.

Once the endolysins were chosen and their annotations were verified, each of the eight amino acid sequences was subjected to mRNA stabilisation and codon optimisation for expression in an *Escherichia coli* background by Eric Altermann (AgResearch) using the on-line tools available from DNA synthesis company, GeneArt. The pET-14b expression vector is comprised of a *lacI* gene that encodes a *lac* repressor, a *lac* operator, a T7 promotor that is specific for RNA polymerase, AMP resistance gene and an origin of replication (Fig. 13). The vector is designed to overproduce proteins fused to the surface of the nanobead by enabling high expression by the T7 RNA polymerase as a result of *E. coli* BL21 production.

More specifically in this project, the mycobacteriophage endolysins (lysin A and lysin B) were each incorporated into the pET-14b expression vector and then transformed into *E. coli*, which contains the plasmid for nanobead production.

3.2 PART TWO: Expression and production of biodegradable lysin nanobeads

This section discusses the results of making the biodegradable nanobeads with lysins fused to the surface *in vitro* both in AgResearch, Palmerston North, as well as Massey University, Albany Campus.

3.2.1 Establishing expression of PhaC in *E. coli* with a Nile Red stain

Once the expression vectors were created they were transformed into *E. coli* and expressed. Briefly, transformation of the expression vectors was confirmed by selection on Amp LB plates (see materials and methods). Cultured representative single colony isolates were frozen down at -80°C. Cultures of each plasmid were induced (see Materials & Methods) and Nile Red stain was used to visually confirm the PHA nanobeads within living *E. coli* cells (Fig. 14). Nile Red dye is a hydrophobic fluorogenic dye that associates strongly with the PHA (Peters & Rehm, 2005; Robins, Hooks, Rehm, & Ackerley, 2013). Nile Red was used to identify the presence of PHA nanobeads prior to *E. coli* cell lysis and also as a qualitative method to determine the yield percentage of each lysin nanobead compared to the other lysin nanobeads.

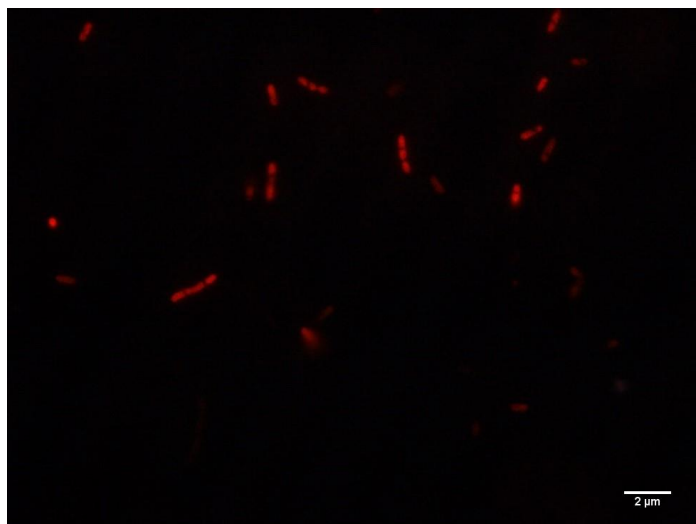


Figure 14: Nile Red stain to detect presence of lipid nanobeads

After the expression of PhaC in the nanobeads through the growth of the *E. coli* culture induced with IPTG, a small volume of beads were treated with Nile Red stain and visualised under the fluorescent microscope to estimate yield. This photo is of the lysin B D29 nanobeads and illustrates the beads that have picked up the stain due to the presence of lipids and have fluoresced red. This evidence was used as further evidence of bead presence prior to lysis.

3.2.2 Purifying nanobeads

Table 6: Amount of nanobeads harvested

A	Lysin	Amount of nanobeads harvested (mg)
	StarStuff (LysA)	589.9
	Pipsqueaks (LysA)	387.2
	D29 (LysB)	366.0
	Jaws (LysB)	453.0
	Inca (LysB)	473.1
	Giles (LysB)	908.0
	Dylan (LysB)	447.2
	Bongo (LysB)	344.9
	PhaC (no lysin)	331.4



A) Table 6. All of the beads yielded at least 300mg of nanobeads. This data was an average of each of the nanobead productions because the tests for cell death often required more production of these nanobeads. There does not appear to be any relationship between the type of lysin and the amount of nanobeads harvested.

B) Figure 15: Purified nanobeads indicated by the white band in the glycerol gradient

These beads were then separated into a Falcon tube by pouring off the glycerol and centrifuged. Beads that were contaminated could not be observed in a white band, instead a sticky white precipitate at the bottom of the polypropylene tube.

3.2.3 Dealing with contamination

When making the lysin nanobeads for the first time at AgResearch, Palmerston North, there appeared to be contamination in the beads when streaking them out on 1.5% LB plates. The suspect colonies looked similar to the *E. coli* colony morphology that had been observed with the *E. coli* BL21 transformed with the plasmid. To confirm this, we streaked out the beads on 1.5% LB + AMP + CM which WT bacteria would be sensitive to and not grow, however the *E. coli* BL21 contamination persisted, suggesting this was the cause of the contamination (Fig. 16). The cause of contamination was probably insufficient lysis. Although the aseptic practices differed greatly at either institution, this could not be ruled out as the cause. At the Massey University, Albany, the chemical lysis using lysis buffer, lysozyme and DNaseI stayed constant, yet the physical lysis step changed from using a microfluidiser at AgResearch to a sonicator at Massey University. I had to change the lysis method when travelling between laboratories, yet the change in physical lysis technique appeared to result in more lysis and therefore less contamination of unlysed *E. coli* BL21 which was an advantage.

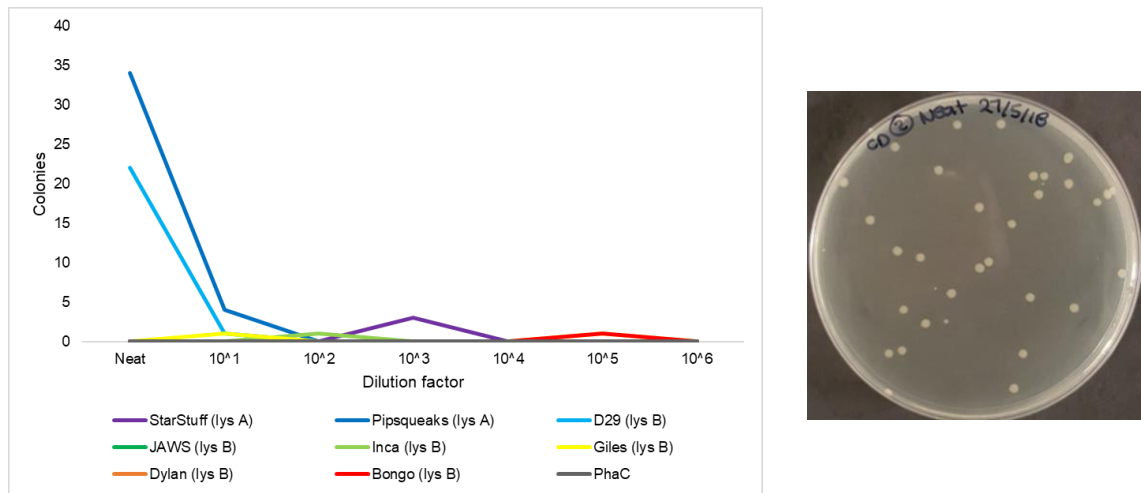


Figure 16: Contamination across increasing dilutions

A) We can see that the number of colonies correlates to the increase in dilution, with each increase in dilution resulting in a 10-fold decrease in colony counts, especially visible for Pipsqueaks and D29. This suggests that the contamination is from the bead solution rather than a chance contamination on a few plates. B) The medium sized, round, off-white colony morphology initially suggested *E. coli* as the likely contaminant. Because this laboratory does not work with this strain of *E. coli* beyond this project, it is likely that this is a result of insufficient lysis.

A Gram stain was carried out on representative contaminating colonies. As can be seen in Fig. 17 below, the pink, rod shaped cells are indicative of Gram-negative *E. coli* and as a result better physical lysis approaches were ensured when moving on to produce more endolysin nanobeads.

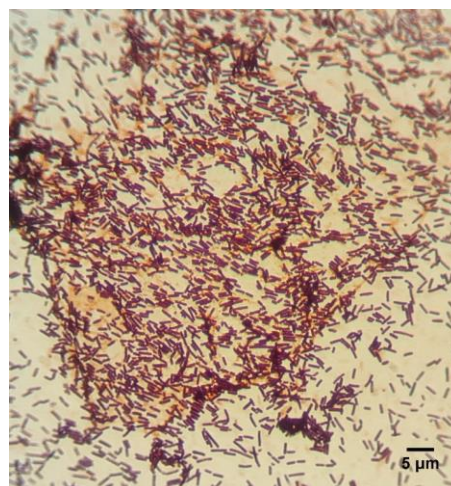


Figure 17: Gram stained contamination indicated Gram-negative bacterium present

The pink stained rod shapes are indicative of a Gram-negative bacterium and the persistence in LB plates supplemented with AMP and CM yet the sensitivity to CB and CHX suggest *E. coli* contamination. Gram-negative bacteria have a thin peptidoglycan layer and outer membrane, therefore they do not take up the primary stain, instead retaining the secondary counterstain (sarafin) illustrating a pink/red colour.

3.2.4 Endolysin nanobead size differences

In order to establish what physical differences might appear in the nanobeads due to fusion and expression we sent samples of the nanobeads for EM. The nanobeads ranged in size from averages of $0.434\mu\text{m} \pm 0.149$ through to $1.787\mu\text{m} \pm 0.456$ (Fig. 18). This box and whisker plot illustrates the difference in mean lysin length in relation to the lysin type. For example, both StarStuff and Pipsqueaks who were lysin A's have mean lysin lengths of $1.787\mu\text{m} \pm 0.456$ and $1.722\mu\text{m} \pm 0.409$. This is different to the lysin B lengths which average from $0.592\mu\text{m} \pm 0.0123$ to $0.896\mu\text{m} \pm 0.0226$. A two sample t-test of the average nanobead sizes of lysin A's compared to lysin B's revealed a p-value of 4.34×10^{-6} , which indicated an extremely significant difference to the lysin B lengths which average from $0.592\mu\text{m} \pm 0.0123$ to $0.896\mu\text{m} \pm 0.0226$.

Table 7: Endolysin nanobead mean bead sizes

Lysin name	Lysin type	Mean bead size
PhaC	No lysin	0.434 ± 0.0149
StarStuff	lysin A	1.787 ± 0.0456
Pipsqueaks	lysin A	1.722 ± 0.0409
D29	lysin B	0.640 ± 0.0189
Jaws	lysin B	0.757 ± 0.0232
Inca	lysin B	0.616 ± 0.0171
Giles	lysin B	0.896 ± 0.0226
Dylan	lysin B	0.592 ± 0.0123
Bongo	lysin B	0.620 ± 0.0197

There is a significant difference ($p=4.34 \times 10^{-6}$) in the size of endolysin nanobeads between lysin A, lysin B and the negative control of PhaC. The largest two bead sizes were StarStuff and Pipsqueaks (both lysin A) and the smallest was the negative control (PhaC).

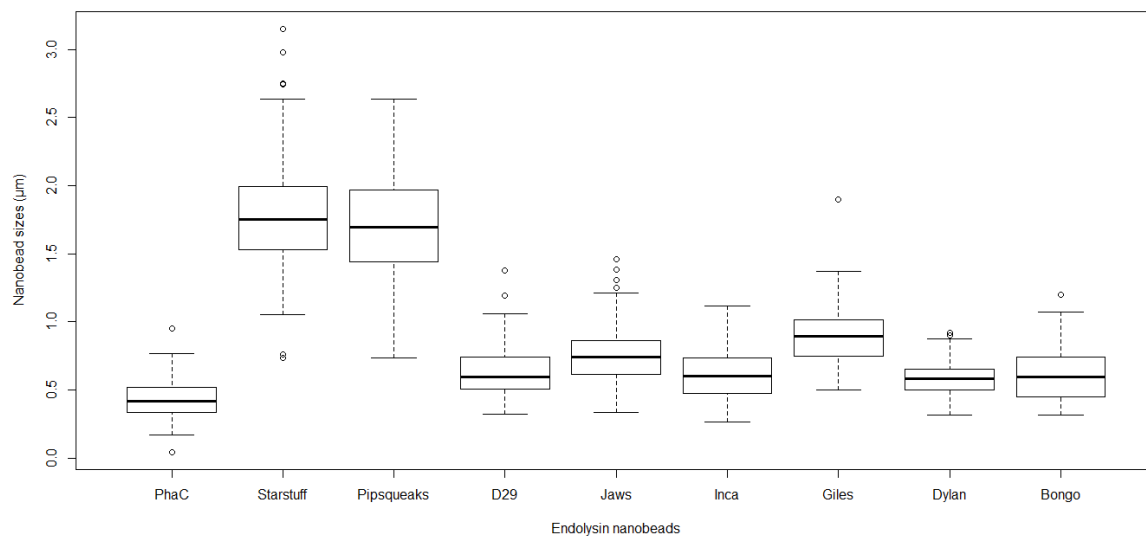
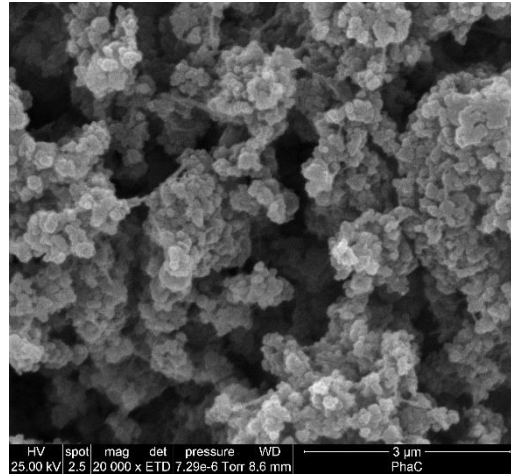


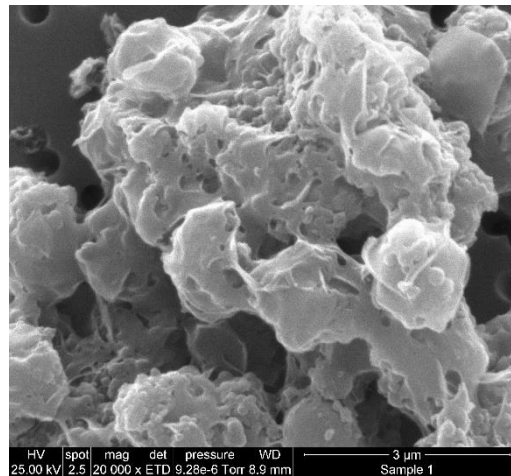
Figure 18: Endolysin nanobead size differences

PhaC (negative control with no endolysin N-terminal fusion) has the smallest size. The lysin A candidates, StarStuff and Pipsqueaks have the largest bead sizes, whilst there is also a noticeable difference between the lysin A and the lysin B candidates, despite the occasional outlier.

PhaC



**StarStuff
(lys A)**



**D29
(lys B)**

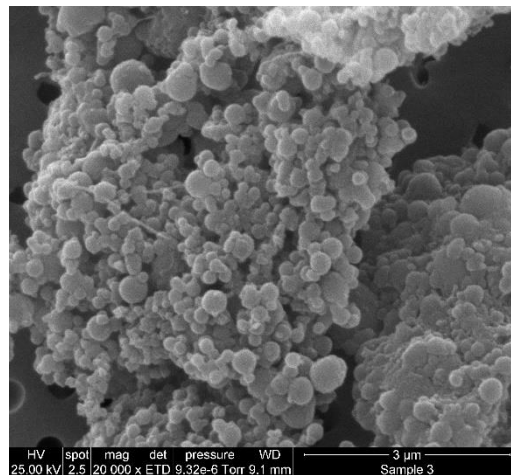


Figure 19: Scanning Electron Microscopy of three lysin nanobeads

A) PhaC nanobeads with no endolysin attached. The mean size of these beads is $0.434\mu\text{m} \pm 0.0149$. B) StarStuff nanobeads with lysin A fused to the surface. The mean size of these beads is $1.787\mu\text{m} \pm 0.0456$. C) D29 nanobeads with lysin A fused to the surface. The mean size of these beads is $0.640\mu\text{m} \pm 0.0189$. Microscopy carried out by the Manawatu Microscopy & Imaging Centre.

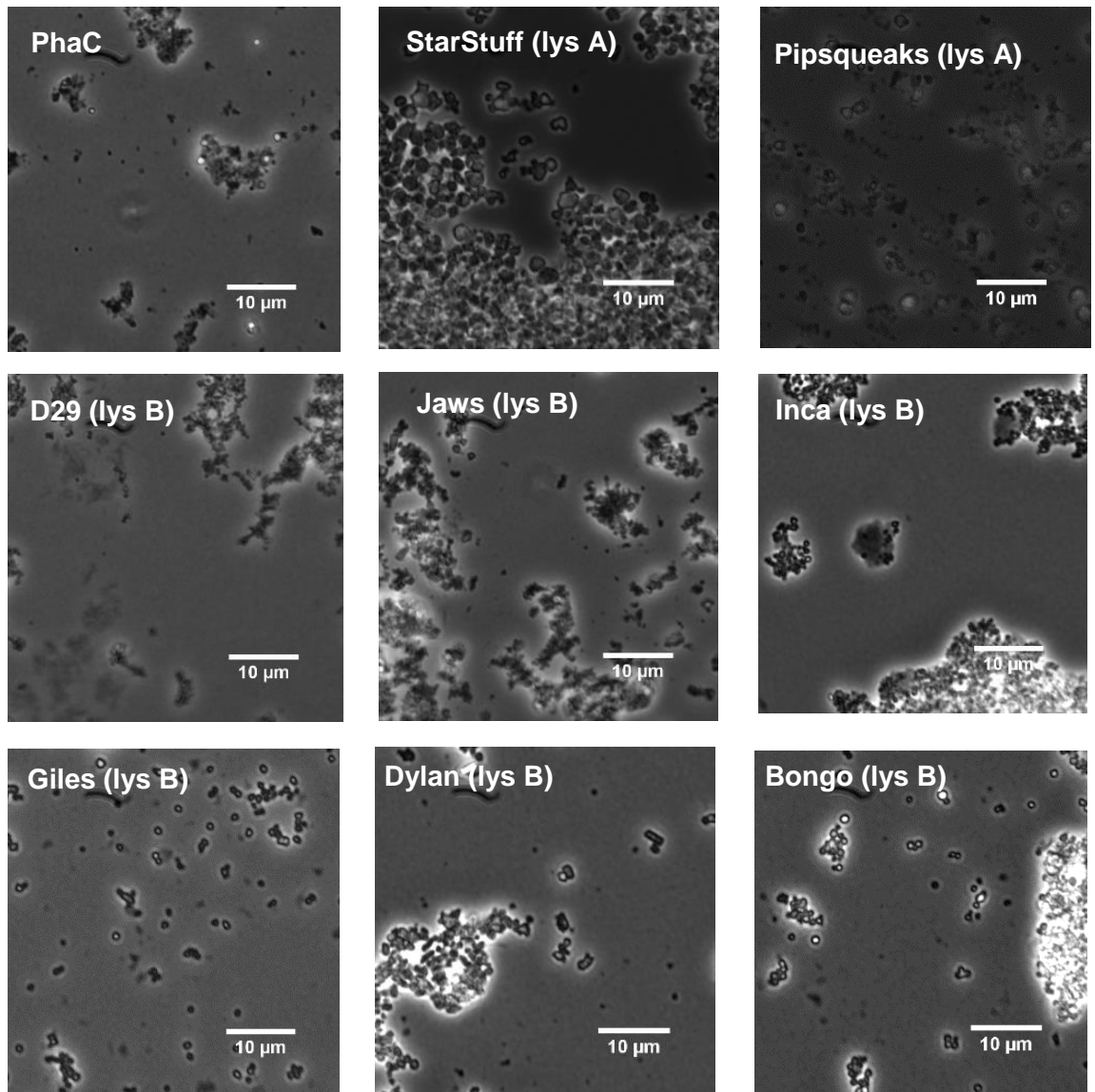


Figure 20: Phase contrast 100X microscopy of unstained lysin nanobeads

Unstained phase-contrast microscopy illustrates the significant size difference between the lysin A and lysin B nanobeads.

Nanobead fusions to lysins appear to have significantly different sizes, depending on the type of lysin (Table 7, Fig. 18 and 20). This was unexpected and may implies some complex biochemical process in action with the different Pha phasins regulating PHA accumulation thus controlling size as well as composition given the particular fusion protein (Możejko-Ciesielska & Kiewisz, 2016; Singh, Kumar, Ray, & Kalia, 2015). This could be a potential reason as to why the size of the two lysin A's are similar to each other, and the six lysin B's are also similar in size, however neither lysin type is similar to the other overall.

Two main hypotheses were suggested as a possible explanation of this result. The first is that perhaps the lysin A nanobeads are much bigger because there is oligomerisation between the C-terminal binding sites of the lysin interacting with each other, resulting in a folding of the protein or larger clumping as the lysin proteins join into an oligomer. When looking at Fig. 19, the beads in StarStuff do not appear any less circular than their smaller counterparts PhaC in nor D29.

Plenty of research presents the idea that holins form holin-oligomerisation compounds when creating a lesion hole in the cell wall for the endolysin to make contact with (Catalão, Gil, Moniz-Pereira, & Pimentel, 2011; Gründling, Bläsi, & Young, 2000; Saier & Reddy, 2015). Catalão and colleagues demonstrate evidence of mycobacteriophage Ms6 lysin A proteins oligomerising with a holin after expressing lysin A (GP4) and holin (GP5) monomers through *E. coli* BL21 membrane fractions and running a Western blot and observing bands indicative of monomers, dimers, whilst also concluding that the final degree of oligomerisation of lysin A is not yet known (Catalão et al., 2011). The oligomerisation potential of the Ms6 lysin A may indicate the risk of oligomerisation with just lysin A monomers such as StarStuff and Pipsqueaks in this trial.

An additional hypothesis is that the lysin B proteins that target the peptidoglycan cell wall are interacting with the *E. coli* cell wall during expression and lysis for nanobead harvest. Consequently, Gram-negative *E. coli* does not have any mycolic acids, as seen in cell wall Fig. 2, which is a unique component of the mycobacterial cell wall. As a result, there could be some biological activity between the peptidoglycan hydrolase lysin B during the isolation process. This will be further explored in section 3.3 as the efficiency of the lysin nanobeads is assessed against *M. smegmatis*.

3.3 PART THREE: Testing antimicrobial activity against *M. smegmatis*

Once the endolysins had been verified and produced in a repeatable, sterile manner, it was time to conduct tests of the antimicrobial properties of these nanobeads by exposing them to *M. smegmatis* cultures. A range of tests including live/dead stain microscopy, shaking cultures nanobead exposure measured by OD in a plate reader, nanobead exposure in static cultures assayed by colony plate counts were attempted first. Late an applied test which used either hospital masks or a filter paper analogue and colony counts as a proof-of-concept approach. In the last instance, we were interested in seeing the degree to which such an approach could be a potential prophylactic tool for health care workers treating tuberculosis in developing nations.

3.3.1 Test one: detecting cell death through fluorescent microscopy

As an initial start point to visualise the presence of dead *M. smegmatis* cells as a result of the endolysin nanobead lysis activity by exposing *M. smegmatis* to two different concentrations of nanobeads to infect for 5 hours before putting 2µl onto an agarose pad and using fluorescent microscopy to measure cell death as seen by live/dead staining with propidium iodide (see Materials and Methods for detailed methods).

The results in Table 8 below are relatively consistent; cell death appears to take place in a very small number of cells by this measure. Between 2.5% and 11% of cells appears to be killed according to this assay. As we considered the results however, we noted the presence of completely lysed cells in our microscopy results. We reasoned that if nanobead exposure results in complete cell lysis then with completely destroyed cells the propidium iodide stain (which has high affinity to DNA) would be unable to stain the lysed cells. After a series of tests using microscopy, this experiment was changed due to inaccuracy and the second test, using a plate reader was initiated.

Table 8: Live/dead stain of *M. smegmatis* after exposure to nanobeads

Lysin	Nanobead concentration (mg/ml)	Live cells (%)	Dead cells (%)
<i>M. smegmatis</i>	Untreated	97.20 ± 0.025	2.80 ± 0.025
	Untreated	96.90 ± 0.029	3.10 ± 0.029
PhaC (no lysin)	100	97.23 ± 0.13	2.77 ± 0.13
	800	97.46 ± 0.14	2.54 ± 0.14
StarStuff (lysA)	100	92.60 ± 0.036	7.40 ± 0.036
	800	92.33 ± 0.46	7.67 ± 0.46
Pipsqueaks (lysA)	100	91.11 ± 0.41	8.89 ± 0.41
	800	90.99 ± 0.32	9.01 ± 0.32
D29 (lysB)	100	95.87 ± 0.015	4.13 ± 0.015
	800	94.32 ± 0.51	5.68 ± 0.51
Jaws (lysB)	100	93.40 ± 0.14	6.60 ± 0.14
	800	94.65 ± 0.42	5.35 ± 0.42
Inca (lysB)	100	92.70 ± 0.25	7.30 ± 0.25
	800	91.58 ± 0.065	8.42 ± 0.065
Giles (lysB)	100	88.50 ± 0.32	11.50 ± 0.32
	800	92.78 ± 0.78	7.22 ± 0.78
Dylan (lysB)	100	96.22 ± 0.002	3.78 ± 0.002
	800	95.76 ± 0.18	4.24 ± 0.18
Bongo (lysB)	100	90.98 ± 0.085	9.02 ± 0.085
	800	94.36 ± 0.096	5.64 ± 0.096

Table showing the cell death (%) of each *M. smegmatis* culture after exposure to the corresponding nanobead at 10mg/ml and 80mg/ml (the lowest and highest concentrations).

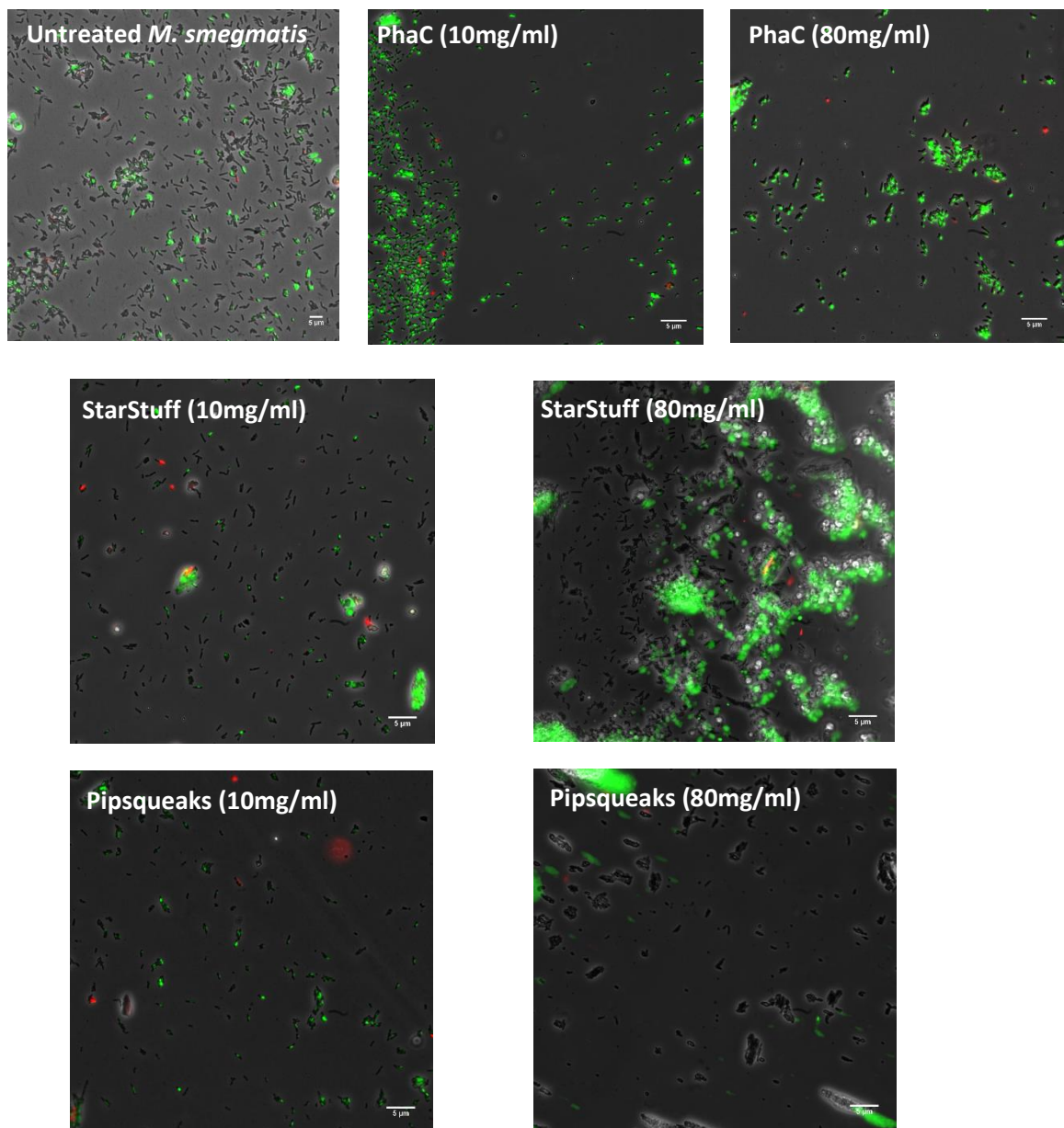


Figure 21: Fluorescent microscopy of *M. smegmatis* exposed to nanobeads (1)

Even though the 80mg/ml exposure concentrations have four times higher lysin concentration, there is still no significant presence of dead cells that would show up in red. A second difficulty is the fluorescent nature of the nanobeads making it difficult to accurately count cells under fluorescence. The scale bar is set to 5μm and each image is one of the three replicates.

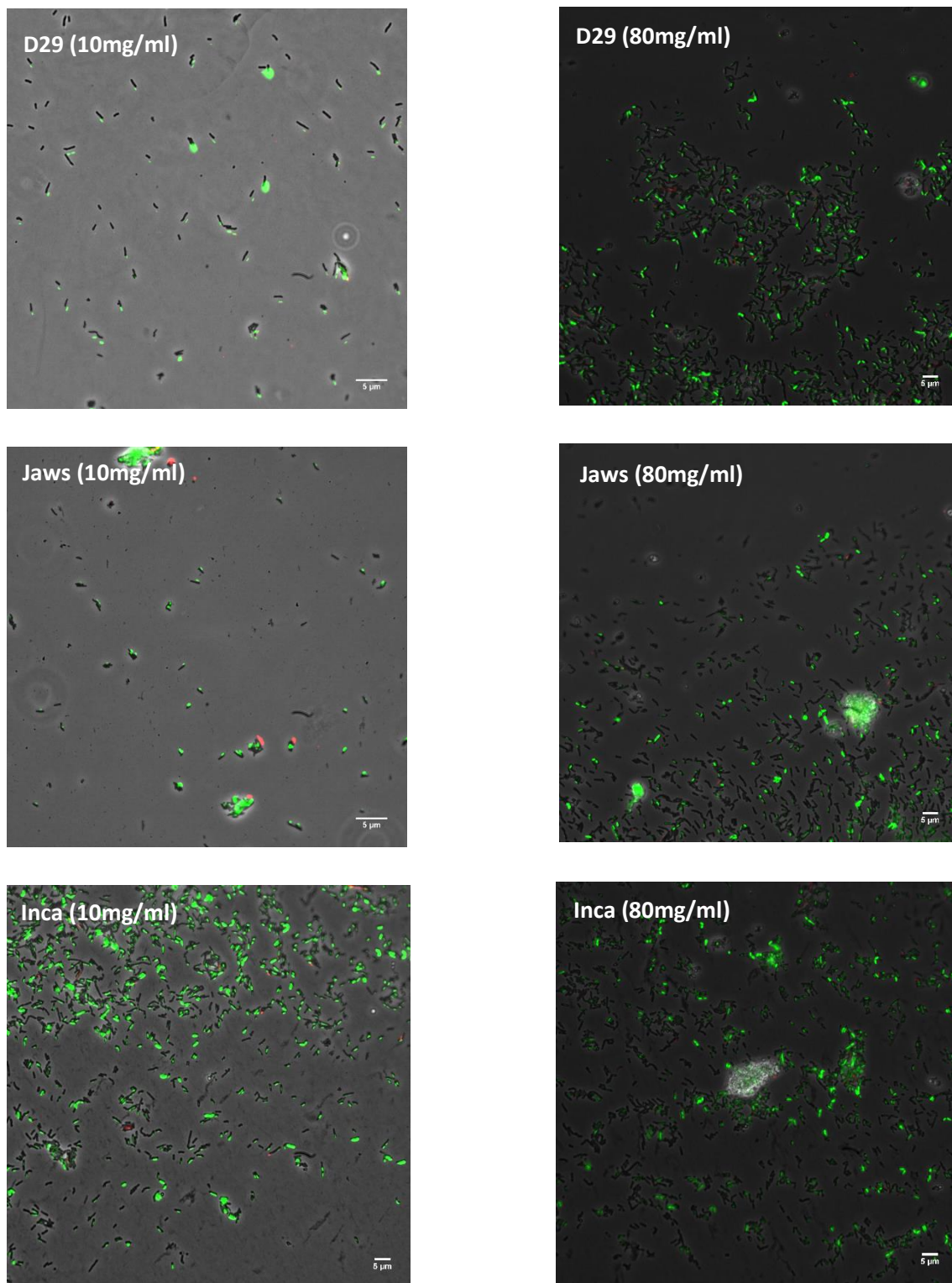


Figure 22: Fluorescent microscopy of *M. smegmatis* exposed to nanobeads (2)

Even though the 80mg/ml exposure concentrations have four times higher lysin concentration, there is still no significant presence of dead cells that would show up in red. A second difficulty is the fluorescent nature of the nanobeads making it difficult to accurately count cells under fluorescence. The scale bar is set to 5µm and each image is one of the three replicates.

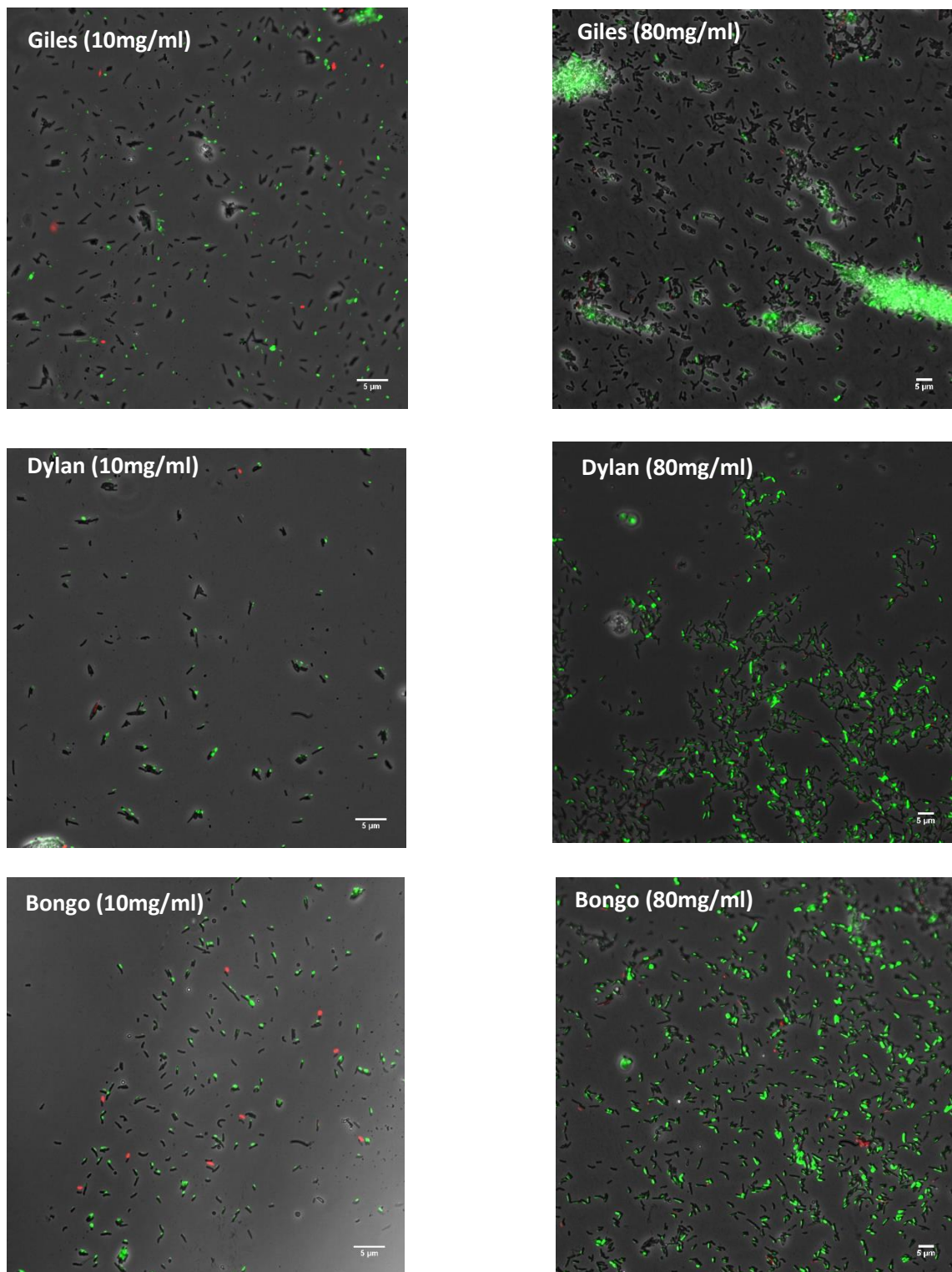


Figure 23: Fluorescent microscopy of *M. smegmatis* exposed to nanobeads (3)

Even though the 80mg/ml exposure concentrations have four times higher lysin concentration, there is still no significant presence of dead cells that would show up in red. A second difficulty is the fluorescent nature of the nanobeads making it difficult to accurately count cells under fluorescence. The scale bar is set to 5µm and each image is one of the three replicates.

The fluorescent microscopy test involved exposing *M. smegmatis* to two different concentrations of nanobeads and the percentage of live and dead cells were recorded.

As can be seen in Table 8 and Fig. 21, 22 and 23, there does not appear to be a lot of cell death, even after exposure at the highest concentration of nanobeads (80mg/ml). We would expect to see a lot more red cells throughout the microscopy, however this is absent. Test three was conducted shortly after to see if these results were indicative of the lytic activity of the nanobeads, or if in fact there was no lysis occurring. Another limitation to this study was that the nanobeads were extremely fluorescent, especially in high quantities and we were only able to view a small section under microscopy.

There also appear to be a few anomalies in the trend of data. We would expect that any cell death beyond what would naturally be occurring in *M. smegmatis* ($2.95\% \pm 0.15$) would be attributed to the increase in endolysin concentration from 10mg/ml to 80mg/ml. We can see that in Bongo, there is more cell death in the lower concentration of 10mg/ml and that is the same situation for Pipsqueaks, Jaws and Giles.

To conclude, using microscopy did not appear to be a reliable way to visualise cell lysis as any completely lysed cells would not pick up the PI stain or appear red. The next test was to use a plate reader to observe the change in optical density (OD) of the cells, where lysed cells decrease in optical density that can be tracked through a plate reader (Newton, Schofield, Vlahopoulou, & Zhou, 2016).

3.3.2 Test two: detecting cell death through a plate-reader assay

Instead of using a live/dead stain to understand the effect the nanobeads had on the cell death of *M. smegmatis* cultures, a kinetic (shaking) 96 well plate reader experiment was set up instead. Because *M. smegmatis* requires a lot of aeration when growing (traditionally grown in an aerated shaking conical flask), we included an autoclaved glass ball as one of the control additions to a second set of *M. smegmatis* wells and corresponding lysin nanobeads (Greening, Villas-Bôas, Robson, Berney, & Cook, 2014).

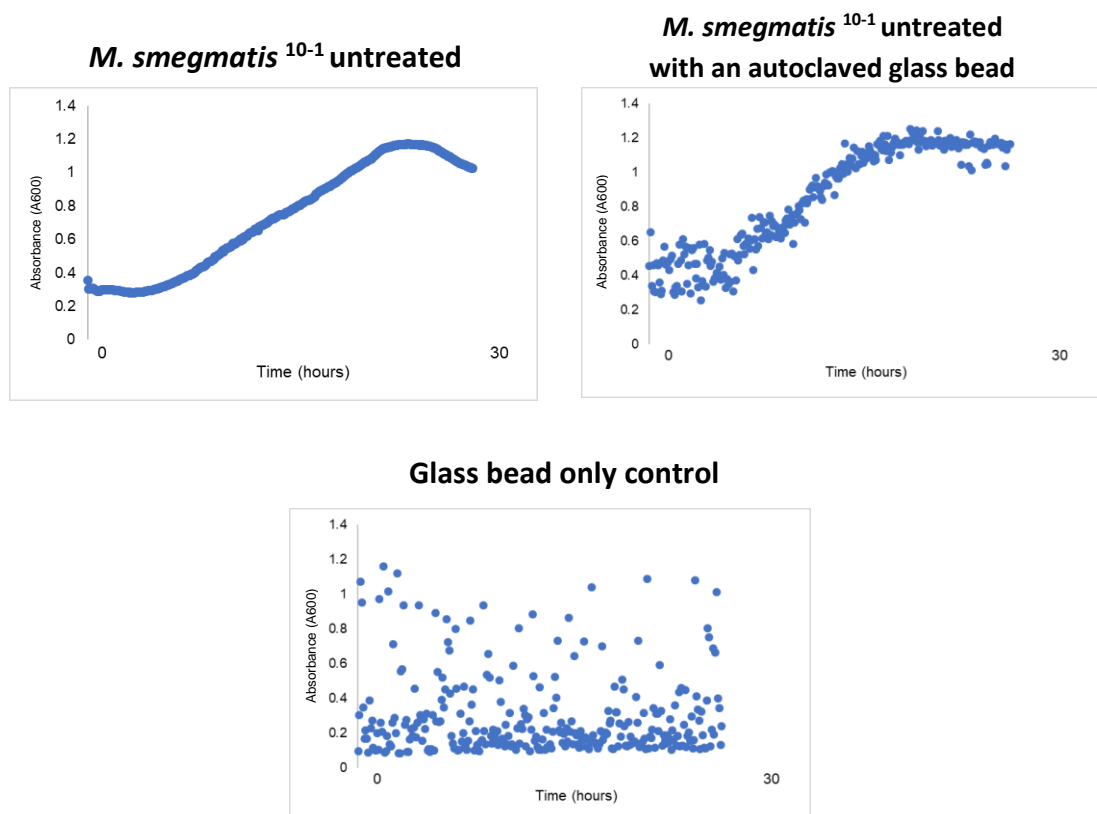


Figure 24: Plate reader graphs of *M. smegmatis* cell states

A) *M. smegmatis* 10^{-1} dilution demonstrating a standard exponential curve. After testing out a series of dilutions, this dilution was the most appropriate to test. B) *M. smegmatis* 10^{-1} dilution with an autoclaved glass bead to stimulate cell growth through increased aeration. Although only 100 μ l of *M. smegmatis* dilution was added to each well, we hypothesise that the increased aeration through a shaking stimulant (the bead) has caused small droplets to stay on the lid and distorted the absorbance reading slightly as C) the glass bead-only control shows a lot of “noise”.

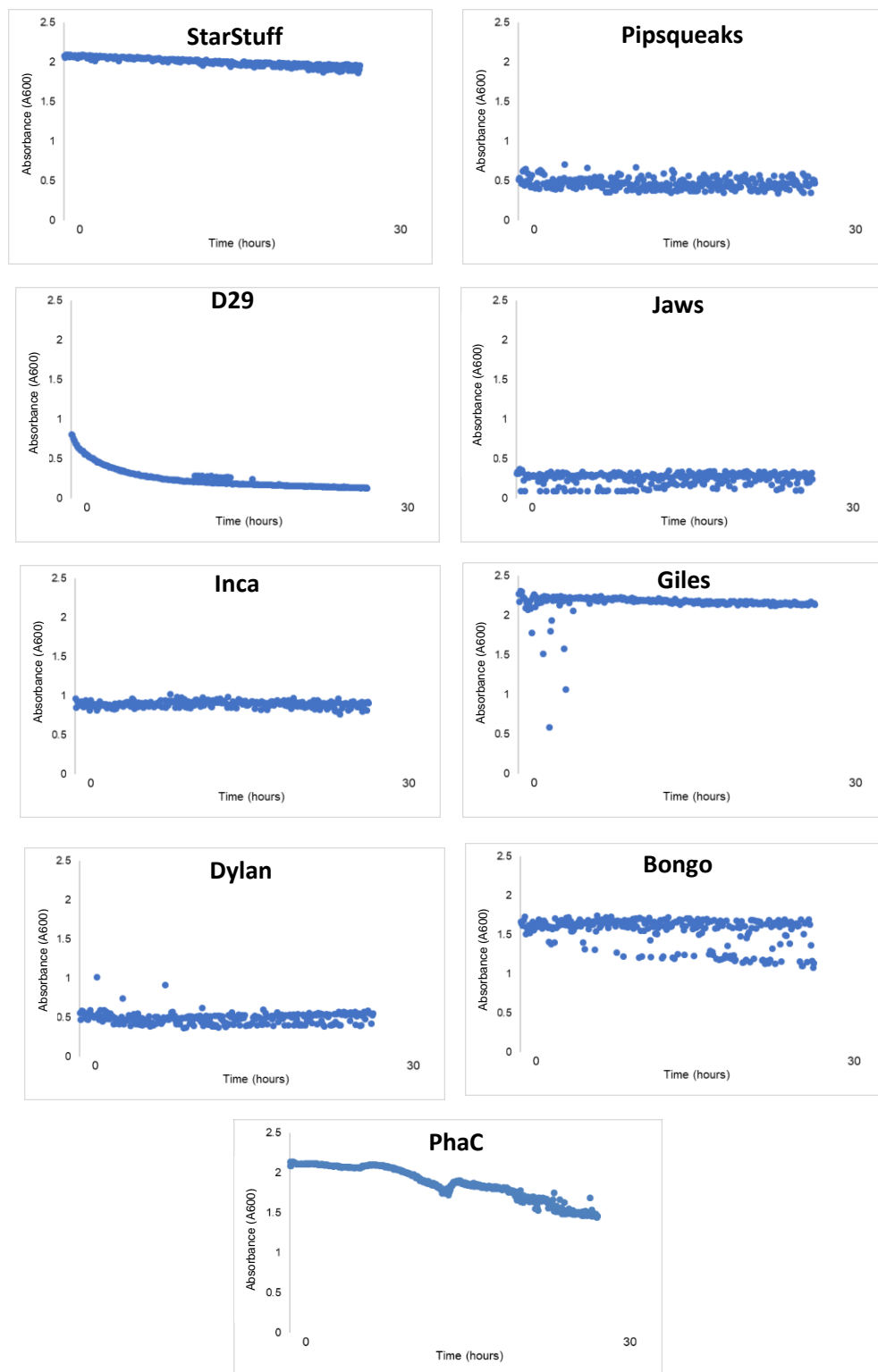


Figure 25: Endolysin nanobead controls in 96-well plate, no bacteria

There does not appear to be a constant absorbance reading between the nanobeads. Taking size into account, we would expect that there would be a larger constant absorbance reading for lysin A's StarStuff and Pipsqueaks as there is more bead mass, however this is only true for StarStuff. Giles and Bongo are both lysin B's that are smaller in size than the lysin A's, however we are seeing a higher OD compared to Pipsqueaks.

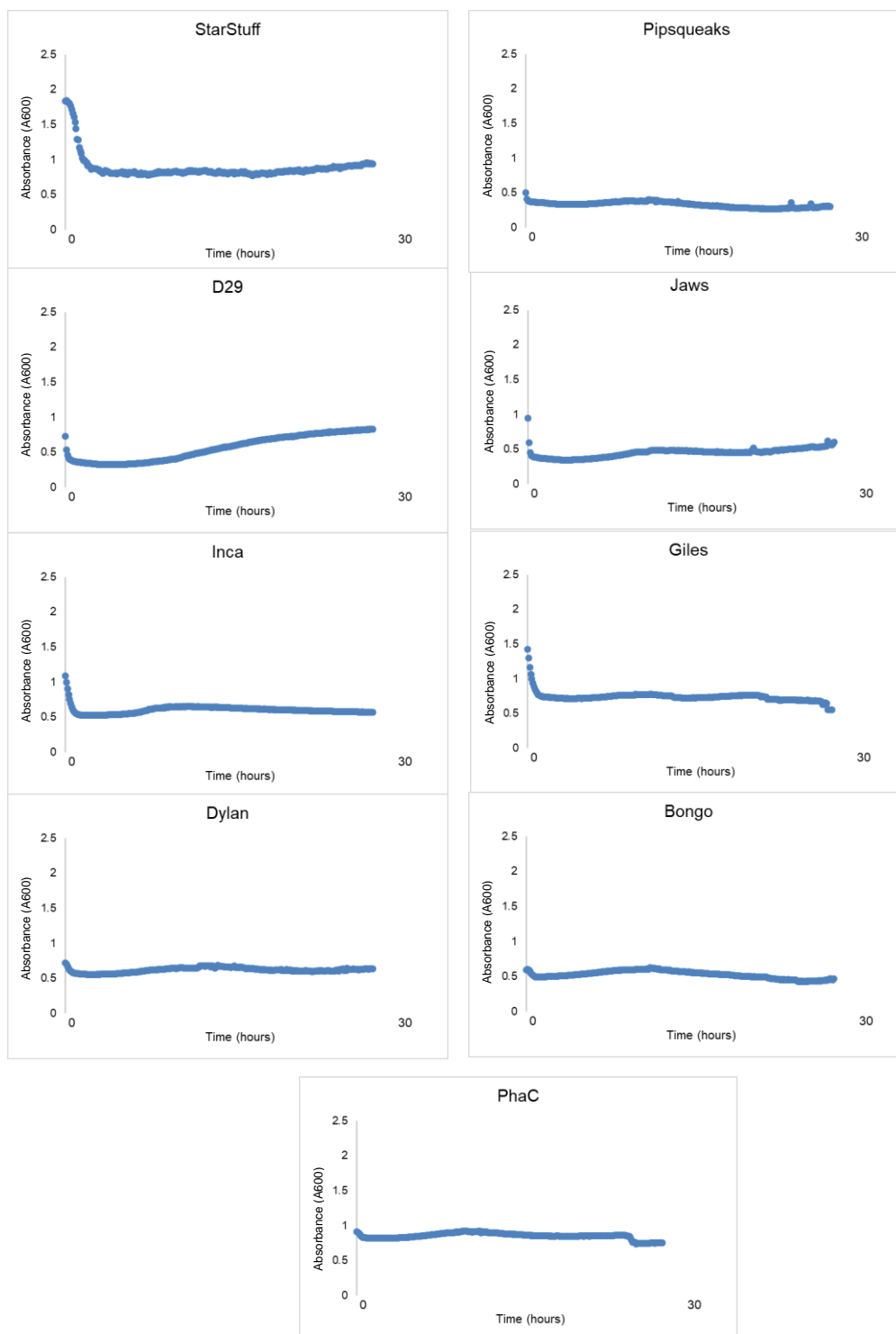


Figure 26: *M. smegmatis* after exposure to 10mg/ml endolysin nanobeads in the 96-well plate reader, shaking

The shaking plate reader resulted in difficult lysis conditions.

We first established the growth curves of the *M. smegmatis* culture in the 96 well plates. We found there was exponential growth under these conditions (Fig. 24). Because *M. smegmatis* requires aerated growth conditions, it seemed reasonable to include the addition of a sterilised glass bead to assist with aeration (Tillich et al., 2014). However, (Fig. 24) show the addition of the bead increased noise, but not to an appreciable degree.

We also wanted to test the nanobeads in order to understand if some of them had different levels of growth, or absorbance that they caused in the 96 well plates. We therefore put the nanobeads alone in the 96 well plate reader and saw that there were different levels of OD that remained constant throughout most of the experiment (Fig. 25). This suggested to us that perhaps the nanobeads were clumping, resulting in different absorbance readings between the nanobeads. This is unlikely related to size as we saw in Fig. 18 that StarStuff and Pipsqueaks (lysin A's) would have had a higher absorbance with a larger mass. We also see that Giles and Bongo (lysin B's) have an average absorbance above 1.5 too.

After establishing the growth of the bacterial cells and the optical properties of the nanobeads we were prepared to combine these in order to determine if the presence of the nanobeads changed the growth dynamics of the cells in 96 well plate readers. We saw uneven growth distributions that were difficult to conclude (Fig. 26), however we can hypothesise that once again there may be some clumping amongst the nanobeads. Nevertheless, we did not observe any prominent cell growth.

In retrospect it is clear that the plate reader was not the most reliable test of the lytic properties of the endolysin nanobeads when exposed to a 10^{-1} *M. smegmatis* culture. This may be because these cultures were shaking on the fastest setting, in excess of 200rpm, making it more difficult for the nanobeads to make contact for long enough to lyse. This

is necessary for culturing the *M. smegmatis* but not ideal for nanobead use. Although lysis in natural systems can take only seconds once the holin protein has created access to the peptidoglycan component of the cell wall for the endolysin to lyse, in our experiment, the endolysins were not in very close proximity to the bacteria, especially in the lower dilutions (10mg/ml and 20mg/ml) which may have made it more difficult to make contact for long enough time to be able to lyse the cell. Pohane and colleague Jain demonstrated cell lysis after 60-90 minutes of continuous infection and Briers and colleagues have observed lysis after 15 minutes (Briers, Peeters, Volckaert, & Lavigne, 2011; A. A. Pohane & Jain, 2015). Of course, those experiments were carried out inducing an internal endolysin-holin co-expression, so those results may not be immediately relevant to a nanobead mediated lysis. There is very little literature on the timing of lysis from without, yet we hypothesise that the concentration and contact time of endolysins has an impact on nanobead mediated cell death.

Because of this, we moved on to the third experiment, using a standing culture of *M. smegmatis* to expose the endolysin nanobeads reasoning that this was likely to be a more reliable test, and a truer mimicry of real-world applications. Spraying nanobeads on hospital masks and allowing surface mediated contact is not very similar to a constantly shaking emulsion.

3.3.3 Test three: detecting difference in colony counts

3.3.3.1 Testing cell death by exposing *M. smegmatis* to endolysin nanobeads for 45 minutes in a standing culture.

In order to test the effect of nanobead exposure in a standing liquid culture we used concentrations of 10mg/ml, 20mg/ml and 80mg/ml in 45 minutes and decided to switch our measurements from a live/dead stain approach, which did not account for cells that had completely lysed, to a method in which we plated the cells out and counted colonies in order to determine the consequences of the nanobeads on the number of live cells. All counts were calculated as percentages of cells grown and cultured in the same way without nanobeads. We observed variation between each of the replicates, but as the concentrations increased we observed a general increase in cell death in comparison to the untreated *M. smegmatis* control and PHA nanobead, which is the PhaC control with no endolysin attached (Fig. 27 and Table 9).

There are distinct differences in the effect of cell death based on concentration of endolysin exposed to *M. smegmatis*. We can see from Table 9, that 80mg/ml is the most effective concentration that results in cell death in most of the trials with Giles having the most lytic effect causing $71.99\% \pm 3.30$ cell death. Jaws (lysB) and Dylan (lysB) are the least effective in cell lysis at 20mg/ml. With only three replicates, we would expect to see a different trend towards increasing lysis with more trials completed. When looking at the raw data (not displayed), although *M. smegmatis* cell death remained constant ~3%, each of the replicates varied, and as cell death point was calculated in respect to the average across the three replicates of *M. smegmatis* cell death, we can see the variation within those plates through the range of points on the graph.

A lot of this variation for all endolysin nanobeads occurs around 10mg/ml. It is important to realise that this may be due to the low concentrations. Some of the nanobeads clumped and as a result, there may be an extremely lytic “burst” of cells if these lytic clumps interacted with the bacterial cells, which may be the reason behind the sudden increase in cell lysis for lysin B nanobeads Jaws and Dylan, causing $55.56\% \pm 7.05$ and $70.14\% \pm 8.87$ cell death, respectively. For the unclumped nanobeads, there is less chance of making contact with the bacterial cells and if they did, there is less chance that the contact time would be long enough to successfully cleave the cell wall components which may indicate why the remaining endolysins only cause around ~40% cell lysis.

Although we cannot claim that there is a significant difference in cell death between D29, Giles and PhaC at 10mg/ml, the average cell death of each respective endolysin nanobead is still above 30%. As this is the shortest exposure time and lowest concentration, these are promising results.

As the endolysin nanobead concentration increased from 10mg/ml to 20mg/ml, we saw an average increase in cell death for each nanobead, except Jaws and Dylan that were previously discussed. This observation fits with the well-known idea that an increase in concentration correlates with an increase in reaction rate (cell death in this case). At 20mg/ml, both lysin A nanobeads had a significant effect on cell death, however only Inca from the lysin B nanobeads had a significant cell death.

Nevertheless, at 80mg/ml of nanobeads in the standing culture with *M. smegmatis*, every endolysin nanobead caused a significant cell death. This result indicates that for applied trials it would be important to have a concentration of at least 80mg/ml of nanobeads.

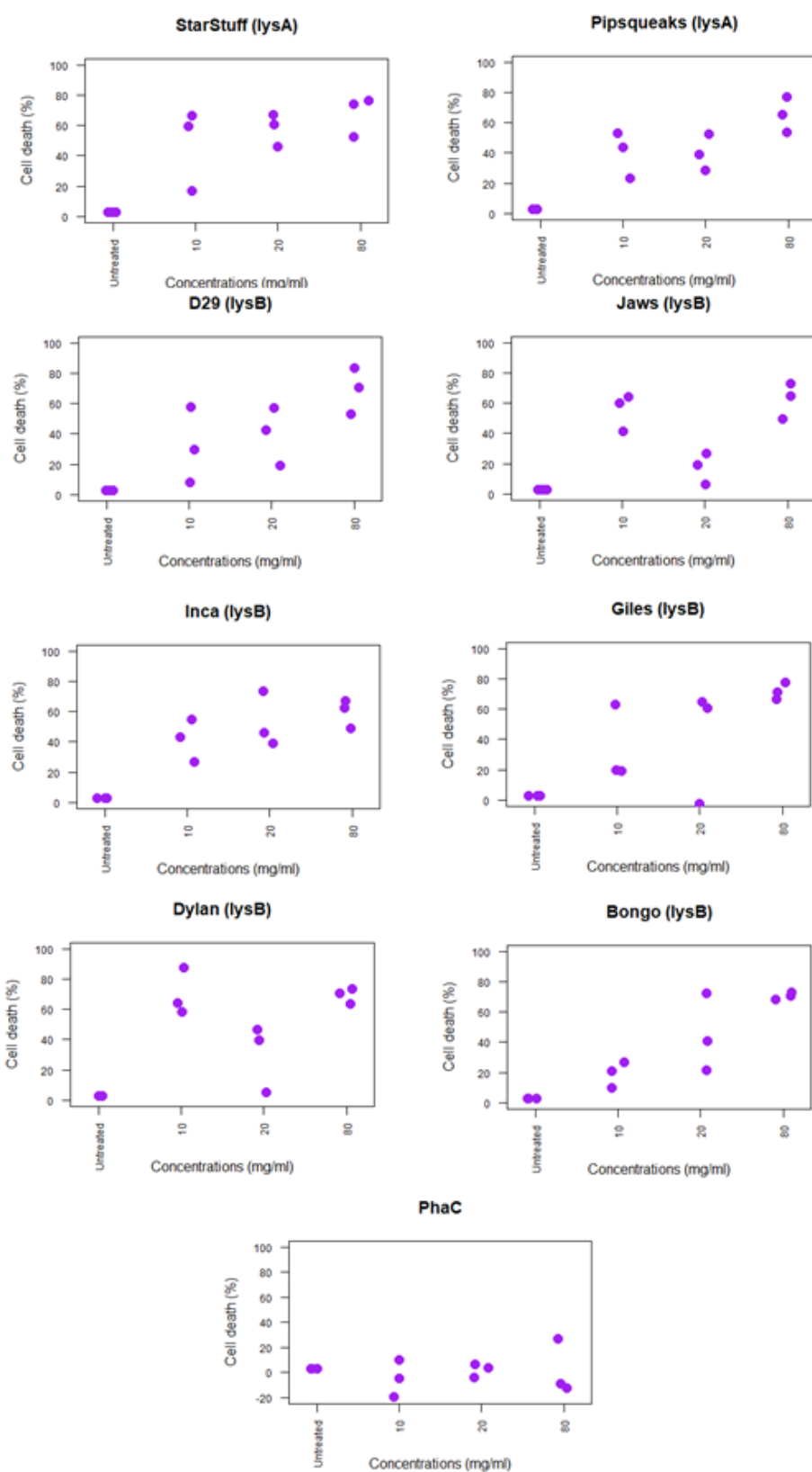


Figure 27: *M. smegmatis* cell death after 45 minutes exposure to 10mg/ml, 20mg/ml and 80mg/ml nanobead concentrations in a standing culture of at room temperature

Across all lysin nanobeads except Jaws and Dylan, there is an increase in cell death as the concentration of nanobeads increases.

Table 9: *M. smegmatis* average cell death and significance after 45 minutes of exposure to 10mg/ml, 20mg/ml and 80mg/ml nanobead concentrations

Lysin	Average cell death at 10mg/ml (%)	p-value	Average cell death at 20mg/ml (%)	p-value	Average cell death at 80mg/ml (%)	p-value
PhaC (no lysin)	-4.86 ± 8.57	0.228	1.91 ± 3.13	0.380	2.12 ± 12.60	0.469
StarStuff (lys A)	47.57 ± 15.59	0.030 *	58.16 ± 6.17	0.00195 **	68.61 ± 7.68	0.0105 *
Pipsqueaks (lys A)	40.10 ± 8.76	0.011 *	40.10 ± 6.94	0.00762 **	65.36 ± 6.76	0.0106 *
D29 (lys B)	31.94 ± 14.33	0.057	39.76 ± 11.07	0.0407 *	69.42 ± 8.78	0.00593 **
Jaws (lys B)	55.56 ± 7.05	0.0028 **	17.53 ± 6.08	0.0532	64.14 ± 6.97	0.0122 *
Inca (lys B)	41.67 ± 8.01	0.0083 **	53.13 ± 10.63	0.0219 *	59.95 ± 5.42	0.0123 *
Giles (lys B)	34.03 ± 14.50	0.052	41.15 ± 21.91	0.109	71.99 ± 3.30	0.0164 *
Dylan (lys B)	70.14 ± 8.87	0.005 **	30.56 ± 12.85	0.0813	68.61 ± 2.95	0.0174 *
Bongo (lys B)	19.10 ± 4.89	0.047 *	44.79 ± 14.88	0.0531	70.64 ± 1.37	0.0160 *

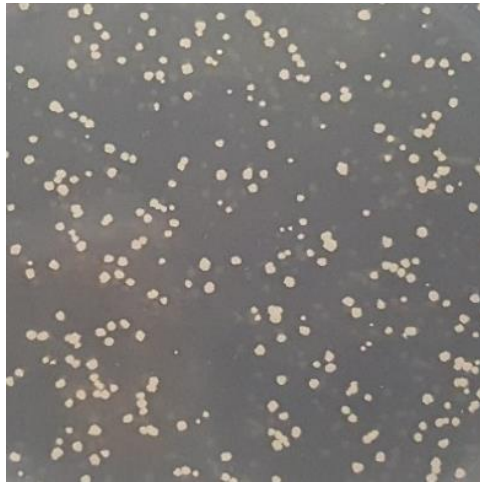
Two-sample t-test (assuming unequal variance) was performed on the above data in relation to the cell death as a result of exposure to PhaC nanobeads (no lysin attached). The most significant difference in cell death occurs at a concentration of 80mg/ml. * = p<0.05, ** = p<0.01, *** = p<0.001.

From the results in Fig. 27 and Table 9 above, when the nanobeads are grouped into their respective “lysin A” or “lysin B” categories, there is no significant difference between the lysin types at 10mg/ml (p=0.212), 20mg/ml (p=0.194) or 80mg/ml (p=0.429). This suggests that when applied “from without” there is no difference between the lytic effect causing cell death of *M. smegmatis* at any concentration point.

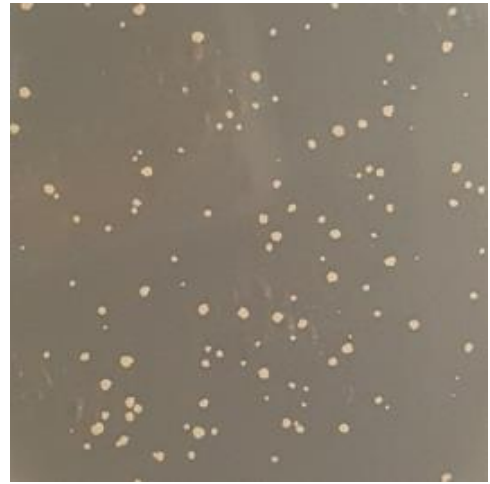
However, we can clearly see the decrease in colony number with Giles (lys B) which caused the most cell death at 80mg/ml at 45 minutes (71.99% ± 3.30), see in Fig. 28.

There is significant variation observed in Fig. 27 however, time constraints limited the opportunity for more replication. Future directions (discussed later) indicate more trials would provide conclusions that are more reliable.

M. smegmatis
untreated colonies



Giles (lys B)
10mg/ml exposure



Giles (lys B)
20mg/ml exposure



Giles (lys B)
80mg/ml exposure

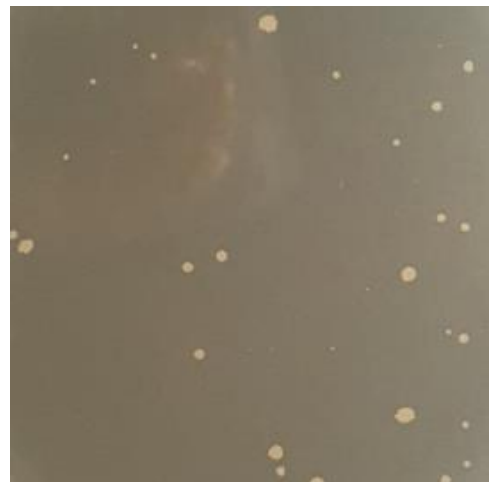


Figure 28: Giles is the most effective endolysin nanobead at 45 minutes

As the concentration of nanobeads exposed to *Giles* increases, cell death increases, indicated by the decrease in observable colonies from the untreated sample to the 80mg/ml exposure sample. Each of these plates is one of three replicates.

3.3.3.2 Testing cell death by exposing *M. smegmatis* to endolysin nanobeads for 5 hours in a standing culture

To understand if the time *M. smegmatis* is exposed to the endolysin nanobeads has any effect on the cell death observed, a second trial repeating the same experiment above, was carried out using an exposure time of 5 hours in the standing culture with three replicates (Table 10).

At 10mg/ml, only D29 (lysB) exposure resulted in a significant *M. smegmatis* cell death of $75.81\% \pm 5.97$. This was the highest cell death that D29 caused throughout the three nanobead concentrations at both time points. This is an outlier compared to the rest of the data, and we would expect that with more trials we would see less cell death at 10mg/ml and more at the higher concentrations, not only for D29 but for the other nanobeads too.

The most cell death was observed when *M. smegmatis* was exposed to 80mg/ml endolysin nanobeads for 5 hours. The most successful nanobead in causing cell lysis was Inca at $78.87\% \pm 5.21$. It is expected that with further trials using higher concentrations, that we would see the percentage of cell death increase. Because endolysins target the cell wall components (peptidoglycan and mycolic acids), a high concentration of these lipases would result in a higher chance of cell death. In regard to bacterial resistance developing, discussed in the introduction, eventually slow bacteriophages have the opportunity to lyse after the previous bacteriophage have “sacrificed” themselves. This links back to the increase in time being beneficial for lysis opportunity as well as increased concentration of the proteins that are able to destroy the bacterial cell wall.

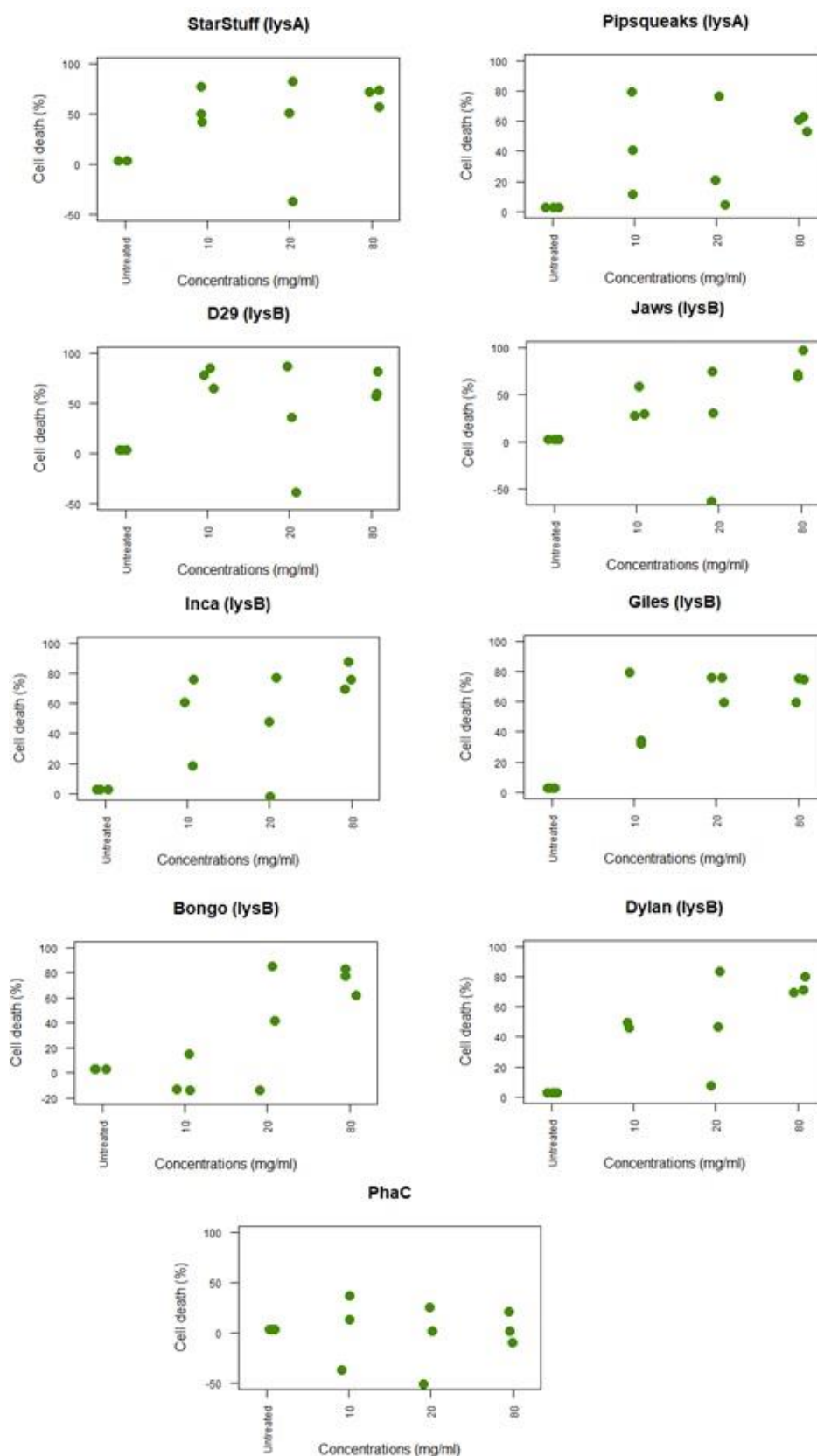


Figure 29: *M. smegmatis* cell death after 5 hours exposure to 10mg/ml, 20mg/ml and 80mg/ml nanobead concentrations in standing culture at room temperature

Across all lysin nanobeads except D29 and Giles, there is an increase in cell death as the concentration of nanobeads increases.

Table 10: *M. smegmatis* average cell death and significance after 5 hours of exposure to 10mg/ml, 20mg/ml and 80mg/ml nanobead concentrations

Lysin	Average cell death at 10mg/ml (%)	p-value	Average cell death at 20mg/ml (%)	p-value	Average cell death at 80mg/ml (%)	p-value
PhaC (no lysin)	4.42 ± 21.91	0.477	-0.66 ± 22.73	0.337	2.33 ± 9.11	0.132
StarStuff (lys A)	56.32 ± 10.53	0.061	57.98 ± 35.65	0.205	67.94 ± 5.53	0.00475 **
Pipsqueaks (lys A)	43.95 ± 19.74	0.126	53.59 ± 21.88	0.126	58.39 ± 2.84	0.0145 *
D29 (lys B)	75.81 ± 5.97	0.0440 *	57.05 ± 36.41	0.230	67.94 ± 7.81	0.00332 **
Jaws (lys B)	38.94 ± 9.74	0.122	44.41 ± 40.62	0.335	78.38 ± 8.78	0.00202 **
Inca (lys B)	51.92 ± 17.22	0.0817	59.04 ± 23.08	0.102	78.87 ± 5.21	0.00297 **
Giles (lys B)	48.67 ± 15.51	0.0873	73.67 ± 5.48	0.0390 *	70.81 ± 5.17	0.00404 **
Dylan (lys B)	24.78 ± 23.03	0.278	64.23 ± 22.09	0.0818	74.42 ± 3.30	0.00279 **
Bongo (lys B)	-4.13 ± 9.59	0.372	60.90 ± 28.62	0.139	74.95 ± 6.38	0.00164 **

Two-sample t-test (assuming unequal variance) was performed on the above data in relation to the cell death as a result of exposure to PhaC nanobeads (no lysin attached). The most significant difference in cell death occurs at a concentration of 80mg/ml. * = $p < 0.05$, ** = $p < 0.01$, *** = $p < 0.001$.

Similarly, to the results from the 45 minute exposure test, the cell death is significant with every endolysin nanobead at 80mg/ml. It would once again be important to use this concentration if developing a prophylactic treatment.

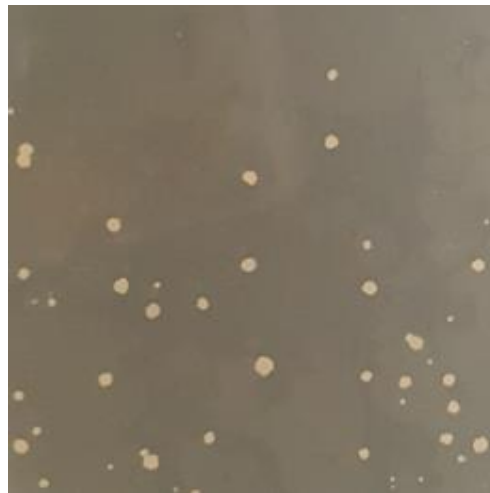
From the results in Fig. 29 and Table 10 above, when the nanobeads are grouped into their respective “lysin A” or “lysin B” categories, there is no significant difference between the lysin types at 10mg/ml ($p=0.213$), 20mg/ml ($p=0.198$) or 80mg/ml ($p=0.137$). This suggests that when applied “from without” there is no difference between the lytic effect causing cell death of *M. smegmatis* at any concentration point.

We can also visually observe the decrease in colonies from Inca (lys B), which caused the most cell death ($78.87\% \pm 5.21$) at 80mg/ml at 5 hours, seen in Fig. 30.

M. smegmatis
untreated colonies



Inca (lys B)
10mg/ml exposure



Inca (lys B)
20mg/ml exposure



Inca (lys B)
80mg/ml exposure



Figure 30: Inca is the most effective endolysin nanobead at 5 hours

As the concentration of nanobeads exposed to *Giles* increases, cell death increases, indicated by the decrease in observable colonies from the untreated sample to the 80mg/ml exposure sample. Each of these plates is one of three replicates.

3.3.3.3 Conclusion of using colony counts to detect cell death

In summary, Fig. 31 below illustrates all of the average cell death data across every time point and endolysin nanobead concentration trialled. As demonstrated in Fig. 27 and 29, both increasing exposure time to the nanobeads and increasing nanobead concentration from 10mg/ml to 80mg/ml at each time point can have a significant increase in observable *M. smegmatis* cell death; 45 minutes ($p=0.00119$) and 5 hours ($p=0.00484$).

When comparing the overall lytic effect of 45minutes exposure with 5 hours exposure in regards to *M. smegmatis* cell death, there is no significant effect at the concentration level; 10mg/ml ($p=0.481$) and 80mg/ml ($p=0.0821$). However, there is a significant effect in the difference in time on cell death at 20mg/ml ($p=0.00265$) where exposure to lysin nanobeads for 5 hours results in significantly more cell death than just 45 minutes.

Nevertheless, at the individual lysin level, we can see that the most significant concentration for cell death above 70% (average cell death is $71.46\% \pm 2.39$) is 80mg/ml nanobeads exposed to *M. smegmatis* for at least 5 hours.

This increasing trend is promising for applied trials, where nanobeads would be sprayed onto hospital masks to act as an initial barrier of defense against airborne bacterial pathogens (such as tuberculosis) when coughed or otherwise transmitted near an orifice. In applied settings, these masks would be worn for long periods of time (~5 hours), therefore it is important that longer exposure continues to increase cell death rather than becoming inactive at room temperature. This experiment is discussed more in depth in section 3.4.

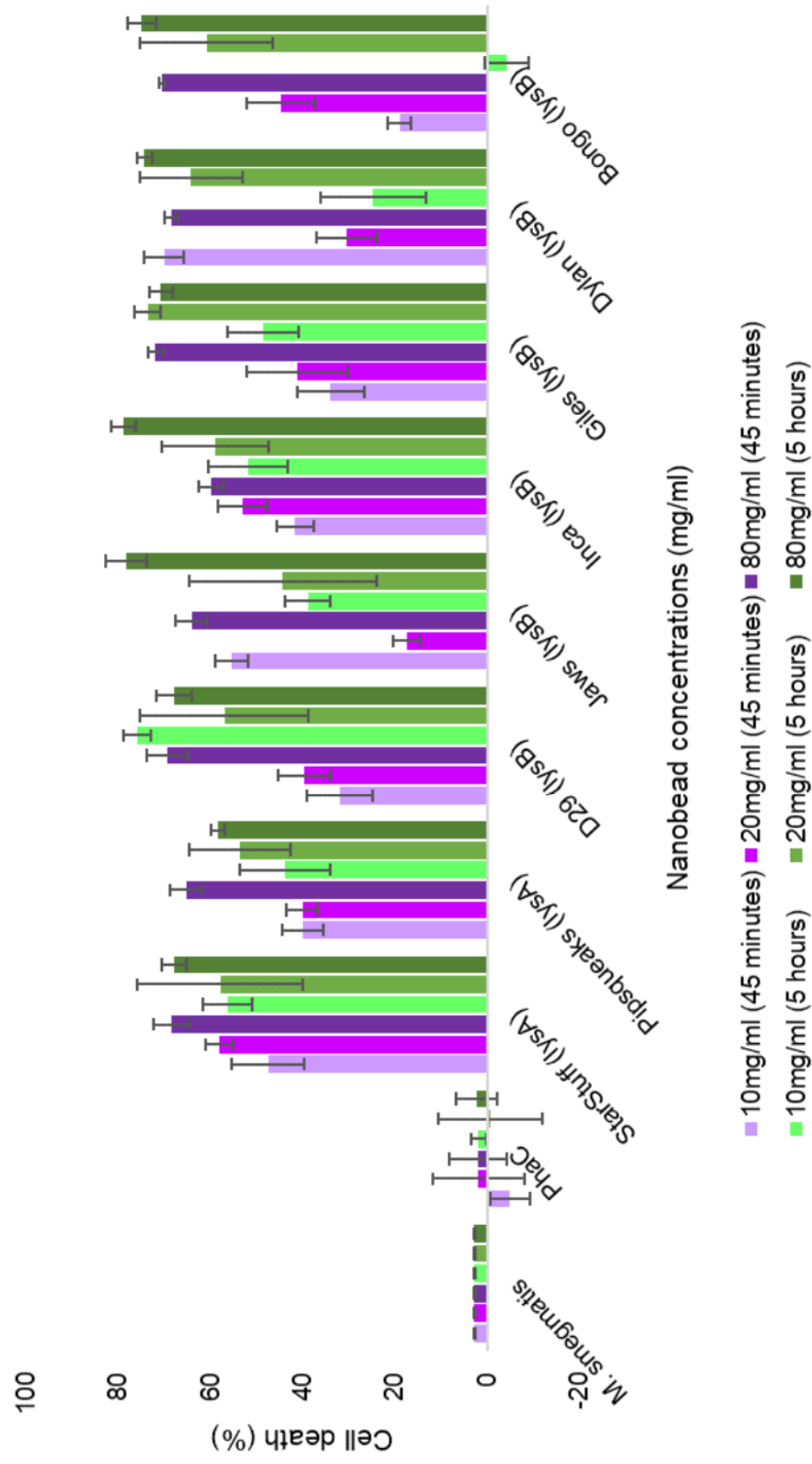


Figure 31: All endolysin combinations at each trial point

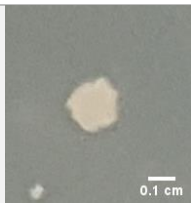
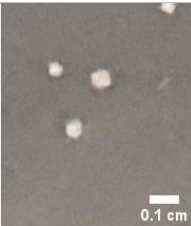
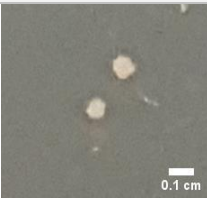
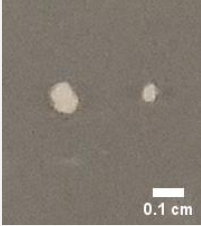
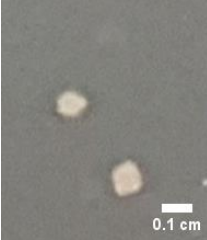
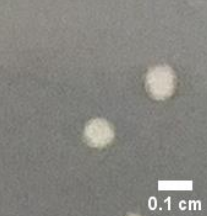
Exposure time clearly has a more pronounced impact on cell lysis than the concentration of nanobeads that *M. smegmatis* is exposed to. We can see that the green bars (representing cell death after exposure to the three concentrations after 5 hours) are larger than the blue bars, in all cases except D29 at 20mg/ml, Jaws at 10mg/ml and Dylan at 10mg/ml.

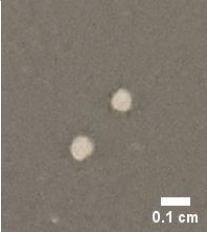
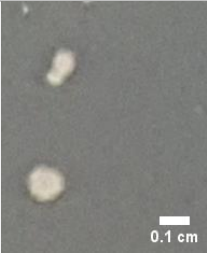
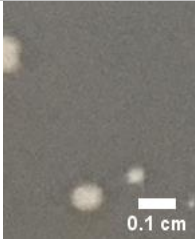
3.3.3.4 Investigating if remaining colonies are resistant

I observed from my colony forming unit plates that the colonies that appeared to have survived exposure to the nanobeads were smaller than *M. smegmatis* colonies generally appear on this media. I was therefore motivated to test these colonies to see if they represented a population of mutants that were able to survive against the nanobeads and would therefore represent a problem for practical applications or if these represented a population that had simply survived by not encountering the nanobeads or lysing. I therefore repeated the exposure test in standing liquid cultures with *M. smegmatis* cultures that were derived from survivor colonies.

The persisting *M. smegmatis* colonies on the agar plate after exposure to 80mg/ml endolysin nanobeads appeared smaller than the colonies otherwise seen. This suggested that there may have been a mutation providing the bacteria with additional defense against the lytic enzymes, allowing them to survive the largest concentration of endolysin nanobeads in the trial, for the longest exposure time of 5 hours (Barsom & Hatfull, 1996). To test this, I picked a surviving colony from each of the plates after 72 hours of incubation (Table 11), regrew them using the methods discussed earlier and repeated the same experiment; exposing *M. smegmatis* to 80mg/ml of each endolysin nanobead for 5 hours, before plating and incubating for 72 hours at 37°C. The colonies were then counted, and the percentage of cell death was recorded, Fig. 32.

Table 11: Comparison of *M. smegmatis* colony morphologies between WT and endolysin nanobead-surviving colonies

Lysin nanobead	Colony morphology and size		<i>M. smegmatis</i> survivor colony size after 80mg/ml 5 hour exposure (cm)
<i>M. smegmatis</i> WT			0.168 ± 0.072
PhaC (no lysin)			0.146 ± 0.023
StarStuff (lys A)			0.059 ± 0.0031
Pipsqueaks (lys A)			0.075 ± 0.0045
D29 (lys B)			0.051 ± 0.0092
Jaws (lysB)			0.073 ± 0.0068
Inca (lysB)			0.080 ± 0.0015

Giles (lys B)		0.067 ± 0.0017
Dylan (lys B)		0.111 ± 0.082
Bongo (lysB)		0.070 ± 0.039

Scale bar is 0.1cm. There are obvious differences between the colony sizes that survived the endolysin nanobead exposure and the WT *M. smegmatis* and PhaC (no lysin nanobead). The survivors are considerable smaller whereas the colonies not exposed to lysins are larger.

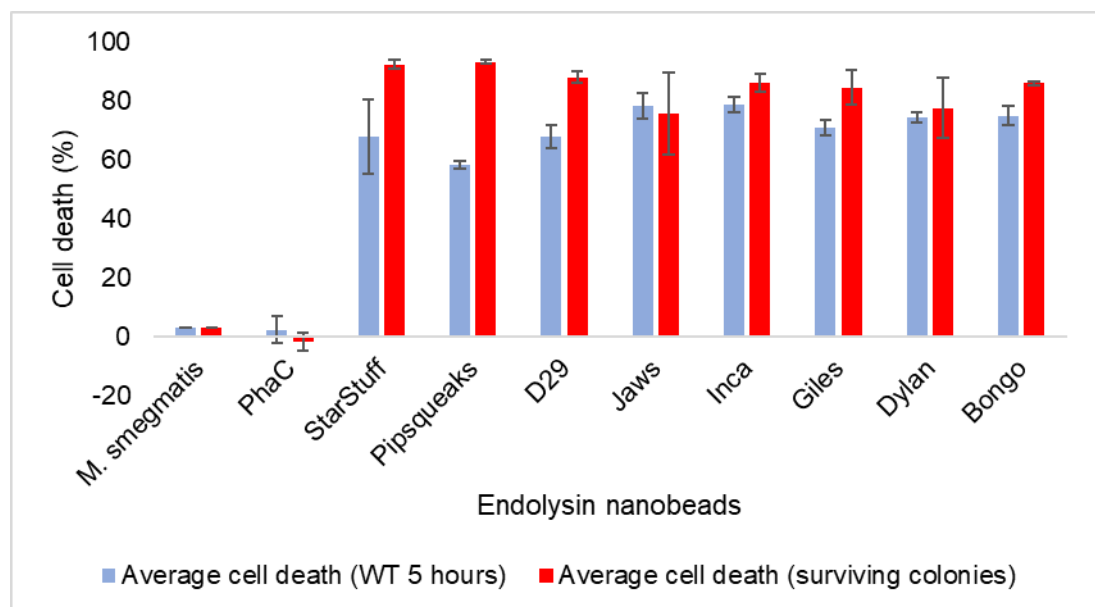


Figure 32: Comparison of cell death with *M. smegmatis* WT and *M. smegmatis* colonies cultured from surviving colonies

In all endolysin nanobeads (except Jaws), we see more cell death when the nanobeads are applied to the colonies that have survived.

The cell death observed in Fig. 32, shows similar *M. smegmatis* cell death between initially exposed WT *M. smegmatis* and the colonies of *M. smegmatis* that survived exposure to each respective nanobead after 5 hours and 80mg/ml. However, given the similarities, we can also see that there is in fact a slight increase in cell death when the remaining colonies are exposed once again to the endolysin nanobeads. We hypothesise that we see increased death due to the sensitivity of these colonies. This hypothesis stems from the idea that the remaining colonies may not be resistant, we may just have not exposed them to enough endolysin nanobeads to completely lyse the whole population and the remaining colonies are those who have just survived and may be sensitive to a second round of lysis proteins. A future trial to test this theory would be to keep increasing the concentration and to keep culturing the surviving colonies after each round of exposure to see if a similar pattern ensues.

I also wanted to test if these colonies had changed in their sensitivity to a bacteriophage sample, as we had mycobacteriophage Inca in the freezer stocks, as well as the endolysin nanobead of Inca lysin B. In order to test this I produced a bacterial lawn from each surviving colony discussed above and spot testing 3µl Inca bacteriophage serial dilution $10^0 - 10^{-9}$ onto it. This way we were able to understand if cell lysis was able to occur from the inside out (as opposed to our proposed mechanism of lysis from without). As can be seen in Fig. 33, the most apparent effect is on the StarStuff (lysin A) plate. We see ~3 plaque forming units (pfu) on every other plate at the 10^{-6} dilution spot, however we see no Inca plaques on the 10^{-6} dilution spot. On the bacterial lawn from the StarStuff colony we can see ~20 pfu/ml on the 10^{-5} dilution spot, whereas the spots are webbed (too many plaques to distinguish the number of plaques) on all of the other plates. This experiment was carried out under identical conditions and each 3µl Inca bacteriophage spot came from the same tube as what was used for the other tests, therefore this would not be a

reason to observe the difference. Therefore, we hypothesise that after exposure to StarStuff, lysin A nanobeads at 80mg/ml for 5 hours, *M. smegmatis* undergoes some type of mutation that not only enables it to survive, but to better persist against the bacteriophage infection compared to the other nanobeads. It is worth noting that the bacterial colony that survived the StarStuff nanobead exposure did not have improved resistance to the StarStuff nanobead exposure in the second round (Fig. 32). This may indicate that the mutation (if there is one) is particular to phage infection or that these results are not significant and should be repeated. If the results proved robust, future research would involve sequencing each of the persisting *M. smegmatis* culture to further understand if this was really a mutation or just “right place, right time” for these bacteria that survived.

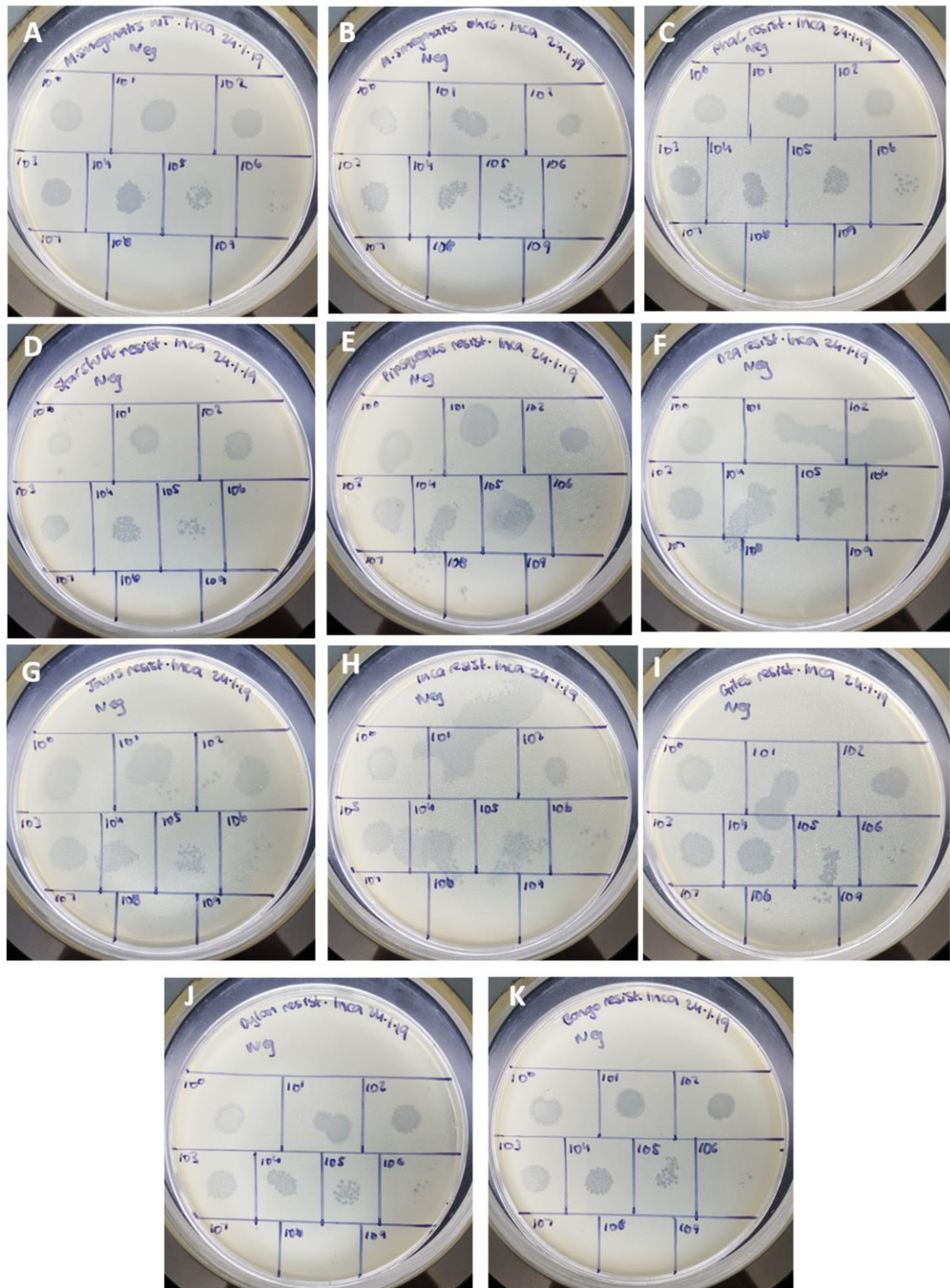


Figure 33: Surviving *M. smegmatis* colonies cultured and infected by Inca bacteriophage serial dilution 3μl spot test

A) *M. smegmatis* WT. Remaining bacterial culture made from surviving colonies of B) *M. smegmatis* WT (from incubator). C) PhaC. D) StarStuff (lys A). E) Pipsqueaks (lys A). F) D29 (lys B). G) Jaws (lys B). H) Inca (lys B). I) Giles (lys B). J) Dylan (lys B). K) Bongo (lys B). StarStuff shows a 10-fold difference in bacteriophage lysis.

Hatfull and Barsom refer to examples of phage-resistance in bacteria, including modified peptidoglycan components of the cell wall and phage-resistant mutants and often these bacteria are resistant to a series of unrelated bacteriophages (Barsom & Hatfull, 1996). More specifically, this paper demonstrated that the overexpression of the *Mpr* gene blocks the access of mycobacteriophage D29 to the membrane, inhibits macromolecular movements or affects membrane potentials that may be required for translocation of bacteriophage DNA across the membrane (Barsom & Hatfull, 1996). In the case of our potentially-resistant colonies, it would be more likely that a random beneficial mutation has arisen, as any pre-evolved mutation in relation to the specific lysin A protein would have been observed to an extent in the other lysin A candidate in this study; Pipsqueaks, which it was not.

3.3.4 Test four: detecting cell death using hospital masks as a proof of concept applied approach

It is important that this antimicrobial tool not only causes cell death in laboratory environments, but also in situations that mimic real-world practices, such as the transmission and infection of hospital workers working with tuberculosis. To test these nanobeads as an applied approach, we used a filter paper, similar to hospital masks, discussed below.

3.3.4.1 Coating hospital masks with nanobeads as a proof of concept

The previous experiment exposed standing cultures of *M. smegmatis* to the different endolysin nanobeads, yet we wanted to attempt a test that would be more similar to a surface contact prophylactic. Initially we proposed submerging a generic-brand hospital mask in endolysin nanobeads and testing *M. smegmatis* survival upon contact. However, we discovered that these surfaces are hydrophobic and commercial nanobead applications use a more intensive adhesive process. The nanobeads were therefore coated onto the 1cm filter paper pieces, left to dry before spraying a bacterial spray of 10^{-5} dilution of *M. smegmatis* spray ($\sim 100\mu\text{l}$) on each piece of filter paper and then stamping onto a 1.5% LB + CB + CHX agar plate before incubating at 37°C overnight for colony forming unit counts.



Figure 34: 10 μl of nanobeads on filter paper compared to a hospital mask

The filter paper (left) is hydrophilic which enabled the even coating of nanobeads on its surface, unlike the hospital mask (right).

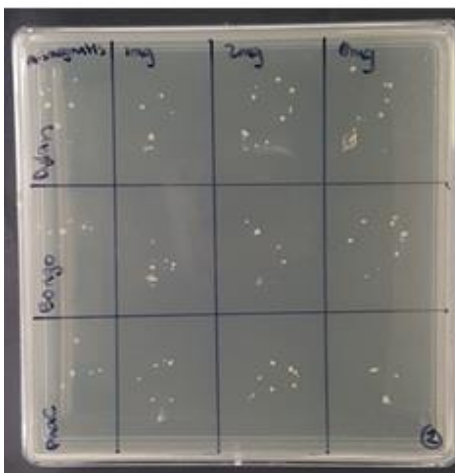
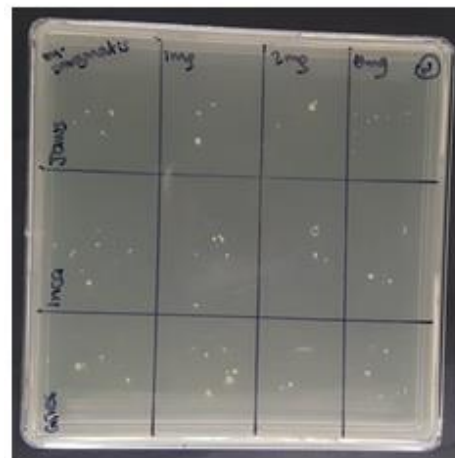
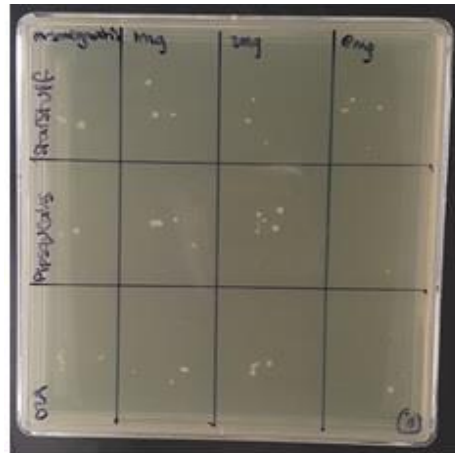


Figure 35: *M. smegmatis* colonies stamped after exposure to nanobeads on filter paper

Example of a stamped plate replicate. The overall trend is that as the concentration of nanobeads increased, cell death decreased. Using a cosmetic atomiser made it difficult to ensure constant spray across each of the filter paper pieces and the small colony counts made it difficult to extrapolate accurate conclusions.

Table 12: Raw colony counts of nanobead stamping experiment

Lysin	<i>M. smegmatis</i> colony count	10mg/ml colony count	20mg/ml colony count	80mg/ml colony count
PhaC (no lysin)	22	20	19	20
	21	19	25	18
	23	24	30	21
StarStuff (lys A)	14	13	10	8
	18	7	4	5
	12	8	2	5
Pipsqueaks (lys A)	11	7	8	5
	11	9	5	7
	16	15	10	9
D29 (lys A)	16	14	3	0
	5	5	4	2
	14	11	8	6
Jaws (lys A)	27	15	9	8
	16	16	16	4
	16	16	10	3
Inca (lys A)	11	14	6	7
	23	7	16	11
	15	14	13	8
Giles (lys A)	12	12	6	2
	12	11	19	10
	25	11	7	6
Dylan (lys A)	19	20	20	15
	23	21	21	18
	27	20	17	16
Bongo (lys A)	14	15	11	12
	21	17	22	16
	25	15	4	13

The *M. smegmatis* colony counts varied throughout this experiment, making it difficult to get reliable averages to make a conclusion.

Table 13: Average cell death of *M. smegmatis* after being sprayed on nanobead-coated filter paper “masks”

Lysin	Average cell death at 10mg/ml (%)	p-value	Average cell death at 20mg/ml (%)	p-value	Average cell death at 80mg/ml (%)	p-value
PhaC (no lysin)	4.76 ± 4.55	0.368	-11.94 ± 13.20	0.188	10.69 ± 1.80	0.340
StarStuff (lys A)	17.65 ± 7.98	0.128	26.19 ± 14.48	0.0618	46.22 ± 6.24	0.00286 **
Pipsqueaks (lys A)	20.26 ± 8.75	0.107	39.78 ± 7.95	0.022 *	44.89 ± 5.28	0.00223 **
D29 (lys B)	11.31 ± 6.21	0.221	48.04 ± 17.87	0.027 *	72.38 ± 13.83	0.0216 *
Jaws (lys B)	14.81 ± 14.81	0.291	34.72 ± 19.29	0.0583	75.54 ± 3.15	0.000107 ***
Inca (lys B)	18.27 ± 26.90	0.335	29.74 ± 9.28	0.0306 *	45.07 ± 4.63	0.00170 **
Giles (lys B)	21.44 ± 17.44	0.226	21.22 ± 40.28	0.258	58.67 ± 21.10	0.0645
Dylan (lys B)	9.79 ± 9.02	0.326	13.49 ± 12.44	0.117	27.84 ± 6.45	0.0210 *
Bongo (lys B)	17.30 ± 13.64	0.237	33.56 ± 26.33	0.110	28.70 ± 10.03	0.0581

The only significant cell death occurred when 80mg/ml of nanobeads were added to the filter paper, with the highest cell death due to Jaws at 75.54% ± 3.15, also at 80mg/ml. * = p<0.05, ** = p<0.01, *** = p<0.001.

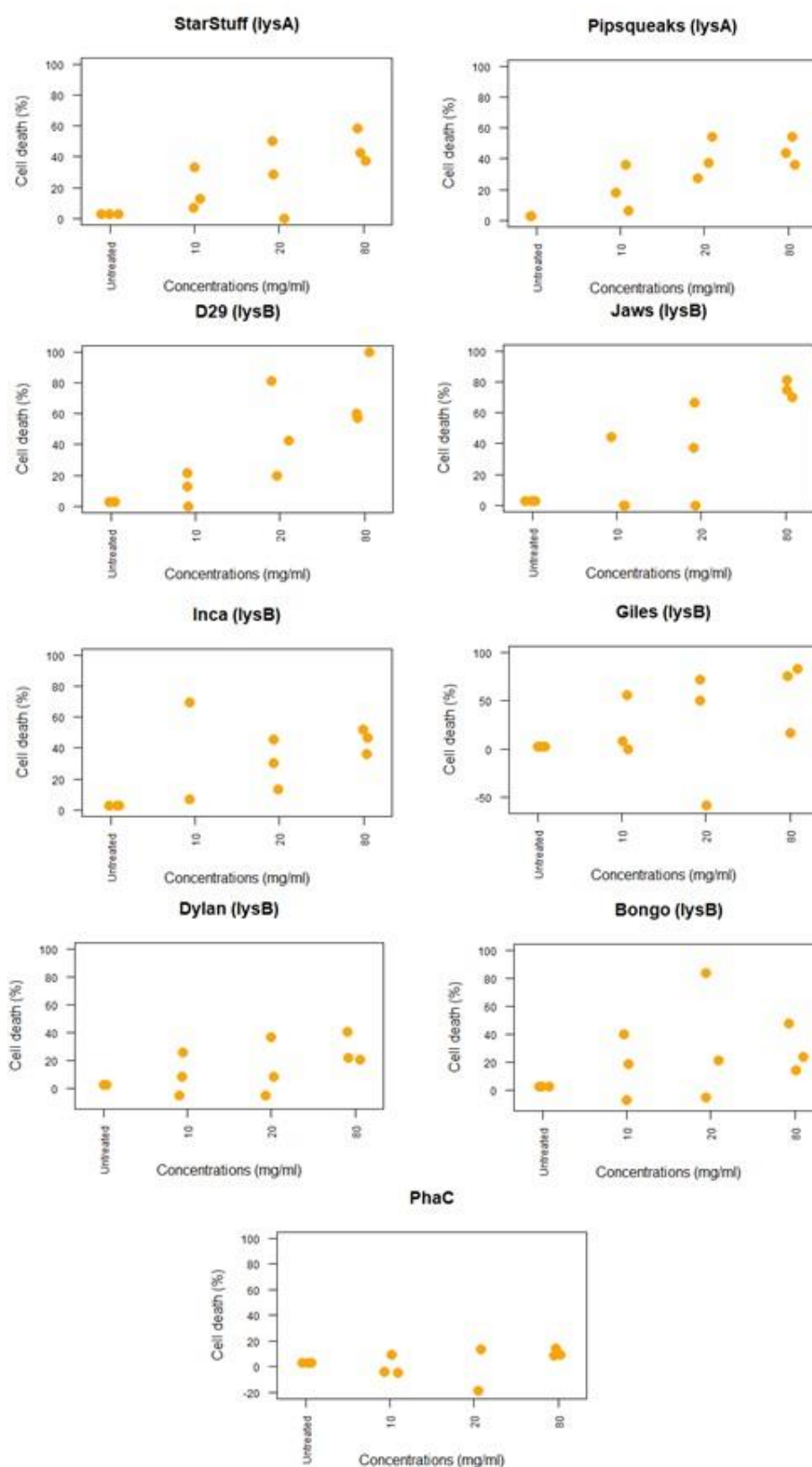


Figure 36: Distribution of colony counts

Example of a stamped plate replicate. The overall trend is that as the concentration of nanobeads increased, cell death decreased. Using a cosmetic atomiser made it difficult to ensure constant spray across each of the filter paper pieces and the small colony counts made it difficult to extrapolate accurate conclusions.

Although the trend of increasing cell death as concentration of endolysin nanobeads increases, in comparison to each concentration equivalent in the standing culture, the average cell death at each concentration decreased to an average across all endolysin nanobeads of 16.95% cell death at 10mg/ml, 29.35% cell death at 20mg/ml and 49.91% cell death at 80mg/ml. One possibility for this may have been the irregularity of using filter paper with some *M. smegmatis* cells absorbing in and not stamping out. During the third experiment (colony counts to observe cell death), we used a 10^{-6} dilution of *M. smegmatis* to get countable colonies with 100 μ l plated, however even though the 100 μ l aliquot was condensed into a smaller surface area, the pilot test (not shown) indicated we would need to decrease the dilution to get countable colonies at 10^{-5} . This experiment was repeated several times in order to see colonies and the results were often inconsistent. We can also see that in Table 12, the colony counts observed on the *M. smegmatis* control were very inconsistent, often with a range between 50% respective to the *M. smegmatis* control. Because we did not get a sample size of at least 30-300 colonies, it becomes difficult to make any definite conclusions about these results without repeating these tests further. Fig. 36 illustrates this variation, especially with Jaws and Bongo at 20mg/ml. Because this part of the experiment became difficult to complete within the timeframe of submitting this thesis, I have decided to present these results to draw some ideas regarding the trend of this data. One overall conclusion (granted the small sample size of colonies), is that while cell death increases as concentration increases, it does not increase as much as the standing culture experiment (test three). One reason these results may have differed from the standing culture colony count experiment could be due to the variability when using the cosmetic atomiser. Unlike a pipette that dispenses the exact aliquot, there may have been variation less or more than the average 100 μ l that each spray released.

Nevertheless, Jaws had the highest cell lysis at $75.54\% \pm 3.15$ at 80mg/ml, with D29 causing the second highest cell death at $72.38\% \pm 13.83$. Inca still had a reasonable cell lysis, causing over 45% cell death and coupled with the bacteriophage of Inca that we have in the freezer stocks, this would make a potential combinatorial “cocktail” therapeutic approach combining the replication ability of the whole bacteriophage and the lysin concentration of the nanobead. More trials would provide directions that are more accurate.

3.4 Summary

I tested a set of nanobeads that were custom-synthesised and attached to mycobacteriophage endolysins in the hopes of developing a tool for easily applying these as an antibacterial to surfaces. The hope is that such a tool can improve defense against pathogenic bacteria in varying aspects of life from health care, agriculture and food production. Through the four main tests carried out, we have discovered that cell death is best observed through cultured plates counting the difference in colonies between treated and non-treated *M. smegmatis* colonies. We also concluded that there is no difference between the lysis ability of lysin A and lysin B across proteins across trials as they average $54.84\% \pm 2.91$ cell death by lysin A's compared to $53.46\% \pm 3.36$ cell death by lysin B's across trials ($p=0.428$).

However, we did observe that the effect of time and concentration appeared to have more of an impact than the species of lysin used. We observed that $50.17\% \pm 8.60$ death happened on average at 45 minutes, $57.45\% \pm 8.52$ death at 5 hours and that increasing the concentration from 10mg/ml to 80mg/ml improved cell death by 24.83% at 45 minutes and 29.42% at 5 hours.

The final test for this project involved applying the nanobeads to a filter paper surface, spraying with bacteria and stamping these onto agar plates. As a result, we saw some cell death, but not as much as in our standing culture tests where we saw on average over 70% cell death as a result of 80mg/ml endolysins exposed to *M. smegmatis* for 5 hours, although the filter paper experiment is more aligned with real world applications.

3.5 Future directions

The premise for this research is that prophylactic treatments against pathogenic bacteria are needed and that bacteriophage endolysins are a promising potential source. Of course, one of the first steps to gaining more reliable answers would be to repeat the experiments discussed above with more replicates. Three replicates was the minimum required and only three were used due to time limitations for submission.

Although not within the scope of this project, there are several opportunities to expand this research and these include; lysin cocktails using a combinatorial approach with both lysin A and lysin B proteins, a step further with “next generation dual-fusion” nanobeads that have both lysin A and lysin B expressed on the surface, inclusion of bacteriophages within the cocktail and *in vivo* tests with other Gram-positive bacterium species (such as *M. tuberculosis* and *M. bovis*) to further understand the specificity of the lysin proteins fused to the nanobeads.

4 Conclusion

Since the discovery of bacteriophage over 100 years ago, the appeal of phage therapy is on the rise due to the increasing threat of antibiotic resistance in everyday lives. This research demonstrated the ability to utilise cell-lysing properties of *M. smegmatis*'s viral predator, the mycobacteriophage, to bypass the opportunity of resistance to the bacteriophage by lysing the cell wall "from without". We fused two lysin A's and six lysin B's to PHA biodegradable nanobeads and observed significant antimicrobial properties against *M. smegmatis* across three different time points and three different endolysin concentrations.

We started this project with an extensive bioinformatic comparison of potential endolysins, which were selected, expressed, produced on nanobeads and purified. We successfully tested the antimicrobial properties of these endolysin nanobead fusions across four tests. We observed some successful results, especially when *M. smegmatis* was exposed to nanobeads in a standing culture, however, when we employed filter paper to mimic a hospital mask with nanobeads coated on the surface we did not see the same levels of cell death, although cell death was still present.

The potential to use the lytic mechanism of the bacteriophage whilst bypassing the existing resistance mechanisms of bacteria indicate that this biotechnology is a potential key to unlocking a safe, economical, environmentally friendly and most importantly, useful tool in combatting antimicrobial resistance.

5 References

- Abedi, D., Beheshti, M., Najafabadi, A. J., Sadeghi, H. M., & Akbari, V. (2012). Optimization of the Expression of Genes Encoding Poly (3-hydroxyalkanoate) Synthase from *Pseudomonas aeruginosa* PTCC 1310 in *Escherichia coli*. *Avicenna J Med Biotechnol*, 4(1), 47-51.
- Abedon, S. T. (2011). Lysis from without. *Bacteriophage*, 1(1), 46-49. doi:10.4161/bact.1.1.13980
- Anderson, A. J., & Dawes, E. A. (1990). Occurrence, metabolism, metabolic role, and industrial uses of bacterial polyhydroxyalkanoates. *Microbiological Reviews*, 54(4), 450.
- Arpigny, J. L., & Jaeger, K. E. (1999). Bacterial lipolytic enzymes: classification and properties. *Biochem J*, 343 Pt 1, 177-183.
- Barsom, E. K., & Hatfull, G. F. (1996). Characterization of a *Mycobacterium smegmatis* gene that confers resistance to phages L5 and D29 when overexpressed. *Molecular Microbiology*, 21(1), 159-170. doi:10.1046/j.1365-2958.1996.6291342.x
- Blatchford, P. A., Scott, C., French, N., & Rehm, B. H. A. (2012). Immobilization of organophosphohydrolase OpdA from *Agrobacterium radiobacter* by overproduction at the surface of polyester inclusions inside engineered *Escherichia coli*. *Biotechnology and Bioengineering*, 109(5), 1101-1108. doi:10.1002/bit.24402
- Brennan, P. J. Structure, function, and biogenesis of the cell wall of *Mycobacterium tuberculosis*. *Tuberculosis*, 83(1), 91-97. doi:10.1016/S1472-9792(02)00089-6
- Brown, L., Wolf, J. M., Prados-Rosales, R., & Casadevall, A. (2015). Through the wall: extracellular vesicles in Gram-positive bacteria, mycobacteria and fungi. *Nat Rev Microbiol*, 13(10), 620-630. doi:10.1038/nrmicro3480
- Brown, L., Wolf, J. M., Prados-Rosales, R., & Casadevall, A. (2015). Through the wall: extracellular vesicles in Gram-positive bacteria, mycobacteria and fungi. *Nature Reviews Microbiology*, 13, 620. doi:10.1038/nrmicro3480
- Butela, K. A., Gurney, S. M. R., Hendrickson, H. L., LeBlanc-Straceski, J. M., Zimmerman, A. M., Conant, S. B., . . . Kagey, J. D. (2017). Complete Genome Sequences of Cluster A *Mycobacteriophages* BobSwaget, Fred313, KADY, Lokk, MyraDee, Stagni, and StepMih. *Genome Announcements*, 5(43).
- Catalão, M. J., Gil, F., Moniz-Pereira, J., & Pimentel, M. (2011). Functional analysis of the holin-like proteins of mycobacteriophage Ms6. *Journal of Bacteriology*, 193(11), 2793-2803. doi:10.1128/JB.01519-10
- Catalão, M. J., & Pimentel, M. (2018). *Mycobacteriophage* Lysis Enzymes: Targeting the *Mycobacterial* Cell Envelope. *Viruses*, 10(8), 428.

- CDC. (2005). *Guidelines for Preventing the Transmission of Mycobacterium tuberculosis in Health-Care Settings, 2005*. Atlanta, Georgia: Department of Health and Human Services Centers for Disease Control and Prevention.
- CDC. (2018). Tuberculosis (TB). Retrieved December 2018 from www.cdc.gov/tb/default.htm
- Chek, M. F., Kim, S.-Y., Mori, T., Arsad, H., Samian, M. R., Sudesh, K., & Hakoshima, T. (2017). Structure of polyhydroxyalkanoate (PHA) synthase PhaC from *Chromobacterium* sp. USM2, producing biodegradable plastics. *Scientific Reports*, 7(1), 5312. doi:10.1038/s41598-017-05509-4
- Chen, J., Kriakov, J., Singh, A., Jacobs, W. R., Jr., Besra, G. S., & Bhatt, A. (2009). Defects in glycopeptidolipid biosynthesis confer phage I3 resistance in *Mycobacterium smegmatis*. *Microbiology*, 155(Pt 12), 4050-4057. doi:10.1099/mic.0.033209-0
- Chen, Z., Franco, C. F., Baptista, R. P., Cabral, J. M., Coelho, A. V., Rodrigues, C. J., Jr., & Melo, E. P. (2007). Purification and identification of cutinases from *Colletotrichum kahawae* and *Colletotrichum gloeosporioides*. *Appl Microbiol Biotechnol*, 73(6), 1306-1313. doi:10.1007/s00253-006-0605-1
- Chibani-Chennoufi, S., Bruttin, A., Dillmann, M.-L., & Brüssow, H. (2004). Phage-Host Interaction: an Ecological Perspective. *Journal of Bacteriology*, 186(12), 3677-3686. doi:10.1128/JB.186.12.3677-3686.2004
- Choudhary, E., Thakur, P., Pareek, M., & Agarwal, N. (2015). Gene silencing by CRISPR interference in mycobacteria. *Nature Communications*, 6, 6267. doi:10.1038/ncomms7267
<https://www.nature.com/articles/ncomms7267#supplementary-information>
- Comeau, A. M., Hatfull, G. F., Krisch, H. M., Lindell, D., Mann, N. H., & Prangishvili, D. (2008). Exploring the prokaryotic virosphere. *Research in Microbiology*, 159(5), 306-313. doi:<https://doi.org/10.1016/j.resmic.2008.05.001>
- Cosivi, O., Grange, J. M., Daborn, C. J., Raviglione, M. C., Fujikura, T., Cousins, D., . . . Meslin, F. X. (1998). Zoonotic tuberculosis due to *Mycobacterium bovis* in developing countries. *Emerging Infectious Diseases*, 4(1), 59-70.
- d'Herelle, F. (1931). Bacteriophage as a Treatment in Acute Medical and Surgical Infections. *Bulletin of the New York Academy of Medicine*, 7(5), 329-348.
- Daniel, T. M. (2001). *Tuberculosis in the Workplace* (M. J. Field Ed.). Washington DC, US: National Academic Press (US).
- Danovaro, R., Corinaldesi, C., Dell'anno, A., Fuhrman, J. A., Middelburg, J. J., Noble, R. T., & Suttle, C. A. (2011). Marine viruses and global climate change. *FEMS Microbiol Rev*, 35(6), 993-1034. doi:10.1111/j.1574-6976.2010.00258.x

- Ehrlich, R. (2018). 1741b Protecting health care workers from occupational tuberculosis and its effects: long on guidelines, short on implementation? *Occupational and Environmental Medicine*, 75(Suppl 2), A222-A222. doi:10.1136/oemed-2018-ICOHabstracts.628
- Fischetti, V. A. (2008). Bacteriophage lysins as effective antibacterials. *Current Opinion in Microbiology*, 11(5), 393-400. doi:<https://doi.org/10.1016/j.mib.2008.09.012>
- Fischetti, V. A. (2010a). Bacteriophage endolysins: A novel anti-infective to control Gram-positive pathogens. *International Journal of Medical Microbiology*, 300(6), 357-362. doi:<https://doi.org/10.1016/j.ijmm.2010.04.002>
- Fischetti, V. A. (2010b). Bacteriophage endolysins: A novel anti-infective to control Gram-positive pathogens. *International journal of medical microbiology : IJMM*, 300(6), 357-362. doi:10.1016/j.ijmm.2010.04.002
- Ford, M. E., Sarkis, G. J., Belanger, A. E., Hendrix, R. W., & Hatfull, G. F. (1998). Genome structure of mycobacteriophage D29: implications for phage evolution11Edited by J. Karn. *Journal of Molecular Biology*, 279(1), 143-164. doi:<https://doi.org/10.1006/jmbi.1997.1610>
- George, S. E., Chikkamadaiah, R., Durgaiah, M., Joshi, A. A., Thankappan, U. P., Madhusudhana, S. N., & Sriram, B. (2012). Biochemical characterization and evaluation of cytotoxicity of antistaphylococcal chimeric protein P128. *BMC Research Notes*, 5(1), 280. doi:10.1186/1756-0500-5-280
- Godde, J. S., & Bickerton, A. (2006). The Repetitive DNA Elements Called CRISPRs and Their Associated Genes: Evidence of Horizontal Transfer Among Prokaryotes. *Journal of Molecular Evolution*, 62(6), 718-729. doi:10.1007/s00239-005-0223-z
- Goujon, M., McWilliam, H., Li, W., Valentin, F., Squizzato, S., Paern, J., & Lopez, R. (2010). A new bioinformatics analysis tools framework at EMBL–EBI. *Nucleic Acids Research*, 38(suppl_2), W695-W699. doi:10.1093/nar/gkq313
- Grage, K., Jahns, A. C., Parlane, N., Palanisamy, R., Rasiah, I. A., Atwood, J. A., & Rehm, B. H. (2009). Bacterial polyhydroxyalkanoate granules: biogenesis, structure, and potential use as nano-/micro-beads in biotechnological and biomedical applications. *Biomacromolecules*, 10(4), 660-669. doi:10.1021/bm801394s
- Grage, K., Jahns, A. C., Parlane, N., Palanisamy, R., Rasiah, I. A., Atwood, J. A., & Rehm, B. H. A. (2009). Bacterial Polyhydroxyalkanoate Granules: Biogenesis, Structure, and Potential Use as Nano-/Micro-Beads in Biotechnological and Biomedical Applications. *Biomacromolecules*, 10(4), 660-669. doi:10.1021/bm801394s
- Greening, C., Villas-Bôas, S. G., Robson, J. R., Berney, M., & Cook, G. M. (2014). The growth and survival of *Mycobacterium smegmatis* is enhanced by co-metabolism of atmospheric H₂. *PLOS ONE*, 9(7), e103034-e103034. doi:10.1371/journal.pone.0103034

- Griebel, R. J., & Merrick, J. M. (1971). Metabolism of Poly- β -Hydroxybutyrate: Effect of Mild Alkaline Extraction on Native Poly- β -Hydroxybutyrate Granules. *Journal of Bacteriology*, 108(2), 782-789.
- Gründling, A., Bläsi, U., & Young, R. (2000). Genetic and biochemical analysis of dimer and oligomer interactions of the lambda S holin. *Journal of Bacteriology*, 182(21), 6082-6090.
- Gründling, A., Manson, M. D., & Young, R. (2001). Holins kill without warning. *Proc Natl Acad Sci U S A*, 98(16), 9348-9352. doi:10.1073/pnas.151247598
- Gupta, R., Gupta, N., & Rathi, P. (2004). Bacterial lipases: an overview of production, purification and biochemical properties. *Appl Microbiol Biotechnol*, 64(6), 763-781. doi:10.1007/s00253-004-1568-8
- Haft, D. H., Selengut, J., Mongodin, E. F., & Nelson, K. E. (2005). A Guild of 45 CRISPR-Associated (Cas) Protein Families and Multiple CRISPR/Cas Subtypes Exist in Prokaryotic Genomes. *PLOS Computational Biology*, 1(6), e60. doi:10.1371/journal.pcbi.0010060
- Hatfull, G. F. (2008). Bacteriophage genomics. *Current Opinion in Microbiology*, 11(5), 447-453. doi:10.1016/j.mib.2008.09.004
- Hatfull, G. F. (2014). Molecular Genetics of Mycobacteriophages. *Microbiology spectrum*, 2(2), 1-36.
- Hatfull, G. F., Cresawn, S. G., & Hendrix, R. W. (2008). Comparative genomics of the mycobacteriophages: insights into bacteriophage evolution. *Research in Microbiology*, 159(5), 332-339. doi:10.1016/j.resmic.2008.04.008
- He, L., Fan, X., & Xie, J. (2012). Comparative genomic structures of Mycobacterium CRISPR-Cas. *Journal of Cellular Biochemistry*, 113(7), 2464-2473. doi:doi:10.1002/jcb.24121
- Higgins, J. P., Higgins, S. E., Guenther, K. L., Huff, W., Donoghue, A. M., Donoghue, D. J., & Hargis, B. M. (2005). Use of a specific bacteriophage treatment to reduce Salmonella in poultry products 12. *Poultry Science*, 84(7), 1141-1145. doi:10.1093/ps/84.7.1141
- Hofnung, M., Jezierska, A., & Braun-Breton, C. (1976). lamB mutations in E. coli K12: Growth of λ host range mutants and effect of nonsense suppressors. *MGG Molecular & General Genetics*, 145(2), 207-213. doi:10.1007/BF00269595
- Hopkins, N., & Ptashne, M. (1971). *Genetics of virulence* (Vol. 2). Cold Spring Harbor Laboratory: Cold Spring Harbor, NY.
- Horvath, P., & Barrangou, R. (2010). CRISPR/Cas, the Immune System of Bacteria and Archaea. *Science*, 327(5962), 167-170. doi:10.1126/science.1179555
- Jacobs-Sera, D., Marinelli, L. J., Bowman, C., Broussard, G. W., Guerrero Bustamante, C., Boyle, M. M., . . . Hatfull, G. F. (2012). On the nature of mycobacteriophage diversity and host preference. *Virology*, 434(2), 187-201. doi:10.1016/j.virol.2012.09.026

- Jayawardana, K. W., Jayawardena, H. S. N., Wijesundera, S. A., De Zoysa, T., Sundhoro, M., & Yan, M. (2015). Selective targeting of *Mycobacterium smegmatis* with trehalose-functionalized nanoparticles. *Chemical communications (Cambridge, England)*, 51(60), 12028-12031. doi:10.1039/c5cc04251h
- Jendrosseck, D. (2009). Polyhydroxyalkanoate Granules Are Complex Subcellular Organelles (Carbonosomes). *Journal of Bacteriology*, 191(10), 3195-3202. doi:10.1128/JB.01723-08
- Jeong, H., Kim, H. J., & Lee, S. J. (2015). Complete Genome Sequence of *Escherichia coli* Strain BL21. *Genome Announcements*, 3(2), e00134-00115. doi:10.1128/genomeA.00134-15
- Jordan, T. C., Burnett, S. H., Carson, S., Caruso, S. M., Clase, K., DeJong, R. J., . . . Hatfull, G. F. (2014). A Broadly Implementable Research Course in Phage Discovery and Genomics for First-Year Undergraduate Students. *mBio*, 5(1), e01051-01013. doi:10.1128/mBio.01051-13
- Jun, S. Y., Jang, I. J., Yoon, S., Jang, K., Yu, K. S., Cho, J. Y., . . . Kang, S. H. (2017). Pharmacokinetics and Tolerance of the Phage Endolysin-Based Candidate Drug SAL200 after a Single Intravenous Administration among Healthy Volunteers. *Antimicrob Agents Chemother*, 61(6). doi:10.1128/aac.02629-16
- Kamravamanesh, D., Lackner, M., & Herwig, C. (2018). Bioprocess Engineering Aspects of Sustainable Polyhydroxyalkanoate Production in Cyanobacteria. *Bioengineering*, 5(4). doi:10.3390/bioengineering5040111
- Kaufmann, S. H. E. (2001). How can immunology contribute to the control of tuberculosis? *Nature Reviews Immunology*, 1, 20. doi:10.1038/35095558
- Keen, E. C. (2015). A century of phage research: Bacteriophages and the shaping of modern biology. *BioEssays : news and reviews in molecular, cellular and developmental biology*, 37(1), 6-9. doi:10.1002/bies.201400152
- King, H. C., Khera-Butler, T., James, P., Oakley, B. B., Erenso, G., Aseffa, A., . . . Courtenay, O. (2017). Environmental reservoirs of pathogenic mycobacteria across the Ethiopian biogeographical landscape. *PLOS ONE*, 12(3), e0173811. doi:10.1371/journal.pone.0173811
- Kingwell, K. (2015). Bacteriophage therapies re-enter clinical trials. *Nat Rev Drug Discov*, 14(8), 515-516. doi:10.1038/nrd4695
- Kovalcik, A., Obruca, S., Fritz, I., & Marova, I. (2019). *Polyhydroxyalkanoates: Their Importance and Future* (Vol. 14).
- Kruger, D. H., & Bickle, T. A. (1983). Bacteriophage survival: multiple mechanisms for avoiding the deoxyribonucleic acid restriction systems of their hosts. *Microbiol Rev*, 47(3), 345-360.

- Labrie, S. J., Samson, J. E., & Moineau, S. (2010). Bacteriophage resistance mechanisms. *Nature Reviews Microbiology*, 8, 317. doi:10.1038/nrmicro2315
- Lee, J. W., Parlane, N. A., Rehm, B. H. A., Buddle, B. M., & Heiser, A. (2017). Engineering Mycobacteria for the Production of Self-Assembling Biopolyesters Displaying Mycobacterial Antigens for Use as a Tuberculosis Vaccine. *Applied and Environmental Microbiology*, 83(5).
- Li, Z., Yang, J., & Loh, X. J. (2016). Polyhydroxyalkanoates: opening doors for a sustainable future. *Npg Asia Materials*, 8, e265. doi:10.1038/am.2016.48
- Lillebaek, T., Dirksen, A., Baess, I., Strunge, B., Thomsen, V. Ø., & Andersen, Å. B. (2002). Molecular Evidence of Endogenous Reactivation of Mycobacterium tuberculosis after 33 Years of Latent Infection. *The Journal of Infectious Diseases*, 185(3), 401-404. doi:10.1086/338342
- Linaz, B. P., Wong, A. Y., Freedberg, K. A., & Horsburgh, C. R., Jr. (2011). Priorities for screening and treatment of latent tuberculosis infection in the United States. *Am J Respir Crit Care Med*, 184(5), 590-601. doi:10.1164/rccm.201101-0181OC
- Liu, F., Hu, Y., Wang, Q., Li, H. M., Gao, G. F., Liu, C. H., & Zhu, B. (2014). Comparative genomic analysis of Mycobacterium tuberculosis clinical isolates. *BMC Genomics*, 15, 469. doi:10.1186/1471-2164-15-469
- Livingstone, P. G., Hancox, N., Nugent, G., & de Lisle, G. W. (2015). Toward eradication: the effect of Mycobacterium bovis infection in wildlife on the evolution and future direction of bovine tuberculosis management in New Zealand. *New Zealand Veterinary Journal*, 63(sup1), 4-18. doi:10.1080/00480169.2014.971082
- Loeffler, J. M., Djurkovic, S., & Fischetti, V. A. (2003). Phage lytic enzyme Cpl-1 as a novel antimicrobial for pneumococcal bacteremia. *Infect Immun*, 71(11), 6199-6204.
- Loeffler, J. M., Nelson, D., & Fischetti, V. A. (2001). Rapid killing of Streptococcus pneumoniae with a bacteriophage cell wall hydrolase. *Science*, 294(5549), 2170-2172. doi:10.1126/science.1066869
- Maestro, B., & Sanz, J. M. (2017). Polyhydroxyalkanoate-associated phasins as phylogenetically heterogeneous, multipurpose proteins. *Microbial biotechnology*, 10(6), 1323-1337. doi:10.1111/1751-7915.12718
- Marraffini, L. A., & Sontheimer, E. J. (2008). CRISPR Interference Limits Horizontal Gene Transfer in Staphylococci by Targeting DNA. *Science*, 322(5909), 1843-1845. doi:10.1126/science.1165771
- McNerney, R., & Traoré, H. (2005). Mycobacteriophage and their application to disease control. *Journal of Applied Microbiology*, 99(2), 223-233. doi:10.1111/j.1365-2672.2005.02596.x

- McWilliam, H., Li, W., Uludag, M., Squizzato, S., Park, Y. M., Buso, N., . . . Lopez, R. (2013). Analysis Tool Web Services from the EMBL-EBI. *Nucleic Acids Research*, 41(W1), W597-W600. doi:10.1093/nar/gkt376
- Mergaert, J., Anderson, C., Wouters, A., Swings, J., & Kersters, K. (1992). Biodegradation of polyhydroxyalkanoates. *FEMS Microbiology Reviews*, 9(2-4), 317-321. doi:10.1111/j.1574-6968.1992.tb05853.x
- Mezzina, M. P., & Pettinari, M. J. (2016). Phasins, Multifaceted Polyhydroxyalkanoate Granule-Associated Proteins. *Applied and Environmental Microbiology*, 82(17), 5060-5067. doi:10.1128/aem.01161-16
- MoH. (2010). *Guidelines for Tuberculosis Control in New Zealand 2010* (Document). Wellington, New Zealand: Ministry of Health New Zealand.
- MoH. (2017). *Antimicrobial Resistance: New Zealand's current situation and identified areas for action*. Wellington, New Zealand.
- Mohan, A., Padiadpu, J., Baloni, P., & Chandra, N. (2015). Complete Genome Sequences of a Mycobacterium smegmatis Laboratory Strain (MC2 155) and Isoniazid-Resistant (4XR1/R2) Mutant Strains. *Genome Announcements*, 3(1), e01520-01514. doi:10.1128/genomeA.01520-14
- Możejko-Ciesielska, J., & Kiewisz, R. (2016). Bacterial polyhydroxyalkanoates: Still fabulous? *Microbiological Research*, 192, 271-282. doi:<https://doi.org/10.1016/j.micres.2016.07.010>
- Nelson, D., Loomis, L., & Fischetti, V. A. (2001). Prevention and elimination of upper respiratory colonization of mice by group A streptococci by using a bacteriophage lytic enzyme. *Proc Natl Acad Sci U S A*, 98(7), 4107-4112. doi:10.1073/pnas.061038398
- Newton, J. M., Schofield, D., Vlahopoulou, J., & Zhou, Y. (2016). Detecting cell lysis using viscosity monitoring in E. coli fermentation to prevent product loss. *Biotechnology Progress*, 32(4), 1069-1076. doi:doi:10.1002/btpr.2292
- O'Flaherty, S., Ross, R. P., & Coffey, A. (2009). Bacteriophage and their lysins for elimination of infectious bacteria. *FEMS Microbiol Rev*, 33(4), 801-819. doi:10.1111/j.1574-6976.2009.00176.x
- O'Neill, J. (2016). *Tackling Drug-Resistant Infections Globally: Final Report and Recommendations*. Review on Antimicrobial Resistance.
- Ojha, A. K., Trivelli, X., Guerardel, Y., Kremer, L., & Hatfull, G. F. (2010). Enzymatic hydrolysis of trehalose dimycolate releases free mycolic acids during mycobacterial growth in biofilms. *J Biol Chem*, 285(23), 17380-17389. doi:10.1074/jbc.M110.112813
- Oliveira, H., Melo, L. D. R., Santos, S. B., Nóbrega, F. L., Ferreira, E. C., Cerca, N., . . . Kluskens, L. D. (2013). Molecular Aspects and Comparative Genomics of Bacteriophage Endolysins. *Journal of Virology*, 87(8), 4558-4570. doi:10.1128/jvi.03277-12

- Oren, E., Bell, M. L., Garcia, F., Perez-Velez, C., & Gerald, L. B. (2017). Promoting adherence to treatment for latent TB infection through mobile phone text messaging: study protocol for a pilot randomized controlled trial. *Pilot and Feasibility Studies*, 3(1), 15. doi:10.1186/s40814-017-0128-9
- Payne, K., Sun, Q., Sacchettini, J., & Hatfull, G. F. (2009). Mycobacteriophage Lysin B is a novel mycolylarabinogalactan esterase. *Molecular Microbiology*, 73(3), 367-381. doi:doi:10.1111/j.1365-2958.2009.06775.x
- Payne, K. M. (2006). *Mycobacteriophage lysins: Bioinformatic characterization of lysin A and identification of the function of lysin B infection*. (Doctor of Philosophy), Pennsylvania State University, University of Pittsburgh. Retrieved from http://d-scholarship.pitt.edu/9933/1/KMPayne_ETD_12-14-2010.pdf
- Payne, K. M., & Hatfull, G. F. (2012). Mycobacteriophage Endolysins: Diverse and Modular Enzymes with Multiple Catalytic Activities. *PLOS ONE*, 7(3), e34052. doi:10.1371/journal.pone.0034052
- Peters, V., & Rehm, B. H. A. (2005). In vivo monitoring of PHA granule formation using GFP-labeled PHA synthases. *FEMS Microbiology Letters*, 248(1), 93-100. doi:10.1016/j.femsle.2005.05.027
- PhagesDB. (2015). Inca. Retrieved from <https://phagesdb.org/phages/Inca/>
- PhagesDB. (2017). Retrieved from <https://phagesdb.org/hosts/genera/1/?sequenced=True>
- PhagesDB. (2019). Phage Isolation Locations by GPS Coordinates. Retrieved 2019 from <https://phagesdb.org/GPSmap/>
- Pohane, A. A., Patidar, N. D., & Jain, V. (2015). Modulation of domain–domain interaction and protein function by a charged linker: A case study of mycobacteriophage D29 endolysin. *FEBS Letters*, 589(6), 695-701. doi:<https://doi.org/10.1016/j.febslet.2015.01.036>
- Pope, W. H., Bowman, C. A., Russell, D. A., Jacobs-Sera, D., Asai, D. J., Cresawn, S. G., . . . Mycobacterial Genetics, C. (2015). Whole genome comparison of a large collection of mycobacteriophages reveals a continuum of phage genetic diversity. *eLife*, 4, e06416. doi:10.7554/eLife.06416
- Pötter, M., Müller, H., Reinecke, F., Wieczorek, R., Fricke, F., Bowien, B., . . . Steinbüchel, A. (2004). The complex structure of polyhydroxybutyrate (PHB) granules: four orthologous and paralogous phasins occur in *Ralstonia eutropha*. *Microbiology*, 150(7), 2301-2311. doi:doi:10.1099/mic.0.26970-0
- Rehm, B. H. (2003). Polyester synthases: natural catalysts for plastics. *Biochem J*, 376(Pt 1), 15-33. doi:10.1042/bj20031254
- Rehm, B. H. (2007). Biogenesis of microbial polyhydroxyalkanoate granules: a platform technology for the production of tailor-made bioparticles. *Curr Issues Mol Biol*, 9(1), 41-62.

- Roberts, R. J., & Macelis, D. (2001). REBASE--restriction enzymes and methylases. *Nucleic Acids Research*, 29(1), 268-269.
- Robins, K. J., Hooks, D. O., Rehm, B. H. A., & Ackerley, D. F. (2013). Escherichia coli NemA Is an Efficient Chromate Reductase That Can Be Biologically Immobilized to Provide a Cell Free System for Remediation of Hexavalent Chromium. *PLOS ONE*, 8(3), e59200. doi:10.1371/journal.pone.0059200
- Rocha, E. P., Danchin, A., & Viari, A. (2001). Evolutionary role of restriction/modification systems as revealed by comparative genome analysis. *Genome Res*, 11(6), 946-958. doi:10.1101/gr.153101
- Russell, D. A., & Hatfull, G. F. (2017). PhagesDB: the actinobacteriophage database. *Bioinformatics*, 33(5), 784-786. doi:10.1093/bioinformatics/btw711
- Saier, M. H., & Reddy, B. L. (2015). Holins in Bacteria, Eukaryotes, and Archaea: Multifunctional Xenologues with Potential Biotechnological and Biomedical Applications. *Journal of Bacteriology*, 197(1), 7. doi:10.1128/JB.02046-14
- Salaniponi, F. M., Harries, A. D., Banda, H. T., Kang'ombe, C., Mphasa, N., Mwale, A., . . . Boeree, M. J. (2000). Care seeking behaviour and diagnostic processes in patients with smear-positive pulmonary tuberculosis in Malawi. *Int J Tuberc Lung Dis*, 4(4), 327-332.
- Samaddar, S., Grewal, R. K., Sinha, S., Ghosh, S., Roy, S., & Das Gupta, S. K. (2015). Dynamics of Mycobacteriophage-Mycobacterial Host Interaction: Evidence for Secondary Mechanisms for Host Lethality. *Applied and Environmental Microbiology*, 82(1), 124-133. doi:10.1128/AEM.02700-15
- Sandhu, G. K. (2011). Tuberculosis: current situation, challenges and overview of its control programs in India. *J Glob Infect Dis*, 3(2), 143-150. doi:10.4103/0974-777X.81691
- Sassi, M., Bebeacua, C., Drancourt, M., & Cambillau, C. (2013). The First Structure of a Mycobacteriophage, the *Myoviridae* genus-species *Mycobacterium abscessus* subsp. *bolletii* Phage Araucaria. *Journal of Virology*, 87(14), 8099. doi:10.1128/JVI.01209-13
- Schmelcher, M., Donovan, D. M., & Loessner, M. J. (2012). Bacteriophage endolysins as novel antimicrobials. *Future microbiology*, 7(10), 1147-1171. doi:10.2217/fmb.12.97
- Schuch, R., Nelson, D., & Fischetti, V. A. (2002). A bacteriolytic agent that detects and kills *Bacillus anthracis*. *Nature*, 418(6900), 884-889. doi:10.1038/nature01026
- Schuster, H. (1962). Bacteriophages, von M. H. Adams. Interscience Publishers, Inc., New York-London 1959. 1. Aufl., XVIII, 592 S., 26 Tab., 16 Abb., geb. £ 6.50. *Angewandte Chemie*, 74(4), 164-164. doi:10.1002/ange.19620740437

<https://seaphagesphagediscoveryguide.helpdocsonline.com/home>

- Sharma, U., Vipra, A., & Channabasappa, S. (2018). Phage-derived lysins as potential agents for eradicating biofilms and persisters. *Drug Discovery Today*, 23(4), 848-856. doi:<https://doi.org/10.1016/j.drudis.2018.01.026>
- Sievers, F., Wilm, A., Dineen, D., Gibson, T. J., Karplus, K., Li, W., . . . Higgins, D. G. (2011). Fast, scalable generation of high-quality protein multiple sequence alignments using Clustal Omega. *Molecular Systems Biology*, 7(1), 539. doi:10.1038/msb.2011.75
- Singh, M., Kumar, P., Ray, S., & Kalia, V. C. (2015). Challenges and Opportunities for Customizing Polyhydroxyalkanoates. *Indian journal of microbiology*, 55(3), 235-249. doi:10.1007/s12088-015-0528-6
- Snapper, S. B., Melton, R. E., Mustafa, S., Kieser, T., & Jr, W. R. J. (1990). Isolation and characterization of efficient plasmid transformation mutants of *Mycobacterium smegmatis*. *Molecular Microbiology*, 4(11), 1911-1919. doi:10.1111/j.1365-2958.1990.tb02040.x
- Sreevatsan, S., Pan, X., Stockbauer, K. E., Connell, N. D., Kreiswirth, B. N., Whittam, T. S., & Musser, J. M. (1997). Restricted structural gene polymorphism in the *Mycobacterium tuberculosis* complex indicates evolutionarily recent global dissemination. *Proceedings of the National Academy of Sciences*, 94(18), 9869-9874.
- Sterling, T. R., Pope, D. S., Bishai, W. R., Harrington, S., Gershon, R. R., & Chaisson, R. E. (2000). Transmission of *Mycobacterium tuberculosis* from a cadaver to an embalmer. *N Engl J Med*, 342(4), 246-248. doi:10.1056/nejm200001273420404
- Stern, A., & Sorek, R. (2011). The phage-host arms race: shaping the evolution of microbes. *BioEssays : news and reviews in molecular, cellular and developmental biology*, 33(1), 43-51. doi:10.1002/bies.201000071
- Stummeyer, K., Schwarzer, D., Claus, H., Vogel, U., Gerardy-Schahn, R., & Mühlenhoff, M. (2006). Evolution of bacteriophages infecting encapsulated bacteria: lessons from *Escherichia coli* K1-specific phages. *Molecular Microbiology*, 60(5), 1123-1135. doi:10.1111/j.1365-2958.2006.05173.x
- Sturino, J. M., & Klaenhammer, T. R. (2006). Engineered bacteriophage-defence systems in bioprocessing. *Nat Rev Microbiol*, 4(5), 395-404. doi:10.1038/nrmicro1393
- Suzanne, M. M., Jennifer, F., Barbara, S., Yael, H.-M., Lori, A., Sundari, M., . . . Kathryn, S. (2014). Treatment Practices, Outcomes, and Costs of Multidrug-Resistant and Extensively Drug-Resistant Tuberculosis, United States, 2005–2007. *Emerging Infectious Disease journal*, 20(5), 812. doi:10.3201/eid2005.131037

- Tillich, U. M., Wolter, N., Schulze, K., Kramer, D., Broedel, O., & Frohme, M. (2014). High-throughput cultivation and screening platform for unicellular phototrophs. In (Vol. 14).
- Vishnoi, A., Roy, R., Prasad, H. K., & Bhattacharya, A. (2010). Anchor-Based Whole Genome Phylogeny (ABWGP): A Tool for Inferring Evolutionary Relationship among Closely Related Microorganisms. *PLOS ONE*, 5(11), e14159. doi:10.1371/journal.pone.0014159
- von Delft, A., Dramowski, A., Khosa, C., Kotze, K., Lederer, P., Mosidi, T., . . . Zumla, A. (2015). Why healthcare workers are sick of TB. *International Journal of Infectious Diseases*, 32, 147-151. doi:<https://doi.org/10.1016/j.ijid.2014.12.003>
- Wang, I.-N. (2006). Lysis timing and bacteriophage fitness. *Genetics*, 172(1), 17-26. doi:10.1534/genetics.105.045922
- Wang, I. N., Smith, D. L., & Young, R. (2000). Holins: the protein clocks of bacteriophage infections. *Annu Rev Microbiol*, 54, 799-825. doi:10.1146/annurev.micro.54.1.799
- Warren, L., & Allen, P. (2017). 9 Developing capacity for farm consultancy in New Zealand. *Management Consultancy Insights and Real Consultancy Projects*.
- White, A., & Knight, V. (1958). Effect of Tween 80 and Serum on the Interaction of Mycobacteriophage D-29 with certain Mycobacterial Species. *American Review of Tuberculosis and Pulmonary Diseases*, 77(1), 134-145.
- WHO. (2010). *Treatment of tuberculosis: guidelines* (Fourth ed.). Switzerland: WHO Press.
- WHO. (2018) Global Tuberculosis Report 2018. In, (pp. 277). Geneva: World Health Organisation 2018.
- Young, R. (2013). Phage lysis: do we have the hole story yet? *Curr Opin Microbiol*, 16(6), 790-797. doi:10.1016/j.mib.2013.08.008
- Zimmermann, L., Stephens, A., Nam, S.-Z., Rau, D., Kübler, J., Lozajic, M., . . . Alva, V. (2018). A Completely Reimplemented MPI Bioinformatics Toolkit with a New HHpred Server at its Core. *Journal of Molecular Biology*, 430(15), 2237-2243. doi:<https://doi.org/10.1016/j.jmb.2017.12.007>
- Zumla, A., Raviglione, M., Hafner, R., & Fordham von Reyn, C. (2013). Tuberculosis. *New England Journal of Medicine*, 368, 745-755. doi:10.1056/NEJMra1299894